NITRIC OXIDE THERAPIES FOR LOCAL INHIBITION OF PLATELETS' ACTIVATION ON BLOOD-CONTACTING SURFACES

by

Kagya Agyeman Amoako

A dissertation submitted in partial fulfillment
of the requirements for the degree of
Doctor of Philosophy
(Biomedical Engineering)
in The University of Michigan
2011

Doctoral Committee:

Associate Research Professor Keith E Cook, Chair
Professor Emeritus Robbert H Bartlett
Associate Professor Joseph L Bull
Associate Professor Mohamed El-Sayed

I dedicate this to my family and friends.

ACKNOWLEDGEMENTS

First and foremost, I wish to express my sincerest gratitude to my advisor, Professor Keith Cook, for his tutelage, inspiration, encouragement and support throughout my doctoral study. His guidance and vision played an important role in this work.

I would like to thank my dissertation committee: Robert Bartlett MD, Joseph Bull PhD and Mohamed El-Sayed PhD for their advice, guidance and encouragement during my study. Their insights and critiques helped improve this work.

I would like to express my thanks to the Extracorporeal life Support (ECLS) Lab and the National Institute of Health for their financial support during and beyond my doctoral study. Their support made my doctoral work possible. All other support from past and present ECLS lab members are also very much appreciated.

I also like to thank MedArray Inc. for providing the manufacturing tools and expertise required for the fabrication of the first nitric oxide generating artificial lung. All artificial lungs used in this work were developed using their facilities.

I would like to acknowledge the Ann Arbor soccer, MI community for providing an outlet for balancing time spent in the lab with outdoor activities. Their friendship is very much appreciated.

Finally I would like to thank my family for their inspiration, constant encouragements and support. They sacrificed their joy of family during my college and doctoral study. For this, I am forever grateful.

TABLE OF CONTENTS

DEDICATION ii

ACKNOWLEDGEMENTS iii

LIST OF FIGURES viii

LIST OF TABLES xi

LIST OF ABBREVIATIONS xii

ABSTRACT xiv

CHAPTER

I. INTRODUCTION 1

1.1 Motivations and Objectives 1
1.2 Coagulation on Artificial Surfaces 2
1.2.1 Platelet Activation 7
1.2.2 Intracellular Mechanisms During Platelet Activation 8
1.2.3 Clinical Consequences of Clotting on Biomaterials . 9
1.3 Clinical Methods used to Control Coagulation 11
1.3.1 Systemic Anticoagulation 11
1.3.2 Clinical Coatings 15
1.4 Experimental Surface Modifications for Improved Hemocompatibility 26
1.5 Long Term Use of Oxygenators 28
1.6 Nitric Oxide: Mechanisms and Physiology 30
1.7 Inhibition of Platelet Activation by Nitric Oxide 32
1.8 NO-releasing and NO-generating Polymers 34
1.9 Sweep Gas Nitric Oxide for Artificial Lungs 38
1.10 Summary of the Study 41
1.11 Reference 44

II. SYNTHESIS AND CHARACTERIZATION OF NITRIC OXIDE-GENERATING SILICONE FOR USE AS A BLOOD-CONTACTING BIOMATERIAL 60

2.1 Abstract 60
2.2 Introduction 61
2.3 Materials and Methods 64
2.3.1 In vitro Test System 64
2.3.2 PMC Surface Analysis 65
2.3.3 Measurement of NO flux and Clotting Times 66
2.3.4 Clot Distribution on NO-generating Cu(II)/Si PMCs 67
2.3.5 Statistical Analysis 67
2.4 Results 68
2.4.1 PMC's Surface Microstructure and Composition . . 68
2.4.2 Relationships among wt% Cu, Surface Expression of Cu and NO Flux and Clotting Times of PMCs . . 71
2.4.3 Clots on Coated Surfaces 72
2.5 Discussion 73
2.6 Conclusion 76
2.7 References 77

III. FABRICATION AND FLUX OPTIMIZATION OF NITRIC OXIDE-GENERATING HOLLOW SILICONE FIBERS . . . 81

3.1 Abstract 81
3.2 Introduction 82
3.3 Materials and Methods 84
3.3.1 Preparation of Hollow Fiber Material 84
3.3.2 Fabrication of NO-generating Hollow Silicone Fibers 85
3.3.3 Characterization of Fiber Structure and Wall Surface 86
3.3.4 Measurement of Nitric Oxide Generation from Fibers 87
3.3.5 Statistical Analysis 87
3.4 Results 87
3.4.1 Structure and Surface of Hollow Silicone Fibers . . . 87
3.4.2 NO Generation from Hollow Silicone Fibers 89
3.5 Discussion 91
3.6 Conclusion 93
3.7 References 94

IV. DEVELOPMENT AND BIOCOMPATIBILITY TESTING OF NITRIC OXIDE-GENERATING HOLLOW FIBER ARTIFICIAL LUNG 97

4.1 Introduction 97
4.2 Materials and Methods 99

4.2.1 Design of NO-Generating Hollow Silicone Fiber Oxygenator . . . 99
4.2.2 ECC Circuit Components . . . 101
4.2.3 Measurement of NO Flux from Fibers . . . 102
4.2.4 Rabbit Thrombogenecity Model for Testing ECC Circuits . . . 103
4.2.5 Blood sampling . . . 105
4.2.6 Plasma Fibrinogen . . . 105
4.2.7 Platelet aggregometry . . . 106
4.2.8 Measurement Plasma Copper . . . 106
4.2.9 Measurement of Blood Flow Resistance . . . 107
4.2.10 Statistical Analysis . . . 107
4.3 Results . . . 107
4.3.1 NO generating Artificial Lung Prototype and their NO generation . . . 107
4.3.2 NO Flux from Fibers . . . 108
4.3.3 Survival of NOgen and Control ECCs . . . 108
4.3.4 Thrombogenecity Outcomes . . . 109
4.3.5 Plasma Copper Concentration: . . . 112
4.3.6 ECC Blood Flow and Artificial Lung Resistance . . . 113
4.4 Discussion . . . 115
4.5 Conclusion . . . 119
4.6 References . . . 120

V. NON-THROMBOGENIC CHARACTERIZATION OF EXTRUDED NITRIC OXIDE RELEASING SILICONE CATHETERS 124

5.1 Abstract . . . 124
5.2 Introduction . . . 125
5.3 Materials and Methods . . . 127
5.3.1 Structure and Composition of NO-releasing Catheters 127
5.3.2 Nitric Oxide Charging of Catheters and NO-release Testing . . . 129
5.3.3 Preparing Catheters for Non-thrombogencity Evaluation . . . 130
5.3.4 Rabbit Thrombogenicity Model for Testing of Catheters 130
5.3.5 Blood sampling . . . 132
5.3.6 Platelet Aggregometry . . . 132
5.3.7 Statistical Analysis . . . 133
5.4 Results . . . 134
5.4.1 Extruded Catheter . . . 134
5.4.2 NO Release from DACA-6 Doped Silicone Catheters 134
5.4.3 Thrombogenicity Testing Outcomes . . . 137
5.5 Discussion . . . 139
5.6 Conclusion . . . 141

5.7 Reference 143

VI. NITRIC OXIDE IN SWEEP-GAS FOR LOCAL CLOT INHIBITION IN OXYGENATORS 147

6.1 Abstract 147
6.2 Introduction 148
6.3 Materials and Methods 152
6.3.1 In vitro Study 152
6.4 Results 156
6.4.1 NO Concentration in Fluid 156
6.4.2 Estimating NO Flux from the Biolung and Capiox RX25 fibers at Time Zero 159
6.5 Discussion 163
6.6 Reference 166

VII. CONTRIBUTIONS, LIMITATIONS AND FUTURE WORKS, AND CONCLUSION 168

7.1 Contributions 168
7.2 Limitations and Future Works 171
7.3 Conclusion 173

LIST OF FIGURES

Figure

1.1 The contact system of blood coagulation. 3

1.2 The contact system, intrinsic, extrinsic, and common pathways of blood coagulation 5

1.3 Intracellular mechanisms during platelet activation 9

1.4 Fibrinogen induced platelet activation 12

1.5 Heparin Coating 16

1.6 Polymer brushes 27

1.7 Biosynthesis of nitric oxide from L-arginine substrate 31

1.8 NO-cGMP dependent pathway to platelet inactivation 32

1.9 Fate of NO in blood 33

1.10 NO-releasing oxygen sensing catheter 38

2.1 Cu-mediated nitric oxide generation from S-nitrosothiols in blood and life dynamics of the nitric oxide gas. 63

2.2 Tube Coating Setup 65

2.3 Chemiluminescence Setup 67

2.4 Dendrites structure 68

2.5 Chemical compostion of surface 69

2.6 Surface expression of Copper 70

2.7 NO generation Profiles 71

2.8 ACT and NO flux graph 72

2.9 Clot formation on PMCs 73

3.1 Synthesis of NO generating polymer 84

3.2 Hollow silicone fiber extrusion process 85

3.3 Hollow silicone fiber extruder 86

3.4 Structure of extruded fibers 88

3.5 Cu nanoparticles' expression on hollow silicone fibers 88

3.6 Representative NO generation profile from hollow fibers 89

3.7 Cu particle size effect on NO generation from hollow fibers 90

3.8 Effect of Cu distribution and particle size on nitric oxide generation 91

4.1 Mechanism of NO generation by fibers 99

4.2 Oxygenator Design 100

4.3 Extracorporeal circulation circuit 102

4.4 Prototype of nitric oxide generating hollow silicone fiber oxygenator 108

4.5 Survival of control and experimental ECC circuits after flow initiation 109

4.6 ECC circuits' platelet consumption during blood flow 110

4.7 Levels of plasma fibrinogen concentration during extracorporeal circulation 111

4.8 Time course of ECC blood flow 112

4.9 Levels of plasma copper at baseline and at the end of extracorporeal circulation 113

4.10 Time course of control ECC resistance to blood flow 114

4.11 Time course of ECC blood flow 115

5.1 Catheter composition 128

5.2 Catheter Extruder 129

5.3 Extruded Catheter 134

5.4 NO release from control and NO-charged catheters 136

5.5 Effect of DACA-6 and Borate on catheters' NO release 136

5.6 NO flux density as a function of wt% DACA-6 137

5.7 Implanted control catheters with clot 138

5.8 Clots on explanted catheters 138

5.9 Survival of implanted catheters 139

6.1 Nitric oxide in sweep gas circulation setup. 153

6.2 Representative profile of nitric oxide degassed from samples. 157

6.3 Representative profile of nitric oxide recovered from nitrites. 157

6.4 NO concentration in fluid as a function of time sweep gas flow. . . . 158

6.5 NO flux from fibers of the Biolung and Capiox RX25 oxygenators as a function of time sweep gas flow 159

6.6 Evolution of the mass transfer coefficient, (k_c), of the Biolung and Capiox RX25 oxygenators at 10, 100, and 1000ppm NO/N_2 sweep gases. 161

6.7 Estimating time-zero NO flux on the Biolung. 161

6.8 Estimating time-zero NO flux on the Capiox RX25. 162

LIST OF TABLES

Table

1.1 Agonists secreted from platelets' dense** and alpha* granules including other potent agonists and their platelet membrane receptors . . 8

1.2 Conventional anticoagulation drugs; indications, mechanism of action and complications 14

1.3 New anticoagulation drugs; indications, mechanism of action and complications 15

1.4 Clinical coatings available for blood-contacting surfaces and estimated quantity used in US Clinics 18

1.5 Nitric oxide (NO) flux levels and inhibition of platelet activation by NO releasing/generating polymers 37

1.6 Sweepgas NO effect on Coagulation. 40

3.1 Nitric oxide (NO) flux levels from hollow silicone fibers 90

5.1 Chemical composition of extruded NO-releasing catheters 128

6.1 Solubilities of NO in fluid. 160

6.2 Predicted NO flux at time zero 163

LIST OF ABBREVIATIONS

ANOVA analysis of variance

AVCO$_2$R arterio-venous CO_2 removal

cGMP cyclic guanosine monophosphate

GP Glycoprotein

CPB cardio pulmonary bypass

DAG Diacylglycerol

DACA-6 N-(6-aminohexyl) aminopropyl-trimethoxysiloxane

ECMO extracorporeal membrane oxygenation

EDS energy dispersive x-ray spectroscopy

GP Glycoprotein

GSNO S nitrosoglutathione

GTP guanosine triphosphate

IP$_3$ inositol triphosphate

LDH lactate dehydrogenase

MetHb Methemoglobin

MLCK myosin light chain kinase

NADPH nicotinamide adenine dinucleotide phosphate

NOHLA NG-hydroxy-L-arginine

NO Nitric Oxide

NOS nitric oxide synthase

NOA Nitric Oxide Analyzer

PC phosphorylcholine

PDMS polydimethylsiloxane

PIP_2 phosphotidyl inositol bisphosphate

PKC protein kinase C

PL phospholipid

PLA2 phospholipase A2

PLC phospholipase C

PMC Polymetric matrice composite

PMP polymethylpentene

PP polypropylene

PPP Platelet-Poor Plasma

PRP Platelet-Rich Plasma

RBC Red Blood Cell

SA surface areas

SAMs self-assembled monolayers

SMAs surface modifying additives

STP Standard Temperature and Pressure

TAL total artificial lung

TATIII thrombin-antithrombin III

t-PA tissue plasminogen activator

TF tissue factor

u-PA urokinase plasminogen activator

vWF von Willebrand factor

ABSTRACT

Nitric oxide therapies for local inhibition of platelets' activation on blood-contacting surfaces

by

Kagya Agyeman Amoako

Chair: Keith E Cook

Blood-contacting devices interact with blood during their function much like the endothelium that modulates hemostasis. The surfaces of these devices however, lack endothelial-like properties, and consequently, upon blood contact, activate clotting factors to form clots. Systemic heparinization for inhibiting clot formation can cause bleeding and surface coatings show insignificant benefits.

This research investigated nitric oxide (NO) production mimicry of the endothelium on artificial lungs (ALs) and pediatric catheters. Their surfaces were functionalized either by (1) entrapping NO donors inside their bulk, (2) incorporating catalysts to generate NO from NO-donors or (3) supplementing NO into sweep gas of artificial lungs. Pediatric catheters functionalized with NO-donor thin coats using method 1 is limited by short NO release duration. Method 2 has not been applied to large surface-area, low-flow devices like the AL.

In this work NO-generating silicone membranes were synthesized and characterized to determine the relationship between surface properties, NO flux, and blood clotting time. These outcomes helped develop and optimize NO-generating gas-

exchange silicone fibers that represent the majority of ALs surface area. The first NO-generating AL prototypes, using those fibers, were manufactured, incorporated into NO-generating circuits and tested for their non-thrombogenicity. To test for NO-release duration and non-thrombogenicity, catheters were fabricated to incorporate NO-donors inside their walls, characterized for NO flux and release duration by chemiluminescence, and tested for patency using a thrombogenicity model in rabbits. Methods 1-2 involve material modification using complicated and expensive chemical formulations and/or manufacturing. Method 3 however, functionalizes ALs by only adding NO into sweep gas. Decade-long anti-clotting testing using a wide range of NO concentrations has been conducted without knowledge of what concentration yields endothelial NO flux levels in the AL. This concentration was determined for the MC3 Biolung and the Terumo capiox rx25 ALs *in vitro*.

All these ideas have shown positive results in short-term studies, and each may play a necessary role in inhibiting clot formation in future ALs. The sufficiency however, of each idea or of a combination for clot inhibition in long-term ALs remains to be determined.

CHAPTER I

INTRODUCTION

1.1 Motivations and Objectives

The biocompatibility of blood-contacting biomaterials are especially important as no biomaterial in blood-contacting devices like gas-exchangers, catheters, stents, and dialysis membranes adequately prevents clot formation without some form of systemic anticoagulation. Systemic anticoagulation is the gold standard for inhibiting clot formation on blood-contacting biomaterials but unfortunately it has been associated with bleeding in many patients. Without systemic anticoagulation however, clotting can lead to: blockage of blood flow paths and increased device resistance, reduced mass transport in artificial lungs and kidneys, and thromboembolic events. Paradoxically, clotting can also cause bleeding complications if platelets and clotting proteins are consumed by artificial surfaces.

To date, clot formation and the accompanying life-threatening complications are key problems clinicians still face. In attempts to reduce or eliminate the use of systemic anticoagulation, two main approaches have been tried: 1) development of surface coatings that inhibit protein adsorption (aka non-fouling surfaces) and 2) heparin-bonded surfaces that inhibit the common branch of the coagulation cascade. Clinical oxygenators that incorporate both of these anti-clotting approaches are available. Some examples are the X-coated Terumo Capiox; Carmeda (heparin-bonded)

and Trillium (polyethylene oxide) Medtronic Affinity, heparin-bonded Medos Hilite, and phosphorylcholine-coated Sorin PrimO2x. However, their clinical testing outcomes have either been marginally beneficial for short term use (up to 4h) in cardiopulmonary bypass settings or not different from controls in long term use (weeks to months) in respiratory support settings[**1-3, 4**].

Because of this unmet need, this research attempts to develop nitric oxide (NO) releasing and generating surfaces and characterize their ability to inhibit clot formation and reduce the use of systemic anticoagulation. It examines a relatively new approach to local inhibition of clotting on biomaterials through the use of NO gas. NO is a free radical gas produced naturally by the endothelium and circulated in biological systems to maintain hemostasis [**5-8**]. Endothelium NO flux levels have been estimated in literature to be 1 - 5 ($x10^{-10}$ mol min^{-1} cm^{-2}).

Specifically, the work examines the synthesis of NO-generating and NO-releasing polymers and determination of their NO flux rates. These NO-generating polymers were then placed in oxygenators, and NO-releseasing materials were used to form catheters. The thrombogenicity of these devices were then examined in vivo using rabbits. Lastly, the NO flux rates were determined in vitro using a representative clinical oxygenator and thoracic artificial lung using different NO concentrations within N_2 as the sweep gas.

1.2 Coagulation on Artificial Surfaces

Under normal physiologic conditions, blood remains in contact only with the normally antithrombogenic endothelium. The endothelium is lined with cells that modulate hemostasis by expressing or secreting NO, thrombomodulin, heparan sulfate, tissue plasminogen activator (t-PA), urokinase plasminogen activator (u-PA) and plasminogen activator inhibitors. Thrombomodulin and heparan sulfate inhibit blood coagulation where as t-PA, u-PA, and plasminogen activator inhibitors modulate fib-

rinolysis [**9**]. Endothelial cells also have a low surface energy that keeps blood proteins from changing conformation [**10**]. Artificial surfaces, however, lack such endothelial properties and thus activate circulating platelets and the coagulation cascade leading to blood coagulation.

Blood coagulation on biomaterials is initiated by the contact system. The liver produces three main zymogens that play key roles in the contact system. These zymogens, namely Factor XII (hageman factor), Factor XI, and high molecular weight kininogen (HK) all exist in plasma. The initiation, activation, and feedback mechanisms of these zymogens at the artificial surface is shown in Figure 1.1. In the ac-

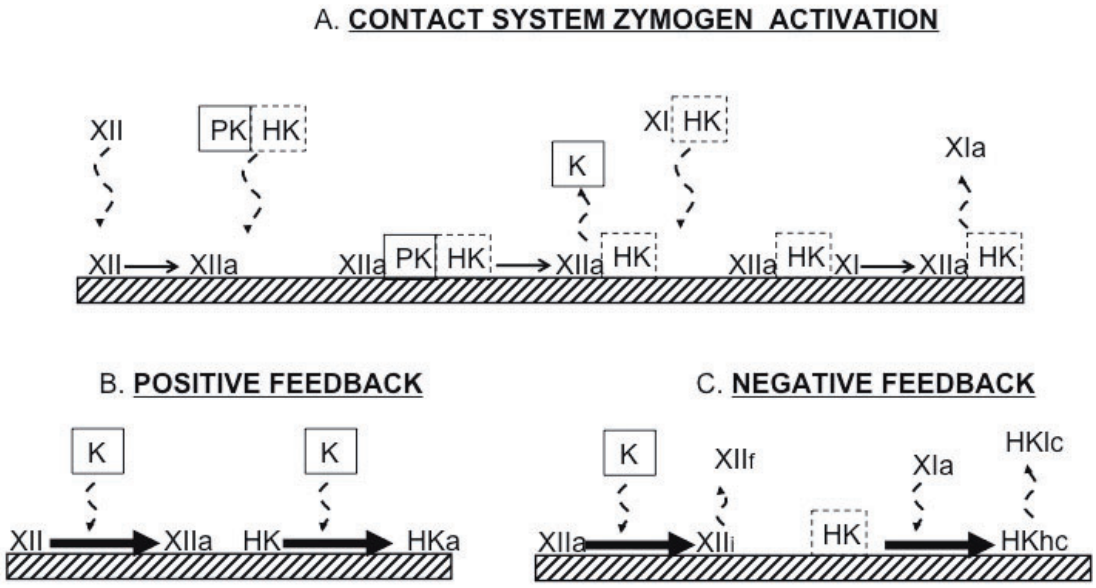

Figure 1.1: The activation phase of the contact system A) starts with adsorption and autoactivation of FXII. Activated FXII help activate prekallikrein (PK) which exists as a complex with high molecular weight kininogen (HK). A similar reaction occurs with FXI-HK complex resulting in the activation of FXI. The system also uses a positive feedback mechanism B) where FXII is rapidly activated by the activated form of PK, kallikrein (K). The activation of HK is also potentiated by K. To balance the positive feedback control, the contact system also uses a negative feedback mechanism C) to halt the activity of XIIa and HK. It fragments XIIa into soluble/low activity XIIf and inactive XIIi using K and fragments HK into surface-bound inactive heavy chain HK (HKhc) and soluble light chain HK (HKlc) using XIa. Modified from biomaterial science text 2nd Edition [**Colman 11**]

tivation phase, zymogen Factor XII first adsorbs to negatively charged surfaces and activates to FXIIa by autoactivation. This process cleaves a single disulfide bridge of FXII allowing its heavy chain to bind to the surface while revealing its active site. At this point FXIIa becomes a co-factor for prekallikrein and FXI which exist in plasma as non-covalent complexes with HK (PK-HK and XI-HK). The PK-HK complex binds to FXIIa to activate prekallikrein into kallikrein. The FXI-HK complex also binds to FXIIa to activate factor FXI into FXIa to complete the activation phase of the contact system. Zymogens XII, XI, and PK at this point have been activated into XIIa, XIa and K enzymes.

Once activated, the contact system uses a positive feedback mechanism potentiated by kallikrein. Kallikrein acts on FXII and HK substrates to speed up their conversion into FXIIa and HKa. For example HKa binds 10 fold faster than HK to PK and FXI thereby accelerating the association PK and FXI. This feedback mechanism serves as the initial driver of all amplification reactions in blood coagulation starting from the contact system down to a formed clot. The contact system also has a negative feedback arm, in addition to the positive feedback mechanism, to modulate the contact system. During negative feedback control, Kallikrein cleaves off a fragment of adsorbed FXIIa, (FXIIf), into plasma leaving behind inactivated FXIIi. Although FXIIf is still active, its participation in blood coagulation is decreased as it looses its affinity for surfaces. It therefore exhibits low activity for prekallikrein to kallikrein conversion. FXIa is also a player for the suppression of contact activation. It cleaves off the light chain of adsorbed HK, HKlc, which contains the active site of HK leaving behind the heavy chain portion (HKhc). This reaction terminates the cofactor activity of HK and thus allows FXIa to desorb from the artficial surface. The effect of the negative feedback mechanism has however, not inhibited the contact system adequately to prevent downstream activation of procoagulant factors in the intrinsic and extrinsic pathways of the coagulation system that lead to clot formation

in blood-contacting devices.

Post contact system blood coagulation has been traditionally viewed in two separate pathways; the intrinsic and extrinsic pathways. See Figure 1.2. Such views are slowly fading as it's now more accepted that the pathways interact *in vivo*.

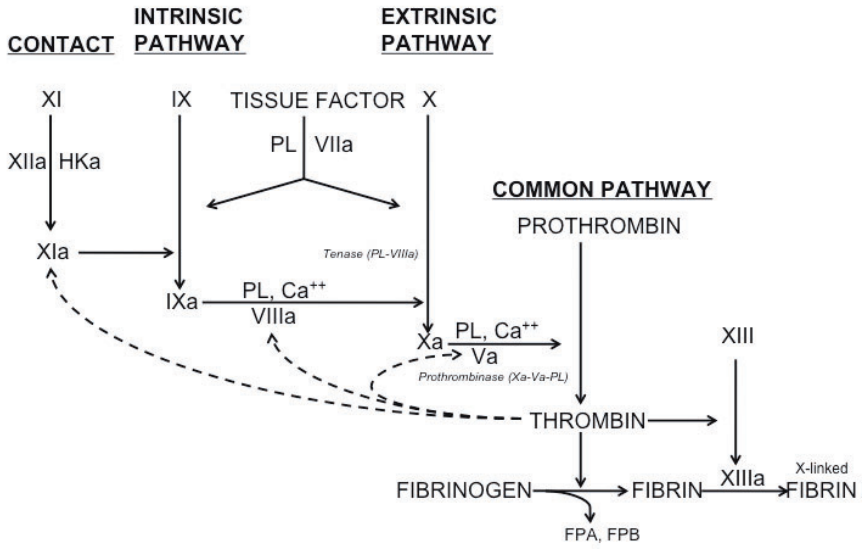

Figure 1.2: The contact system involves the adsorption and activation of zymogens FXII, FXI, and HK. FXIa from the contact system activates FIX of the intrinsic pathway. A tenase complex consisting of FIXa and a phospholipid surface (PL) in the presence of VIIIa and Ca^{2+} activates the FX. FX activation marks the beginning of the extrinsic pathway and can occur independently of TF (VIIa). However TF in the presence of a PL can influence both pathways. With the production of Xa, a prothrombinase complex is formed between FXa and FVa in the presence of a PL surface (eg platelet's membrane) to initiate the common pathway. Prothrombin is converted into thrombin inside the platelet. After secretion from platelets, thrombin potentiates the activation of XI, VIII and V to amplify blood coagulation. Thrombin cleaves fibrinogen into fibrinopeptides A and B so the peptides can polymerize into fibrin resulting in more fibrinogen-GP IIb/IIIa interaction for a stable clot. Finally thrombin, activates FXIII to cross link fibrin for a solid clot to form. Modified from biomaterial science text 2nd Edition [**11**]

The contact system is viewed as part of the intrinsic pathway because it initiates that branch of blood coagulation. The intrinsic pathway is associated with artificial surfaces and consists of reactions involving only vascular elements that can occur

independently of VIIa whereas the extrinsic branch consist of blood in addition to vascular elements. The main difference between the branches lies in the way they activate FIX. The intrinsic system uses FXIa in the presence of Ca^{2+} whereas the extrinsic system requires tissue factor (TF) usually embedded in cell membrane lipid bilayer in addition to calcium.

The intrinsic pathway is initiated by the activation of IX to IXa by Factor XIa which is activated in the contact system. FIX can also be activated by TF in the presence of a phospholipid (PL) surface and cofactor VIIa. For the next reaction to occur, calcium, FIXa together with the tenase complex (phospholipid surface-cofactor VIIIa) must work together to activate FX. This marks the end of the intrinsic pathway. Activation of the extrinsic pathway is achieved again by TF in the presence of PL and VIIa, the same coagulant elements association utilized in the intrinsic pathway. As TF is present in endothelial tissue, activation of the intrinsic pathway is usually associated with tissue damage. However, biomaterial-induced platelet activation and inflammation can also activate the intrinsic branch, as TF is also present in platelets and leukocytes. When TF associates with a PL and cofactor VIIa, FX is activated into FXa marking the end of the extrinsic pathway and the beginning of the common pathway of blood coagulation.

The common pathway is activated by the promthrombinase complex consisting of FXa, cofactor Va on platelets' membrane and a PL surface in the presence of calcium. With FVa serving as the platelet membrane receptor for FXa, the activated platelet produces and secrets prothrombin. The complexing of these four elements to form prothrombinase increases prothrombin activity by 300,000 fold compared to that achieved by FXa and prothrombin alone. Adsorbed and activated platelets on the artificial surface, at this point, are connected by fibrinogen-glycoprotein IIb/IIIa platelet membrane receptor bridges following cleavage of fibrinopeptide A and B from fibrinogen. Platelet aggregation achieved by interconnecting-platelet- secreted fibrino-

gen bridges is still a premature clot until thrombin crosslinks the platelet aggregate by converting fibrinogen into longer fibrin strands that bind to activated platelets multiple times. Finally a solid clot is formed when thrombin activates FXIII to FXIIIa to cross link the interconnecting fibrin.

Thrombin also potentiates the clotting process by activating FV, FVIII and FXI (broken line in Figure 1.2). It is therefore viewed as the most potent clotting factor in blood coagulation.

1.2.1 Platelet Activation

Circulating platelets are activated either after damage to healthy endothelium or after blood exposure to an artificial surface. After damage to the endothelium for whatever reason, the endothelium looses its integrity and has to remedy its environment in order to restore its vascular tone. To achieve normal haemostasis, ruptured endothelial cells secret a "sticky" protein called von Willebrand factor (vWF) to bind to collagen in the exposed sub-endothelial layer so that circulating platelets can bind to the opposite ends of vWF to form a seal at the damaged area. Glycoprotein Ib/IX receptor on platelets membrane allows binding of vWF to activate platelets.

On artificial surfaces, the contact system activation leads to generation of FXa. This, in turn, binds to FVa on platelet membrane to activate platelets. After the initial phase where few platelets are activated, a second and massive platelet activation phase ensues. The release of clotting factors from platelets' granules during the first wave of activations acts to systemically activate a substantially large amounts of circulating platelets to potentiate coagulation. Among the granule content released, those of greatest physiological importance and their platelet membrane receptors are listed in Table 1.1

During blood flow in blood-contacting devices, flow-induced shear stresses can also lyse platelets to expel their procoagulant factors or just activate them. Platelets

Table 1.1: Agonists secreted from platelets' dense** and alpha* granules including other potent agonists and their platelet membrane receptors

Agonist	**Receptor**
**Adenosine diphosphate (ADP)	P2Y12 receptor
**Serotonin	5-HT2A receptor (Serotonin receptor)
*Platelet activating factor (PAF)	PAF receptor
*vonWillebrand factor (vWF)	glycoprotein Ib/IX
*Platelet factor 4 (PF4)	PF4 receptor
*Thromboxane A2 (TxA2)	TxA2 receptor
*Thrombin	Protease-activated receptor -1(human)
Collagen	glycoprotein IV
Fibrinogen	glycoprotein IIb/IIIa

[11]

can thus be activated by such mechanical force in addition to chemical induction explained above.

1.2.2 Intracellular Mechanisms During Platelet Activation

Platelets are about 3-4 μm in diameter and have a trilaminar phospholipoprotein membrane. The membrane (Figure 1.3) consists of a plasmatic surface with mucopolysaccharides and glycoproteins, a filamentous submembranous area serving as a contractile system and a peripheral zone filled with adhesion and signal transduction receptor sites **[11]**. As shown in Figure 1.3, these surface receptors activate phospholipase C (PLC) after interacting with platelet agonists.

PLC activation is mediated by glycoproteins (G proteins). After PLC is activated, it cleaves phosphotidyl inositol bisphosphate (PIP_2) into Diacylglycerol (DAG) and inositol triphosphate (IP_3). IP_3 then mobilizes Ca^{2+} from a dense tubular system within the platelet cytosol to activate myosin light chain kinase (MLCK), which phosphorylates the myosin light chain (MLC). This reaction is responsible for the membrane contraction that changes the platelet's shape from discoid to spherical. Dense and alpha granules migrate to the center of platelet at this point. The Ca^{2+}also activates phospholipase A2 (PLA2) to initiate a series of reactions to produce throm-

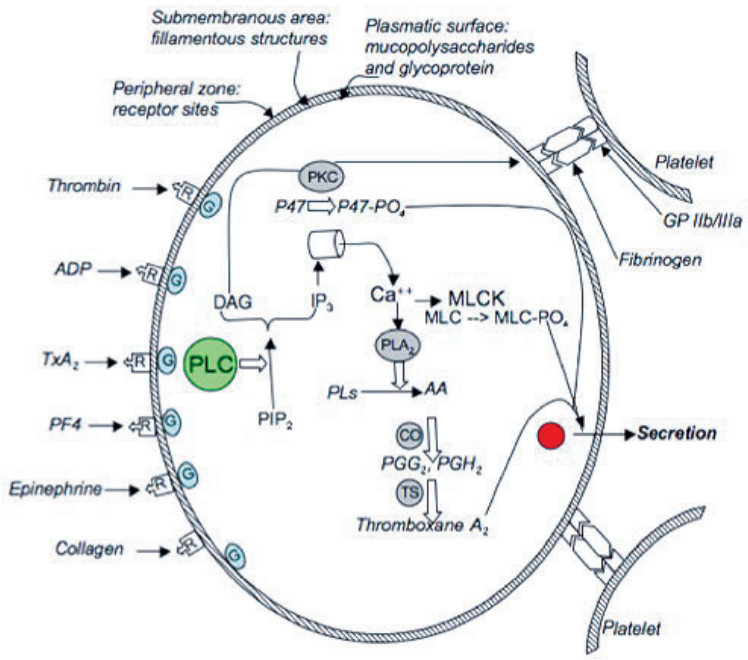

Figure 1.3: Intracellular mechanisms duing platelet activation: Modified from Overview of Hemostasis [**11**]

boxane A2. On the other hand, DAG stimulates protein kinase C (PKC) which in turn phosphorylates P47. The P47-PO_4 then interacts with G proteins to expose the platelet receptors active sites. Finally MLCK, P47-PO_4, and thromboxane A2 together stimulate the secretion of platelet granules [**11**].

1.2.3 Clinical Consequences of Clotting on Biomaterials

The sequelae of blood activation in medical devices vary depending on the device and its duration of use. During the use of extracorporeal membrane oxygenation (ECMO), total artificial lung (TAL), arterio-venous CO_2 removal ($AVCO_2R$), ECMO, TAL or AVCO2R, clots can impede gas transfer in and out of blood and increase resistance to blood flow. In the case of a TAL, this can also increase the loading on the right ventricle. Clots can also shed off the membranes and travel back into the vasculature, lodge in major organs, cause organ dysfunction or failure, and potentially lead to death.

Because of such complications, some form of systemic anticoagulation is administered to prevent thrombus formation in all of these applications. During ECMO, the level of anticoagulation is monitored hourly by the whole blood activated clotting time (ACT) method. Many extracorporeal life support centers maintain the ACT between 180-200 seconds compared to a normal reference value between 70-80 seconds. During clinical TAL use and in low dose ACT $AVCO_2R$ regiment, ACTs are maintained between 180-200 seconds [**12-13**]. Such tight increments in average ACT from baseline require much care, as small downturns in ACT can lead to significant clot formation. High ACT, on the other hand, helps avoid clot formation but also predisposes the patient to bleeding. For example, high ACT during cardio pulmonary bypass (CPB) can lead to post-op bleeding complications, and high ACT during ECMO can lead to bleeding complications, particularly in kids.

Clotting-related complications can also occur in total artificial lungs. Unlike ECMO, where a pump is used to drive flow, here, TALs utilize the right ventricle as the pump. Therefore, an increase in device resistance is especially problematic, as it abnormally stresses the heart. Pumpless $AVCO_2R$ also lacks a pump, and can suffer the low flow and reduced gas transfer problems seen in TALs.

The function of other blood-contacting devices like catheters and whole blood sensors are also adversely affected by protein adsorption and clot formation. Their small surface areas (SA) decrease their platelet consumption compared to devices with large SA to volume ratio. For such devices with large SA to volume ratios, clotting can lead to rapid failure since it doesn't take a large body of clot to occlude the device. For example, the diameters of pediatric catheters are so small (21- 24 ga) that it takes little masses of clot for occlusion to occur.

Clot formation also adds a finite layer of clot material onto biomaterials and can lead to decreased gas diffusion across the biomaterial. In artificial lungs, for example, the layer of clot creates an added physical barrier between the gas exchange fiber

wall and flowing blood. During oxygenation, the sweep gas not only will travel the normal fiber-wall length but also cross the clot thickness to reach flowing blood. The increased gas diffusional distance is also true for $AVCO_2$ where CO_2 travels out from blood into sweep gas.

Reduced gas transfer in gas exchange devices, increased resistant to blood flow, and thromboembolic complications are all real clinical problems as a result of clotting on biomaterials. These problems still need to be addressed with new approaches that do not elicit other equally life-threatening complications.

1.3 Clinical Methods used to Control Coagulation

There are two main approaches being followed by current clinical practice to minize the effects of blood-biomaterial interactions. They include 1) systemic anticoagulation and 2) surface modification of biomaterials.

1.3.1 Systemic Anticoagulation

The mechanism of action of these drugs on platelets and on the intrinsic pathway of blood activation is summarized in Figure 1.4. The most commonly used systemic anticoagulant is heparin, but other agents such as clopidogrel, aspirin, and warfarin are also used. Heparins role in inhibiting clot formation is multi-faceted. It inhibits factor Xa from activating prothrombin into thrombin and, when complexed with antithrombin III, it directly inhibits thrombin from binding to platelets. It also partially inhibits the activation of FXII and FXI. Warfarin inhibits Factors II and VII of the extrinsic coagulation pathway, Factors IX, X, and prothrombin of the intrinsic pathway. The points of action of both these anticoagulants are downstream of the onset of blood coagulation and have no effect on protein adsorption. Furthermore, these anticoagulants may compromise hemostasis and cause hemorrhage as it acts systemically [**14**]. Aspirin and clopidogrel are also among the commonly used systemic drugs

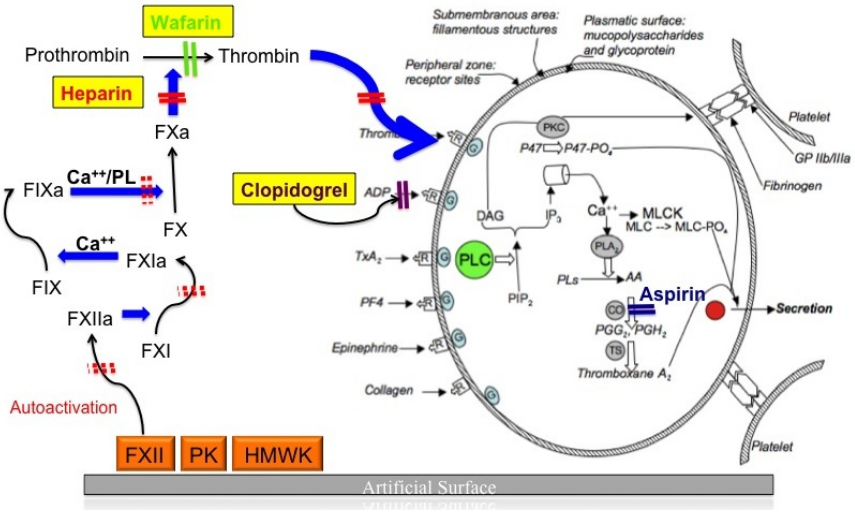

Figure 1.4: Fibrinogen-induced platelet activation on artificial surfaces

to inhibit platelet activation. Asprin irreversibly inhibits the synthesis of Thromboxane A2 and prostaglandins inside platelets and Clopidogrel binds to platelets ADP receptor, P2Y12, to block ADP from activating platelets. They inhibit the clotting cascade at the biomaterial's surface and inside platelets in an irreversibly manner that can lead to bleeding complications [**14**].

The compilations from the use of both conventional and newer anticoagulation drugs, their mechanisms of action, indications, and complications is summarized in Tables 1.2 and 1.3 [**15-19**].

The response to these drugs differ from patient to patient. In fact, many patients are resistant to the effects of a single oral anticoagulation drug, so sometimes a therapy that embodies multiple drugs having different mechanisms of action is often used. The problem with this approach is that although the mechanisms of action for current antiplatelet agents are known, their combined effect may induce an anticoagulation effect whose magnitude may be too large to allow restoration to normal hemostasis. Therefore administering these agents concomitantly further increases the potential of bleeding and of other unforeseen complications [**20**]. Ultimately, these drugs increase the risk of bleeding complications because of their prolonged half lives. Bleeding

complications become even more devastating in patients with renal insufficiency who cannot efficiently clear these long lasting drugs. The effects of systemic anticoagulation swing from bleeding in cases where it overwhelms hemostasis to device clotting when inadequate concentrations are used. In devices with large surface area, both effects (bleeding and depletion of systemic clotting factors and platelets) can occur.

Bleeding complications from systemic heparinization are the most common and life-threatening. For example, the Michigan ECMO experience with neonatal mortality is one that can still be improved if bleeding complications due to systemic anticoagulation are reduced. According to the most recent report on the impact of ECMO on neonatal mortality [**21**], bleeding is the most frequent cause of death in newborns managed with ECLS. In this population, intracranial hemorrhage occurred in approximately 13% of neonates, 5% of pediatric patients, and 4% of cardiac patients. Clotting complications are also common, occurring in 26% of patients [**22**].

Table 1.2: Conventional anticoagulation drugs; indications, mechanism of action and complications

Conventional Anticoagulants			
Drug	**Mechanism**	**Indication**	**Complications**
Heparin	Binds and activates AT-III to inhibit factor IIa and Xa	Prophylaxis in general surgery, prevention and treatment of arterial and venous thrombosis	Heparin-induced thrombocytopenia (HIT): treatment involves activation of platelets with PF4 complexes
Warfarin (Coumadin)	Inhibits synthesis of vit-K dependent factors II, VII, IX and X	Venous thrombosis and prevention of venous thromboembolism in patients with MI	Severe bleeding -Black stool or bleeding from the rectum, -Skin conditions such as hives, a rash or itching,-Swelling of the face, throat, mouth, legs, feet or hands, -Bruising -Chest pain or pressure, -Nausea or vomiting, -Fever or flu-like symptoms, -Joint or muscle aches, -Diarrhea, -Difficulty moving, -Numbness and tingling, -Painful erection lasting four hours or longer
Aspirin	Irreversibly inhibit enzyme COX to block thromboxane A2	Prevention of thrombosis in established vascular disease patients	-GI toxicity from gastric acid secretion: Aspirin inhibits PGI2, PGE2, PGD2 whose expression are necessary for the inhibition of gastric acid secretion from the mucosa. -Renal toxicity: Aspirin inhibits vasodilatory effects of prostaglandins and thus can decrease renal blood flow leading to renal insufficiency (microalbuminuria @ 325mg daily), Significant reduction in Na excretion to 1500mg daily., -Hemorrhagic Stroke: cerebral bleeding @ higher doses)
Clopidogrel	ADP-platelet aggregation irreversible	Patients with a history of ischemic stroke, MI	Inhibition effect lasts over 4-5days and bleeding times maximizes in 3-7days.

[15, 17 - 19]

Table 1.3: New anticoagulation drugs; indications, mechanism of action and complications

New Anticoagulants			
Drug	**Mechanism**	**Indication**	**Complications**
Abciximab (Reopro)	High affinity for GP IIb-IIIa non-competitive, slowly reversible, effect duration = 24-48h, detected on circulating platelets 2wk after treatment	Prevention of cardiac ischemia in PCI, ACS (unstable angina)	Dosage led to 90% blocking of GPIIb-IIIa receptors, marked inhibition of aggregation and prolonged bleeding time. Platelet and RBC transfusion are required in CBP and stenting. Near normal bleeding time seen after 12h
Tirofiban (Aggrastat)	Highly specific but low affinity for GP IIb-IIIa, rapidly reversible, effect duration = 4-8h	Acute coronary syndrome (ACS)	Excessive bleeding, pelvic pain, slowing heart rate and dizziness
Eptifibatide (integrilin)	Highly specific but low affinity for GP IIb-IIIa, highly reversible, effect duration =2-4 h	Acute coronary syndrome, Percutaneous coronary intervention	Case study result:- Groin hematoma: 179(1020), GI bleading: 11(1020), Pulmonary: 1(1020), all in PCI patients. Legend: observed(total)

[15, 17 - 19]

1.3.2 Clinical Coatings

In addition to systemic anticoagulation, biomaterial surface coatings are being used clinically to control clotting. These coatings are largely of two types. The first type attempts to bind heparin to the surface in order to inhibit coagulation specifically at the surface of the biomaterial. The second focuses on limiting protein adsorption to the biomaterial in order to inhibit activation of the contact system and the intrinsic branch of the coagulation cascade.

Coatings that utilize heparin include of Duraflo II, Bioline, Sarns/3M and Carmeda Bioactive Surface. As shown in Figure 1.5, the working principle of heparin for inactivation of thrombin is a two-step process. Anti-thrombin III, secreted by the liver into systemic circulation, must first bind to a specific pentasaccharide sequence on

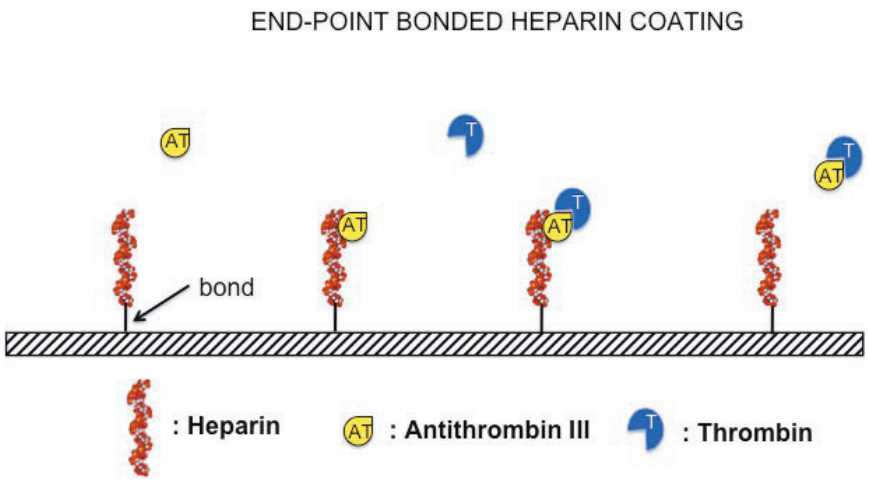

Figure 1.5: End-point bonded (ionic or covalent) heparin coating and mechanism of inactivating thrombin (not drawn to scale).

immobilized heparin molecules to induce conformational changes in ATIII. In the second step, systemic thrombin released from activated platelets binds to ATIII. The ATIII-thrombin complex then turns off thrombin and dissociates it from the immobilized heparin molecule. Whether immobilized in its unfractionated or fractionated form, heparin's activity is reduced for two reaons: 1) it is fixed and thus has limited interaction with ATIII and with thrombin by extension and 2) its pentasaccharide active site can be broken up due to processing.

Coatings that attempt to limit protein adsorption are Sorin and Dideco's phosphorylcholine, trillium, and Terumo's poly(2- methoxyethylacrylate) aka X-coating. These coatings are designed to incorporate charge polarity to increase the hydrophilicity and lower the surface energies of biomaterials by attracting water molecules[**23-24**]. Water molecules cluster around polar functional groups of long chain grafted molecules to create an aqueous layer at the blood/biomaterial interface. The functional groups is believed to limit protein and platelet adsorption by presenting an environment similar to aqueous state of plasma.

The Sorin phosphorylcholine (PC) coating consist of is a polar zwitterionic phospholipid molecules. One end of the molecule is positively charged and the other

phosphate end is negatively charged. Because of this zwitterionic nature, it's able to be absorbed on negatively charged surfaces with the phosphate end free. The interaction of free end with water leads to water retention near the blood/biomaterial interface [25]. Trillium coating consist of polyethylene oxide polymer chains that are hydrophilic along its entire chain to create an insulating water layer [**23-24**]. X-coating also consist of long chain polymers with a polar property and thus work in a similar way as trillium and PC.

The effectiveness of repelling plasma protein and platelets by these coatings depends on how well they retain their water content. Although there isn't data on that under physiological flow conditions, these polymer chain coatings are prone to leach, as is common in most coatings, and lose water retention during flow.

These coatings and their usage are summarized in Table 1.4. The two most common heparin coatings (Duraflo II and Carmeda Bioactive surface) have so far received only general acceptance in routine clinical practice and their current use in the United States is estimated at about 17% of all perfusions [**26**].

Table 1.4: Clinical coatings available for blood-contacting surfaces and estimated quantity used in US Clinics

Coating	**%Usage in all perfusion**	**Manufacturer**	**Current location**
Duraflo II [heparin coating]	ca 8.5	Edwards Life-Sciences	Irvine, CA
Surface Modifying Additive [polydimethylsiloxane polycaprolactone oligomer]	—	COBE Cardiovascular	Arvada, CO
Phosphorylcholine	—	Dideco	Mirandola, Italy
Sorin Synthesis [Phosphorylcholine]	—	SORIN Group USA, Inc	Arvada, CO
Bioline [heparin coating]	—	Jostra AG	Hirrlingen, Germany
X Coating [poly(2-methoxyethylacrylate)]	—	Terumo Cardiovascular	Ann Arbor, MI
Sarns 3M Heparin	—	Sarns 3M Cardiovascular Systems	Ann Arbor, MI
Trillium Biopassive Surface [polyethylene oxide]	—	Medtronic Cardiopulmonary	Minneapolis, MN
Carmeda Bioactive Surfaces [heparin coating]	ca 8.5	—	—

[26- 33]

Surface coating with heparin is currently achieved mostly by ionic or covalent attachment (see Figure 1.5). Carmeda, Bioline, and Sarns 3M covalently attach the heparin by a general method described by Larm et al [**28**] whereas Duraflo II surfaces are coated with heparin by ionic attachment. There are however, slight variations in the method of covalent heparinization used by Bioline and Sarns 3M. Biolines coating method employs a linker molecule (e.g. natural material such as polypeptides) to bind the heparin to the polymer. The linker molecule provides sites of both ionic and covalent interactions with heparin and as a result a more stable bonding of the heparin molecule is achieved [**29**]. The heparinization technique of 3M company is similar to that used by Carmeda Bioactive coatings. It involves a covalent binding of an oxidized heparin to a layer of coated biomaterial. Duraflo II heparin coating

is an ionically bound benzalkonium- chloride complex which enables relatively firm connections with the surface compared to Carmeda. However, a general disadvantage of this method is the rapid release of heparin upon exposure to blood or plasma [**30**]. In the covalent attachment method, the reaction in heparin can occur only at one end allowing the heparin molecule to be tethered only at one end with the remainder containing the active site free to interact with flowing blood. Theoretically, this end-point attachment method may be effective than ionic attachment, as the free end of the heparin would increase its interaction with blood.

In a study conducted by **Niimi et al** [**34**] where heparin-coated polypropylene surfaces and uncoated controls were primed with whole blood and incubated for 3hrs, no change in platelet activation between groups was observed. Also there was significant platelet adhesion within each group ($p < 0.05$). A decade later, **Fluger et al** [**35**] also studied the effect of ionically bonded heparin coating on fibrinogen (Fg) adsorption, platelet counts and activated partial thromboplastin tim(aPTT) in 60 CPB patients. Half of the patients were assigned to a tip-to-tip heparin coating circuit and the other half were put on uncoated circuits. The levels of Fg in the coated and non-coated groups dropped significantly ($p<0.0001$) from 2.90 to 2.44 mg/dL and from 2.73 to 2.40 mg/dL respectively after 2hrs postoperative. There were also no differences in aPTT and platelet counts between the two groups.

In works involving PMEA coatings, **Tanaka et al [36], Kocakulak et al [37], and Demirkilic et al [38]** conducted an *in vitro* study where various forms of poly (meth) acrylates were tested for platelet adsorption and an *in vivo* study using PMEA coated CPB circuits in 96 patients. Platelet deposition in the Tanaka study was lowest (4×10^4 cells/μm^2) on PMEA out of six other forms of poly (meth) acrylates tested. Kocakulak et al found significant loss of platelets in coated and uncoated groups by the end of surgery ($p<0.01$). Also, significantly more platelets were lost in the uncoated group (116 000 cell/mm^3) than in the coated group (36 000 cell/mm^3),

$p < 0.01$. Plasma Fg was also lost more in the uncoated group (1.3 g/L) than in the coated group (0.25 g/L) although both groups significantly ($p<0.01$) lost Fg at the end of CPB. Demirklic et al's work where they combined PMEA tip-to-tip coating of CPB circuits and optimized extracorporeal circulation for reduced turbulent flow showed especially fascinating results. Baseline Fg and platelet count levels were not different from levels at the end of CPB in 41 patients. The only weakness in that study is that PMEA-coated circuits were not controlled for with uncoated circuits and therefore it's difficult to evaluate the anticoagulatory property of the PMEA coating. Was the result solely PMEA-coating effect one?, a combination of flow optimization and coating?, or just flow optimization?

Studies similar to those described have also been conducted with Trillium, phosphorylcholine, surface modifying additives and modified heparin coatings. **Stammer et al [2], Ereth et al [1], Noora et al [39], and Van den Goor et al [40]** have studied Trillium biopassive coated oxygenator versus uncoated ones in a CPB setting. In Ereth's study only the oxygenator was coated and their results suggest that Trillium coating showed no clinical benefit. Levels of BTG, Fg and platelet count were no different between coated and uncoated oxygenators ($p=0.05$). Stammers et al raises a good question about this study; "Was the treatment of the oxygenator alone, and not the entire circuit, sufficient to show efficacy?". A definite interpretation of Ereth's study is therefore difficult to make. In other work conducted by **Noora et al**, coated CBP circuits containing a Trillium-coated Medtronic membrane oxygenator was compared to uncoated circuits in 256 patients. Noora et al concluded that the coating showed no inter-group differences in platelet counts. This observation was also confirmed in Van den Goor's work where no difference in platelet count ($p=0.17$) was observed between two groups (N=10 patients/ group). One group were treated on Trillium-coated circuits and another on uncoated CPB circuits. There was also no difference ($p=0.47$) in contact system FXIIa between groups.

The water retention property of polar zwitterionic phosphorylcholine head groups has established the molecule as a potential material for coating biomaterials to inhibit blood coagulation [**25**]. Some research groups have classified it as a biocompatible material based on *in vitro* and *in vivo* studies in animals [**33, 43**]. Outcomes from clinical studies however don't quite put PC coating in such light. In a study conducted by **De Somer et al [41], Farneti et al [42] and Stefano et al [43]**, PC coating was evaluated for its ability to inhibit blood coagulation during CPB in many patients. In De Somer's work, randomly selected 25 patients were treated with PC-coated CPB circuits whereas the other 25 received uncoated circuits. No differences in generated thrombin and platelet counts were observed between the groups ($p < 0.01$). Platelet factor 4 and BTG levels in the uncoated group (22192 ± 17931, 8040 ± 3986 IU/mL) were however significantly higher ($p=0.01$, $p=0.005$) than in the coated group (9338 ± 17303, 3790 ± 4104 IU/mL). A different outcome in BTG levels was reported by Ferneti and Stefano. In their studies a tip-to-tip PC-coated CPB circuits and uncoated controls were evaluated in a total of 50 adult patients. No significant differences in BTG and sP-selectin was observed between tip-to-tip PC-coated and uncoated groups ($p>0.05$). Furthermore when CPB was performed under different blood management conditions (blood suction, shed blood separation and without shed blood separation) to reduce blood trauma associated with CPB, platelet counts still decreased with no differences observed between PC-coated and uncoated groups ($p>0.05$). In all three conditions, however, platelet counts did not drop significantly ($p= 0.2, 0.13, 0.46$) in both control and PC-coated groups.

Other polymers with similar hydrophilic properties exhibited by PC has also been developed and tested clinically. These polymers termed surface modifying additives (SMAs) are incorporated into the blood-contacting biomaterial during processing. SMAs such as polycaprolactone and PDMS are amphiphilic so they poses both hydrophilic and hydrophobic groups. When incorporated into biomaterials dur-

ing processing in aqueous conditions, the surface of the biomaterial gains hydrophilicity as the hydrophobic tails of SMAs orient towards and attach to the biomaterial. Based on this chemistry, SMA-coated surfaces have been tested clinically for its anticoagulatory properties. In one such study **Defraigne et al [44]** compared COBE SMARxT extracorporeal Circuits (COBE Laboratories, Gloucester, England) to uncoated controls using procoagulant markers' levels as metrics in 100 CPB patients. The coated surface preserved more platelets (165±9 X $10^3/mm^3$) than in uncoated circuits (137±8 X $10^3/mm^3$). However, platelet counts decreased and BTG levels increased significantly in both groups ($p< 0.01$). In addition the biocompatibility of SMA-coated surfaces was not adequate to eliminate or reduce the normal systemic heparinization regiment (ACT $>$ 400) common to all the CPB studies described herein.

A relatively new form of surface coating consisting of heparin modified with long chain dialkyl group has also been tested in goat for its antithrombogenecity in a tip-to-tip coated ECMO system in Japan by **Nishinake et al [45]**. Hydrophobicity of dialkyl groups is proposed to reduce heparin leaching from coated polymethylpentene hollow fiber membrane oxygenator and other ECMO circuitry during blood circulation. This group provided long-term respiratory support for 151 days with small doses of heparin infusion while maintaining the concentration of pro-coagulant markers close to physiological levels. Baseline, week 1 and 21 ACTs were 118, 125 and 133 s respectively. ACTs were stable between during the test period. Platelet counts remained almost steady for 4 weeks and gradually decreased thereafter. Baseline, week 1 and 21 values were 51.9, 48.5 and 15 X $10^4/mm^3$ respectively. ATIII levels remained in physiological range with baseline, week 1 and 21 values of 127, 124 and 138%. Unfortunately no clinical trials of this coating exist.

Of the several studies comparing different surface coatings using identical or almost identical research protocols to allow for direct and accurate evaluation, the

most relevant work starting from about a decade ago is discussed here. **Palanzo et al** [**46**] and **Hoel et al** [**47**] compared Duraflo II (ionic bonded heparin) to Trillium (polyethylene oxide) coatings in a total of 90 CPB patients using procoagulant markers' levels as metrics for blood coagulation. In both studies there were no differences in the demographic data of patients who were attached to Duraflo II or to Trillium coated circuits. The Palanzo study reported a 6.2±10.2% drop in platelets (corrected for hemodilution) after 20 mins in patients who were assigned Trillium coating and 3.6±15.8% in the Duraflo II coating group. Platelet count drop were not significantly different within and between groups. Platelet counts within groups may have been different if blood samples were drawn at the end of the CPB and analyzed for counts. In addition to platelet counts, Hoel et al also monitored beta thromboglobulin (BTG) concentration. Platelet counts in their study decreased significantly ($p < 0.0005$) in Duraflo II and Trillium groups with no significant inter-group differences. There was a 40% and 60% drop in platelet counts in the Trillium and Duraflo II groups respectively. Correspondingly, BTG also increased significantly ($p = 0.02$) in both groups. The authors concluded that using either the Carmeda-coated oxygenator or the Trillium-coated oxygenator affords similar benefits in regards to preserving circulating platelet counts during bypass.

In 2000, Larson et al.[**48**] compared Duraflo II and Sarns 3M heparin-coated arterial filters. The heparin-coated surfaces were evaluated for thrombus formation in a 4hr veno-venous extracorporeal circulation models using adult pigs. Clots formed on coated arterial filters were analyzed with macro-densitometry, light microscopy, and scanning electron microscopy. The conclusions drawn from this study were that the 3M circuit had significantly less gross thrombus ($p < 0.001$), 66% and 84% less microscopic thrombi and five-fold less SEM-measured aggregates ($p = 0.03$) compared to the Duraflo II and uncoated groups. This may be interpreted to mean that the Sarns 3M surface is less thrombogenic. However, if closely inspected, another interpretation of

the data emerges; there was a 25% decrease in platelet count in the 3M and uncoated groups and a 13% decrease in the Duraflo II group over the study period. Perhaps, adhered platelets on the Sarns 3M coating remained in the state of microaggregates. The surface areas of circuits used in respiratory support methods are quite larger than an arterial filter's surface area. Hence a better study approach would have been testing tip-to-tip coated circuits. This work, perhaps, does not provide enough scientific evidence to conclusively compare the two heparin-coated surfaces. Thiara et al [**49**] have also studied another heparin-coating product called Bioline. Bioline surfaces are composed of covalently-bonded heparin coating similar to Sarns 3M coating. Bioline and PC-coated CPB circuits were evaluated for their anti-coagulability in 30 patients undergoing either valve replacement or coronary artery bypass grafting. Platelet count was used as the metric for measuring anti-coagulability of coatings. Platelet counts decrease significantly in PC (15% drop) and Bioline (17%) groups ($p = 0.01$). No difference in platelet counts was observed between groups ($p = 0.66$).

In a slightly different study, the additive anti-coagulation effect of heparin covalently bonded on arterial line filters and oxygenators in PC-coated CPB circuits was evaluated in 15 patients. The other 15 patients were attached to uncoated oxygenators in PC-coated circuits. Jacobs et al 2011 [**50**]observed a significant increase in platelet factor 4 (PF4) in both groups after the CBP procedure ($p < 0.001$). PF4 level in both groups increase from about 25 IU/ml to about 150 IU/ml. No additional benefit in combining both coatings was observed.

The Thiara group further evaluated a tip-to-tip PC-coated PVC circuit connected to PC-coated Avant oxygenator and a tip-to-tip X-coated PVC circuit connected to X-coated Terumo oxygenator for anti-coagulability in 30 CPB patients [**51**]. Platelet count, thrombin-antithrombin III (TATIII), and lactate dehydrogenase (LDH) levels were used as metrics for analyzing anti-coagulation. TATIII levels significantly increased from 6.1 and 7.4 μg/L at baseline to 12.5 and 10 μg/L at the end of surgery

in PC and X-coated groups respectively ($p < 0.05$). Platelet count also significantly decreased from 220 X 10^9/L and 198 X 10^9/L at baseline to 186 X 10^9/L and 172 X 10^9/L in PC and X-coated groups respectively ($p < 0.05$). Expectedly, LDH levels significantly increased in both groups ($p < 0.05$).

Gunaydin et al [52], Marcoux et al [53] and Hussaini et al [54] have conducted anti-coagulability studies on multiple clinical coatings including carmeda, trillium, x-coating, bioline and phosphorylcholine in CPB procedures. On average, platelet count drop of 39.2 ± 6.2% was recorded across all 5 coating groups. Other procoagulant markers such fibrinogen consumption, BTG and PF4 all change at significant ($p < 0.05$) or close to significant levels in the direction indicating inadequate inhibition of coagulation.

The recurring theme in blood anti-coagulability testing of commercial coatings in CPB is one that range from marginal clinical benefits to generally non-significant differences when compared to non-functionalized biomaterials. It is however, important to note that CPB is a highly invasive procedure associated with a substantial amount of trauma on blood elements as a result of surgery and chest tube drainage of blood. Blood elements can thus be activated by CPB procedures completely independent of blood-biomaterial interaction. Perhaps, this is the reason why these coatings have performed better in ECMO and *in vitro* settings. For example, Nojiri et al group were able to support adult sheep on an ECMO circuit coated tip-to-tip with heparin for up 168 h with minimal heparinization (ACT = 150 sec). Gas transfer remained stable and platelet count remained within the physiologic range throughout the experiment **[55]**. Matsuwaka et al 1990 also evaluated covalently bonded heparin ECMO circuits with an uncoated pedriatric centrifugal pump in dogs for 12 h without systemic heparinization. No significant differences in gas exchange and no apparent macroscopic thrombus formation was observed. **[56].**Similar conclusions have also been reached by Palmer et al 1995 **[57].** Taken together this body of knowledge on commercial coat-

ings show better anticoagulation in less invasive test settings like simulated ECMO, and no significant anti-coagulatory benefits in CPB [**58-60**].

1.4 Experimental Surface Modifications for Improved Hemocompatibility

There are other surface modification techniques being experimentally tested in *in vitro* settings. These methods are highly experimental in nature and may take years of research to advance it to clinical testing. They include attachment of charged (negatively, positively or zwitterionic) molecules, polymer brushes, albumin, derivatives of hydrophilic groups (ethylene glycol, ethylene oxide, methyl ether methacrylate)[**61**], and air, oxygen or nitrogen plasma treatment of biomaterials' surfaces. A few of these methods have been reported on extensively in the literature and are discussed herein. The immobilization of hydrophilic groups (eg tetraglyme) on biomaterials keep a hydration layer on their surfaces to prevent protein adsorption and their subsequent denaturation that initiates activation. Hydrophilic groups are mostly either attached as self-assembled monolayers (SAMs) with differing terminating groups or as brushes of different chain lengths. The ability to control the terminating groups (e.g. hydrophobic (methyl), hydrophilic (hydroxyl and carboxyl), and a binary mixture of both) lends this technique a great versatility in chemically modifying the surfaces of biomaterials.

An *in vitro* study by the Ratner group, [**62**] showed that by varying ratios of hydroxyl and methyl terminations of SAMs different effects on human fibrinogen adsorption and platelet adhesion and activation can occur. Platelet adhesion was about 50 and 98 % less ($p < 0.05$) on SAMs with 65% and 100% hydroxyl groups, respectively when compared to a gold surface and SAMs terminated with less than 65% hydroxyl after exposure to plasma. This could be explained by the higher albumin

affinity for the SAMs with 65% hydroxyl and the lower total protein adsorption associated with SAMs with 100% hydroxyl. After exposing these surfaces to a protein solution with a similar ratio of fibrinogen and albumin to that existing in blood (0.1 mg/ml fibrinogen +1mg/ml serum albumin), SAMs with 0%, 36% and 65% hydroxyl showed c.a. 70%, reduction in fibrinogen adsorption. On the same SAMs configurations but with lower serum albumin (0.1mg/ml serum albumin), a 30% reduction was observed indicating, perhaps, a higher albumin affinity of SAMs with 65% hydroxyl. This raises the question of whether engineering surfaces to create higher affinities to specific plasma proteins can reduce the adsorption of procoagulant ones. Most of these new surfaces are yet to be to applied to commonly used blood-contacting biomaterials and tested in *in vivo* settings for thrombogenicity evaluation.

Anchorage of polymer brushes to glass, silica, aluminum and gold is another surface modification method being tested. Polymer brushes are end-tethered (anchored, grafted) polymer chains stretched away from the substrate due to excluded-volume effect. See Figure 1.6.

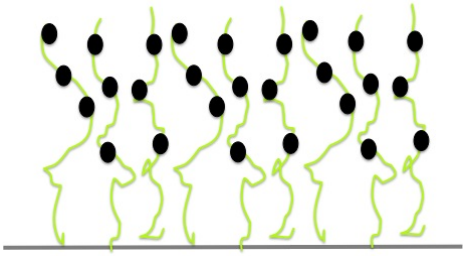

Figure 1.6: High density grafting of polymer brushes

The concept of excluded volume, introduced by a Physical Chemist Werner Kuhn, states that the excluded volume is the volume inaccessible to other molecules in the system as a result of the presence of the first molecule. This effect help brushes extend out from their base into the interacting medium creating a larger physical barrier between substrate and particulates of medium. In the case where hydrophilic brushes are used, blood elements may perhaps interact less with substrate due to such

large hydration layer sequestered by brushes. Single type polymer brush or a mixture of polymer brush grafting is a reality today and have been tested for biocompatibility [**63**] and microbicidal and biofilm resistance properties in some cases [**64**]. Because these brushes can be terminated with antimicrobial peptides (AMPs) like cathelicidin, not only can the surface be imparted with hydrophilicity arising from a polar brush but it can also actively kill microbes and thus prevent biofilm formation.

1.5 Long Term Use of Oxygenators

Artificial lungs are built to function similar to the natural lung: transport oxygen into the bloodstream and remove carbon dioxide from it. These devices work in a similar fashion to the natural lung, with the gas flowing on one side and blood on the other side of a gas permeable membrane. Gas exchange occurs by diffusion of the gases across the membrane. Artificial lungs are used in several different long-term applications: ECMO, AVCO2R, and TAL. The design, surface area, and clot formation in these devices varies based on application. Typical ECMO, AVCO2R, and TAL artificial lungs have gas exchange surface areas of 2.5, 1.3, and 1.7 m^2 respectively, and the typical gas exchange membranes are composed of polypropylene (PP), polymethylpentene (PMP), or polydimethylsiloxane (PDMS). In ECMO circuits, up to 0.5 m^2 additional surface area is possible when one considers the pump, heat exchanger, reservoir, and tubing in the system. The AVCO2R and TAL circuits only consist of the device and its cannulae or vascular grafts, and thus contain less than 0.1 m^2 additional surface area. Extracorporeal membrane oxygenation (ECMO) involves the use of a modified heart-lung machine to support life for patients with severe, acute respiratory or cardiac illness [**65**].

Total artificial lungs (TALs) have been used to support animals [**65**] for up to 30 days. In humans, the duration of respiratory support continues to push to the limit. The maximum time on ECMO for newborns is usually around 21 days, and

the record for longest survivor on ECMO in the US is at 62 days [**66**]. This record was broken in January 30, 2008, when a patient at National Taiwan Univeristy hospital, Taiwan survived a drowning accident after 117 days of ECMO application [**67**]. These durations of support are isolated cases. Problems that limit long-term ECMO support includes bleeding associated with heparinization, thrombus formation in circuit, oxygenator failure, plasma leakage in some oxygenators, and decreased immune function. ECMO is generally a bedside technology so patients are less ambulatory which may lead to muscle atrophy and reduced immune function.

Gas transfer membrane materials of oxygenators are a key design choice for all of these devices. They must be highly gas permeable to allow gas diffusion for blood oxygenation and/or carbon dioxide removal, be highly non-thrombogenic to reduce blood activation and subsequent thrombus formation on their surfaces, and ideally prevent plasma leakage through the membrane during long term support. Commonly used materials in clinical oxygenators include polypropylene (PP), polymethylpentene (PMP) and silicone rubber. Polypropylene fibers are microporous, PMP fibers are porous on the gas side but contain a solid skin on the blood side, and silicone rubber fibers are solid throughout.

Microporous membranes create smaller gas diffusional distances and are thus more efficient at oxygenation and CO2 removal. As published by Gaylor et al. [**68**], the resistance to O_2 and CO_2 transfer in microporous membranes is small and their hydrophobic property is maintained during conditions pertaining to CPB. In long term extracorporeal life support however, membrane resistance may increase due to progressive wetting of the microporous structure which lead to plasma leakage, a condition marked by yellowish to orange coloration in the oxygenator. To resolve this problem, plasma tight PMP microporous membranes were introduced. This hybride membrane is microporous with a thin solid wall to separate blood and gas sides. Until a couple of years ago, there were no reported incidences of plasma leakage with the

hybrid membranes. In 2009, Luis et al [**69**] described the occurrence of plasma leakage in a plasma-tight polymethylpentene type oxygenator after 24h of ECLS. Obviously, there is no denying the fact that the three primary complications of ECLS described above can and need to be improved; some more than others.

The outstanding challenge in extracorporeal life support today is limiting complications due to biomaterial-induced blood activation and subsequent thrombus formation. Many of the current solutions to these problems are decades-old, and alternate ideas for controlling blood coagulation should be pursued.

1.6 Nitric Oxide: Mechanisms and Physiology

Nitric oxide gas holds significant promise as an antiplatelet agent at a biomaterial surface. It affords the luxury of local inhibition of clotting without the use of systemic anticoagulation. Nitric oxide is synthesized by the brain, macrophages [**70**], liver [**71**], and most importantly by endothelial cells. NO production by endothelial cells is most relevant for regulating blood tone. Other regulatory functions within cells and tissues include vasodilation, neurotransmission and as a bactericidal agent secreted by macrophages. NO is formed in the body directly from guanidino nitrogen of the amino acid L-arginine through a two-step reaction catalyzed by nitric oxide synthase (NOS).

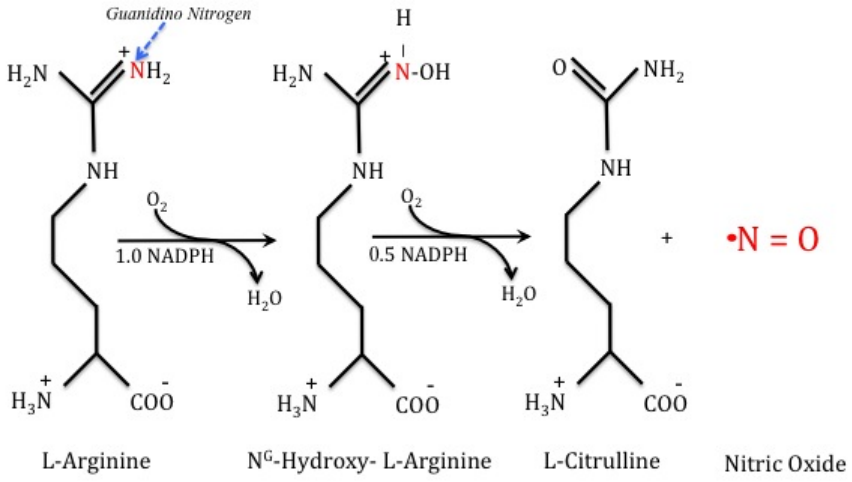

Figure 1.7: Biosynthesis of NO. L-arginine is converted to NO in two successive steps of which a two-electron oxidation of L-arginine to N-w-hydroxy-L-argninie is the first, then converted to NO and citrulline, utilizing one and half NADPH and O_2. Both steps require Ca^{2+} and calmodulin as activators and are accelerated by tetrahydrobiopterin [**72**]

It's a process that consumes five electrons, and results also in the formation of L-citrulline. The complete reaction is shown in Figure 1.5. NG-hydroxy-L-arginine (NOHLA) is formed in the intermediate step and the overall reaction consumes 1.5 moles of nicotinamide adenine dinucleotide phosphate (NADPH) [**73**] and 2 moles of molecular oxygen [**74**]. The unpaired electron on the biosynthesized NO gas makes it highly reactive giving the molecule extremely short half life (2-5 seconds) in blood [**75**]. Such a short half life limits the molecule to act local to the site of production. Since it is both water/lipid soluble, it diffuses freely within tissues from its site of formation to its site of action. It has been reported to bind to the heme moiety of guanylate cyclase, an important molecule also present in platelets, and cause a greater than 400-fold activation of the enzyme[**76**]. These properties are essential for applications that require fast-acting and potent effect of NO on platelets.

1.7 Inhibition of Platelet Activation by Nitric Oxide

In the vasculature, endothelial cells produce NO as described in 1.6 for regulating several physiological processes. After production, the gas diffuses into flowing blood and it's either oxidized or taken up by blood elements like the platelet. Because NO is lipohilic, it freely crosses the lipid bilayer of platelets to indirectly activate several intracellular reactions leading to inhibition of platelet activation. See Figure 1.8.

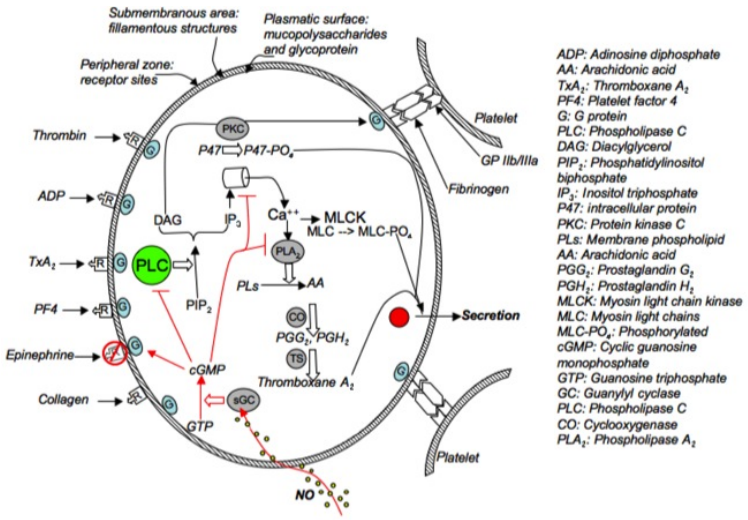

Figure 1.8: Intracellular nitric oxide-cyclic Guanosine Monophospate dependent pathway model that keeps platelets from activation

These reactions termed the NO/cyclic cGMP pathway are initiated by the activation of soluble guanylyl cyclase after NO binds to its heme centers [**75 - 76**]. Soluble guanylyl cyclase then hydrolyzes guanosine triphosphate (GTP) into 3', 5'- cGMP. To inhibit platelet activation, the activated cGMP prevents several of the intracellular platelet activation reactions from occurring [**77**]. It can phosphorylate G protein-coupled surface receptors of the platelet. Their phosphorylation results in a change in their conformation which disorients their binding sites to decrease binding affinities of agonists. Commonly known G protein-coupled receptors on the platelet include thrombin, thromboxane A2, and adenosine diphosphate receptors. Other ways that

cGMP helps inhibit platelet activation include blocking the activation of PLC, blocking the intracellular release of calcium, and blocking the activation of PLA2. The blocking mechanisms are important because PLC is required to initiate G-couple protein mediated platelet activation, calcium release is needed for actin-myosin interaction so that platelets can contract and release their granules and PLA2 is needed to synthesize the secreted clotting agent thromboxane A_2. Collectively, these effects on adhered platelets or those proximal to the source of NO production reduce secondary activation of circulating platelets.

As shown in Figure 1.8 NO produced by the endothelium can also end up binding to other NO scavengers like ceruloplasmin and hemoglobin in RBCs [**78 - 79**].

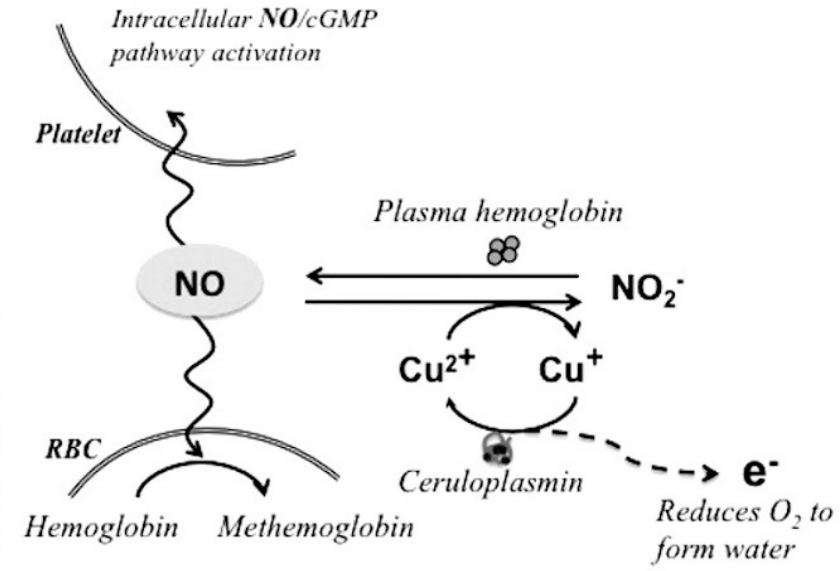

Figure 1.9: Fate of NO in blood. After production, NO can be taken up by platelets, RBCs, or oxidized into nitrites by ceruloplasmin, a multicopper oxidase concomitantly with cupric (Cu^{2+}) to cuprous (Cu^{+}) reduction. Perhaps, with other NO scavengers in plasma, only a fraction of the NO generated diffuses into platelets to activate the NO/cGMP pathway to inhibit platelet activation.

Therefore, the availability of NO to platelets not only depend on the quantity of NO produced by a surface but also on competitive binding to NO by other scavengers. Physiological reactions of NO with Hb during respiratory cycle in RBCs has shown

interesting dynamics contrary to the general knowledge of which NO irreversibly bind to Hb. In this model, NO binds to Hb, dissociates and gets transnitrosated to cysteine in a cycle as a mechanism for controlling the bioactivity of NO in blood vessels. These interactions occur during the journey of relaxed Hb (Hb fully saturated with oxygen) from arterioles back to arteries after crossing the lung. Transnitrosation occurs at the beta subunits of Hb so potentially in one cycle at least 50% of bound NO could be transferred to cysteines as 2 out of the 4 subunits of Hb are of the beta type [**80-83**].

The gas could also be oxidized into nitrites by ceruloplasmin, a plasma oxidase produced by the liver. Ceruloplasmin is a multicopper oxidase and converts NO into nitrite concomitantly with cupric (Cu^{2+}) to cuprous (Cu^{+}) reduction.

Ultimately, the different fates of NO reduces its immediate availability to platelets. The gas can however be recovered from blood thiol groups that received NO from Hb and from nitrates by catalytic decomposition and reduction reaction. It's important to also note that the gas will again be presented with the same fates all over again.

1.8 NO-releasing and NO-generating Polymers

As knowledge of NO inhibition of platelet activation expanded, it was only a matter of time until the multifaceted molecule found its way into blood-contacting materials. The first work on diazeniumdiolate NO donors incorporation in polymers was published in 1996 [**84**]. In the past decade however, published work in this research area has mainly focused on material synthesis optimization methods for controlled and sustained NO concentration at the blood/polymer interface. Polymers functionalized in attempts to impart those properties have been done by 1) entrapping of NO donors in their matrices, 2) doping their surfaces with catalysts to either catalyze endogenous NO donors or both endogenous and exogenous NO donors, and 3) tethering peptides that have high affinity for NO (e.g cysteine) onto their surfaces to direct transnitrosation towards the polymer.

Entrapment methods studied so far include direct dispersion of diazeniumdiolates ($N_2O_2^-$) in polymers, covalent attachment of the $N_2O_2^-$ either to side chain groups or to the backbone of the polymer, and dispersion of amines in the polymer followed by pressurising the polymer with NO in a high pressure atmosphere [**84-96**]. These different entrapment mechanisms, including covalent bonding of $N_2O_2^-$ to nano/micro spheres which are then dispersed in a polymer, are done to increase the NO storage capacity of polymers, and control the release of the gas.

In works involving entrapment of $N_2O_2^-$, Smith et al showed an NO flux of about 0.0001 x 10^{-10} mol/min/mg for 160 hrs from poly(caprolactone) doped with $N_2O_2^-$, Zhang et al [**95**]showed 4 x 10^{-10} mol/min/cm^2 for 4 hours from silicone rubber doped with DACA-6, Robbins et al [**96**]showed 3.6 x 10^{-10} mol/min/cm^2 for 24 h from sensors coated with sol-gel siloxanes previously doped with amines and pressurized under 5 atm of NO(g) for 24 h, Stasko et al [**94**] showed 5.6 μ mol/mg for 16 h from generation 5 dendrimers that were functionalized with amines and then pressurized with NO (5 atm), Riccio et al [**90**] showed 1.31 μ mol/mg (1 x 10^{-10} mol/min/cm^2) for 2 weeks from xerogels doped with NO using similar conditions, and later showed 4.39 μ mol/mg total release from nanometer silica particles modified with $N_2O_2^-$. These fluxes demonstrate the ability to functionalize polymers to release NO at levels comparable to that produced by the endothelium (0.4 - 5 x 10^{-10} mol/min/cm^2). However, these relatively short release duration do not to satisfy clinical requirements for long-term usage of NO releasing materials. They must be able to sustain endothelial levels of NO release for months, however the limited amount of $N_2O_2^-$ that blood-contacting devices can hold makes such long-term release a difficult challenge.

Other research groups have therefore investigated catalytic methods to extend the useful lifespan of these materials. This approach does not rely on storing NO inside the polymer but rather on catalysts to react with blood-borne or exogenous NO donors to

generate NO. The production of NO at the biomaterial's surface continuously occur as long as the catalyst and NO donor interaction remains intact. Oh et al [**97**] showed $\geq$ 1 x 10^{-10} mol/min/cm^2 NO flux from PVC doped with lipophilic Cu(II) complex using 0.5 mM nitrite as the NO donor and 1 mM ascorbate as the Cu(II) reducing agent, Cha et al [**98**]showed a 200 ppb NO generation from Polyethylenimine and 3, 3' dipropionicdiselenide mixed with selenium in solution phase using 0.5 mM EDTA as the NO donor and 250 mM GSH as the reducing agent, Hwang et al [**99**] showed 2 x 10^{-10} mol/min/cm^2 from polymethacrylate doped with lipophilic Cu(II), and Major et al [**100**]showed 12 x 10^{-10} mol/min/cm^2 from PVC doped with 10 wt% 80nm Cu(II) particles used for coatings on extracorporeal circulation circuits using 0.5 mM nitrosogluthation and 1 mM gluthathion. The fact that these catalytic methods also yield endothelial NO flux levels provides a potential solution for long term generation of NO.

Tethering of cysteine on biomaterials for production of NO at their surfaces via transnitrosation has been reported by Duan et al [**101**]. To measure transnitrosation, cysteine tethered polyethylene terephthalate films were exposed to bovine serum albumin-NO (BSA-NO) NO donor in 20 mM PBS for 3 hrs and the transnitrosation was measured by the drop in BSA-NO concentration BSA-NO concentration monitored. After 3 h, BSA-NO concentration decreased by 67% from 4.50 to1.5 μM indicating a transfer of NO from BSA to cysteine. Such surfaces have not produced high NO fluxes, as seen in a study published in 2010 by Kushwaha et al [**102**] where a flux of 0.019 x 10^{-10} mol/min/cm^2 was recorded. An new functionalization paradigm that is now receiving increased attention is the combination of NO and other endothelial-like properties like heparan sulfate and thrombomodulin. This research area, however, has not evolved enough to evaluate its potential. One such study that demonstrates this paradigm was conducted by the Zhou et al [**103**] group. They attempted this approach to some degree but much about their function is still a puzzle. Important

conclusions that can gathered from those *in vitro* studies are that, the activity of heparan sulfate and thrombomodulin diminishes when immobilized and longer chain linkages between the base polymer and tethered agent may improve activity. The effect of adding other functional groups on NO production at the biomaterials surface is yet to be fully evaluated.

The performance of the above NO functionalized surfaces in terms of flux levels and *in vitro* and *in vivo* are summarized in Table 1.5. These results collectively show that NO-functionalized polymers with higher levels of endothelial NO flux inhibited platelets activation more that polymers with low NO flux levels. For instance, as shown in Figure 1.10, surfaces that released $\geq 1\text{x}10^{-10}$ mol/min/cm^2 of NO showed a significant inhibition of clot formation compared to non-NO releasing controls after 16 h implantation in porcine arteries [**104**].

Table 1.5: Nitric oxide (NO) flux levels and inhibition of platelet activation by NO releasing/generating polymers

Test duration (h, h*)	**Average NO flux (x10^{-10} mol/min/cm^2)**	**Effect on Platelets (control/NO polymer)**	**REF**
160,1**in vivo*	0.0001	2.5/0.25 billion ^{a,1}	[84]
4,4**in vivo*	4	35±5/14±3%^{a,2}	[95]
24,24**in vitro*	3.6	120± 47/28±18% coverage ^{b,3}	[96]
16, —	5.6 μ mol/mg	—	[94]
336,1**in vitro*	1.31μ mol/mg	205±64/149±8 ^{a,4}	[90]
0.5, —	4.39μ mol/mg	—	[93]
NA, –	≥ 1	—	[97]
NA, —	200ppb (liquid sample)	—	[98]
NA, —	2	—	[99]
NA, 4**in vivo*	12	42.5±4.3/15±2 % ^{a,2}	[100]
30, 48**in vitro*	0.019	73000±22000/470±220 ^{a,5}	[102]

h,h* : Test durations for NO flux, and material biocompatibility

^{3} : Platelet coverage measured by percent opaqueness in a 167x167 μm^2 image area relative to glass control

^{1} : Platelets deposited, ^{2} : Platelets lost, ^{4}: Adhered platelets, ^{4}: Adhered platelets/ cm^2

NA : No NO production limit on NO generating sample, ^{a}: p<0.05, ^{b}: p<0.001

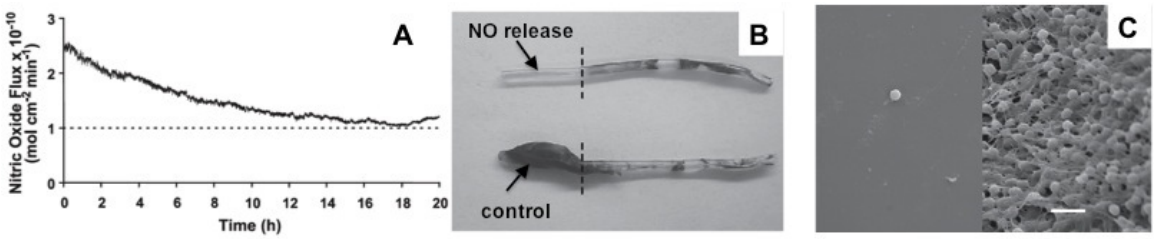

Figure 1.10: NO flux profile (A) of an electrochemical oxygen sensing catheter coated with DACA-6/$N_2O_2^-$/silicone rubber. NO release was measured via chemiluminescence in PBS buffer (pH 7.4) at 378C. Representative digital (B) and SEM (C) images of DACA6/N2O2SR-coated sensors and control sensors after implantation in porcine arteries for 16 h[**104**].

1.9 Sweep Gas Nitric Oxide for Artificial Lungs

Previous methods of functionalizing biomaterials with NO via entrapping finite amounts NO donors and by means of catalytic decomposition of endogenous NO donors involve a chemical modification of the biomaterial. These methods have not yet been applied to artificial lungs as fiber fabrication is a highly specialized process. The application of such methods to artificial lungs requires a merger of industrial type facilities and engineering/chemistry expertise currently unique to the academic setting. With blood clotting in artificial lungs still a problem, an easier alternative for supplying NO to the biomaterial surface is delivering NO gas directly to the sweep gas. In this approach, NO gas is flowed simultaneously with oxygen into oxygenators in order to reduce clot formation inside the device.

A wide range of sweep gas NO concentrations have been supplemented in sweep gas to reduce platelet adhesion, activation, and coagulation within oxygenators *in vitro* and *in vivo* with mixed results. Platelet inhibition by low sweep gas NO concentrations have shown mostly positive results *in vitro* and negative ones *in vivo*. Results from *in vivo* studies conducted using higher sweep gas NO concentrations (>500ppm) have, however, trended towards higher significance in terms of inhibiting

blood anticoagulation.

Mellgren et al [**105**] evaluated the non-thrombogenecity of extracorporeal circulation circuits during heparinized blood flow through a (Dideco D-901 hollow fiber oxygenator) for 24 h using three different sweep gas concentrations (15, 40, and 75 ppm) that were infused at 0.6 L/min. Plasma nitrate, cyclic guanosine monophosphate, and platelet count were significantly higher and Beta thromboglobulin was significantly lower in the NO circuits than in the control circuits ($p<0.01$). No difference was observed in platelets serotonin content and membrane glycoprotein Ib density between circuits. There were no dose-response effects in all measured variables for the NO concentrations tested. Similar positive results using low sweep gas NO concentration (20ppm) were also reported by Keh et al 1999 [**106**]. In their study, the NO gas was supplied into M18 Jostra oxygenators in a simulated ECMO circuit primed with 1IU/ml heparinized blood. Platelet count, betathromboglobulin, and methemoglobin concentrations were monitored in the circulating blood (0.6 L/min) for 4h. Platelet count and methemoglobin concentrations were significantly higher ($p<0.01$) in NO group than in controls. Betathromboglobulin was also significantly lower in the NO group ($p<0.05$).

In an *in vivo* study conducted by Lowson et al. such positive results seen in the above *in vitro* low-dose NO settings were not observed even at a slightly higher sweep gas NO concentration of 100ppm. Inhibition of platelet activation in membrane oxygenators attached to 47 CPB patients was no significantly different from controls. Furthermore, NO had no effect on betathromboglobulin concentration and bleeding. Methemoglobin concentration also remained below 4% in both NO and control groups during the 3 h procedure [**107**]. In a different study where 500ppm sweep gas NO concentration was used in swine undergoing CPB, platelet adherence and aggregation decreased compared to their controls ($p<0.05$) [**108**]. NO also had no effect on blood flow, mean arterial pressure, and hematocrit concentration. A summary of these

studies and other relevant work indicating sweep gas NO concentration and their effect on blood clotting is presented in Table 1.6.

Table 1.6: Effect of sweepgas NO concentrations on blood coagulation

Sweepgas NO concentration (ppm)	**Test duration** (h, setting)	**Inhibition of blood coagulation** (control/NO sweep)	**REF**
15, 40, 75	24, *in vitro*	162/175 x 10^{11} ^{Pct,**} 2000/2600 (IU/ ml) ^{bTG}	[105]
20	4, *in vitro*	50/72% ^{Pct,**} 3000/2500 (IU/ ml) ^{bTG,*} 1.25±.07→1.38±.06/1.43±.05→3.5±.23 (IU/ ml) ^{metHb,**}	[106]
80 (in O_2)	6, *in vivo*	5.78±3.8/0.54±0.41% ^{Sc,*} 62/58 (%) ^{Pct,*}	[107]
40	3, *in vivo*	60/60% ^{Pct} 100/100% ^{Pfunc} <1%/<1% ^{metHb}	[108]
100	3, *in vivo*	<1%/<4% ^{metHb} 153±32/178±57 x$10^3/\mu$L % ^{Pct,*}	[109]
500, 1000	1.5, *in vivo*	2/0.2 x 10^{11} ^{Pct,*} <1%/4% at 500ppm and 8% at 1000ppm ^{metHb}	[110]

^{Pct,**} : Platelet count, p<0.01, ^{bTG} : Beta-thromboglobulin, ^{Sc,*} : Surface coverage, p<0.05

^{Pfunc} : Platelet function, ^{metHb} : methemoglobin

The mixed results may be due to wide variations from study to study in NO concentrations, oxygenator types, blood flow rates, and in vitro and in vivo models. The *in vivo* models were all CPB models, a procedure accompanied with a substantial amount of biomaterial-independent platelet activation. So evaluating sweep gas NO

concentration using only a CPB model, perhaps, doesn't effectively access the anticoagulatory effect of the NO gas. Each of the factors above is, however, likely to affect NO flux rates from the gas exchange membrane. These flux rates have never been measured or modeled, making interpretation of the results difficult. A visit back to the drawing board to investigate what sweep gas NO concentration would produce endothelial levels of NO flux in various commercially available oxygenators is a good metric for evaluating NO's anti-coagulatory performance.

1.10 Summary of the Study

In brief, this study presents a motivation behind the need to explore alternative methods for controlling thrombus formation on blood-contacting biomaterials. Especially, coagulation on artificial surfaces, clinical consequences of clotting for various artificial devices, current methods used to control clotting, the current state of long-term use of respiratory support devices (oxygenators), the potential of nitric oxide releasing and generating surfaces and in sweep gas for controlling thrombus formation on blood-contacting surfaces, and future biomaterials are addressed in Chapter I. For research work involving biocompatibility testing of the gas exchange membranes of oxygenators, NO generation via catalytic decomposition of endogenous NO donors and sweep gas NO were selected a the methods for surface functionalization with NO. These methods allow for long-term release of NO and thus may work for long-term respiratory support. NO donor entrapment method was utilized in the catheter research work to lay a foundation for optimizing catheters for a long term NO release and non-thrombogenecity testing.

Chapter II explores the synthesis and characterization of NO generating silicone for use as a blood-contacting biomaterials. In this alternate approach, copper at the biomaterial surface is utilized to generate NO from donors within the blood flow. Surfaces with various copper concentrations were characterized for NO flux, clotting

times, and platelet adhesion. The applicability and limitations of the NO-generating surface are also presented.

With knowledge gained from Cu-mediated NO generation from silicone membranes, Chapter III explores the application of Cu catalyst to hollow silicone fibers for NO generation. In brief the development and NO flux characterization of hollow silicone fibers are presented here. Small diameter fibers were extruded to incorporate various Cu particle sizes and different particle distribution using similar manufacturing conditions used in industry. Their NO generation as a function of particle size and distribution was evaluated so that the best combination of particle size and distribution may be used for developing the first NO-generating artificial lung.

In the next chapter, Chapter IV, our in-house material synthesis conditions were carried over for the fabrication of gas-exchange hollow silicone fibers that can also generate NO at Medarray Inc. facilities. NO flux from these fibers was characterized before fabricating the first NO-generating oxygenator prototypes. The prototypes were evaluated for their thrombogenicity against non-NO-generating controls in an extracorporeal circulation thrombogenecity model using a tip-to-tip coated circuits and adult rabbits. In brief this chapter provides the first thrombogenicity outcomes of a Cu-mediated NO-generating oxygenators.

Chapter V explores the application of NO-donor dispersion approach for NO release, as opposed to NO generation, to small diameter silicone catheters. The chemistry of NO-releasing material synthesis, NO-releasing catheter fabrication and their non-thrombogenicity were characterized *in vivo* using a thrombogenic rabbit model. Specifically, the thrombogenicity of controls (non NO-releasing) are compared to NO-releasing catheters in a 4h study. This chapter provides a fabrication method for developing NO-releasing catheters, a thrombogenicity testing regiment and points the way forward for long-term NO-releasing catheter fabrication and testing.

NO releasing and generating methods of functionalizing blood-contacting surfaces

show a promising future. However what if we can bypass the chemistry involved by just purfusing artificial lungs with commercial sweep gas NO? With a wide range of sweep gas NO concentration tested with mixed results, Chapter VI, explores the use of nitric oxide sweep for reducing thrombus formation in oxygenators by characterizing the nitric oxide flux in two different commercial oxygenators *in vitro*. Estimation of NO flux across clinical oxygenator membranes are made for several nitric oxide sweep gas concentrations. This study provides a better estimate of what sweep gas NO concentration will yield endothelial NO flux levels for starters. This results may find importance in nitric oxide sweep gas studies where flux control is pertinent.

Finally Chapter VII discusses contributions, limitations, and future works.

1.11 Reference

1. Ereth MH, Nuttall GA, Clarke SH, Dearani JA, Fiechtner BK, Rishavy CR, et al. Biocompatibility of trillium biopassive surface-coated oxygenator versus uncoated oxygenator during CBP. Journal of Cardiothoracic and Vascular Anesthesia **2001**, 15 (5): 545-550

2. Stammers AH. Biocompatibility of trillium biopassive surface-coated oxygenator during cardiopulmonary bypass. Journal of Cardiothoracic and Vascular Anesthesia **2001**, 15(5): 539-541

3. Vijay V and Kevin F. Recent advances in biocompatible surface-modifying additives for cardiopulmonary bypass. Perfusion **2003**, 18:41-45

4. Hsu LC: Issues of biocompatibility: Heparin-coated extracorporeal circuit. Int Anesth Clin **1996**, 34:109-122

5. Boudko DY. Bioanalytical profile of the L-arginine/nitric oxide pathway and its evaluation by capillary electrophoresis. Journal of Chromatography B **2007**, 851:186-210

6. Murad F. Discovery of some of the biological effects of nitric oxide and its role in cell signaling. Bioscience Reports **1999**, 19: 453-474

7. Napoli C, De Nigris F, Williams-Ignarro S, Pignalosa O, Sica V and Ignarro L J. Nitric oxide and atherosclerosis: An update. Nitric Oxide **2006**, 15: 265-279

8. Rabelink TJ and Luscher TF. Endothelial nitric oxide synthase, host defense en-

zyme of the endothelium? Arterioscler Thromb Vasc Biol **2006**, 26: 267-271

9. Colman RW, Hirsh J, Marder VJ, Clowes AW, and George NJ. **(2001)** Hemostasis and Thrombosis: Basic Principles & clinical Practice, 4th Edition: Lippincott Williams & Wilkins, Philadelphia, PA, USA.

10. Walter JC. **(1976)** Blood vessels: Biological structure and function:6 Cambridge University Press, Cambridge, UK

11. Kwaan HC and Walter Bowie EJ. **(1982)**Thrombosis: W.B. Saunders Company, Philldelphia, PA, USA.

12. Sato H, Griffith GW, Hall CM, Toomasian JM, Hirschl RB, Bartlett RH and Cook KE. Seven-Day Artificial Lung Testing in an In-Parallel Configuration, Ann Thorac Surg **2007**, 84:988-994

13. J. Murphy, C. Savage, S. Alpard, D. Deyo, et al. Low-dose versus high-dose heparinization during arteriovenous carbon dioxide removal Perfusion. **2001**, 16(6); 460-468

14. Rapaport SI and Rao VM. Initiation and regulation of the tissue factor-dependent blood coagulation. Arterioscler Thromb **1992**,12:1111-1121

15. Lee LY, Debois W, Krieger KH, Girardi LN et al. The effects of platelet inhibitors on blood use in cardiac surgery. Perfusion **2002**, 17(1); 33-37

16. Chun R, Orser B A, Madan M. Platelet glycoprotein IIb/IIIa inhibitors: overview and implications for the anesthesiologist. Anesthesia and analgesia **2002**, 95(4):879-

88

17. Kidane AG, Salacinski H, Tiwari A, Bruckdorfer KR and Seifalian AM. Anticoagulant and antiplatelet agents: their clinical and device application(s) together with usages to engineer surfaces. Biomacromolecules **2004**, 5: 798-813

18. Lemmer JH and Vlahakes GJ. **(2010)** Handbook of Patient Care in Cardiac Surgery, 7th Edition Lippincott Williams & Wilkins, Philadelphia, PA, USA

19. Ali A, Hashem M, Rosman HS, Moser L, Rehan A, Davis T, et al. Glycoprotein IIb/IIIa receptor antagonists and risk of bleeding: a single-center experience in 1020 patients. Journal of Clinical Pharmacology **2004**, 44(11): 1328-1332

20. LaBan MM, Whitmore CE, Taylor RS. Bilateral adrenal hemorrhage after anticoagulation prophylaxis for bilateral knee arthroplasty. Am J Phys Med Rehabil **2003**, 82:418-420

21. Campbell BT, Braun T, Schumacher R, Bartlett RH, Hirschl RB. Impact of ECMO on neonatal mortality in Michigan (1980-1999). J Ped Surg **2003**, 38(3):290-295

22. Bartlett RH, Roloff DW, Custer JR, Younger JG, Hirschl RB. Extracorporeal Life Support. The university of michigan experience. JAMA **2000**, 283(7):904-908

23. Lee JH, et al. Blood compatibility of polyethylene oxide surfaces. Prog Polym Sci **1995**, 20:1043-1079.

24. Lee JH, et al. Platelet adhesion onto segmented polyurethane film surfaces modified by addition and crosslinking of PEO-containing block copolymers. Biomaterials **2000**, 21:683-691

25. Hayward JA, Chapman D. Biomembrane surfaces as models for polymer design: the potential for hemocompatibility. Biomaterials **1984**, 5:135-142.

26. Mejak BL, Stammers AH, Rauch E, et al: A retrospective study on perfusion incidents and safety devices. Perfusion **2000**, 15:51-61

27. Larson DF, Arzouman D, Kleinert L, Patula V and Williams S. Comparison of Sarns 3M heparin bonded to Duraflo II and control circuits in a porcine model: macro- and microanalysis of thrombi accumulation in circuit arterial filters. Perfusion **2000**, 15:13-20

28. Larm O, Larsson R, Olsson P. Biomater. Med. Devices Artif. Organs **1983**, 11: 161-173.

29. Tayama E, Hayashida N, Akasu K, Kosuga T, Fukunaga S, Akashi H, Kawara T, Aoyagi S. Artif. Organs **2000**, 24:618-623.

30. Engbers GH, Feijen J. Int. J. Artif. Organs **1991**, 14:199-215.

31. Palanzo DA, Zarro DL, Manley NJ, Montesano RM, Quinn M, Elmore BA, Gustafson PA, Castagna JM. Effect of Carmeda-BioActive surface coating versus TrilliumTM Biopassive surface coating Bypass coating of the oxygenator on circulating platelet count drop during cardiopulmonary bypass. Perfusion **2001**; 16; 279-283

32. Hoel TN, Videm V, Baksaas ST, Mollnes TE, Brosstad F and Svennevig JL. Comparison of a Duraflo II-coated cardiopulmonary bypass circuit and a trillium-coated oxygenator during open-heart surgery. Perfuaion **2004**, 19: 177-84

33. Babapulle MN, Eisenberg MJ. Coated stents for the prevention of restenosis: Part I. Circulation **2002**, 106:2734-2740

34. Yoshinari Niimi, Fumito Ichinose, Yoshiki Ishiguro, Katsuo Terui, Shoichi Uezono, Shigeho Morita,and Shingo Yamane. The Effects of Heparin Coating of Oxygenator Fibers on Platelet Adhesion and Protein Adsorption. Anesth Analg **1999**, 89:573-9

35. I Fluger, K Maderov, M Simek, R Hjek, J Zapletalov and V Lonsk? . The effect of a cardiopulmonary bypass system with biocompatible coating on fibrinogen levels determined by the TEG - functional fibrinogen method: preliminary results. Perfusion **2001**, 20(10): 1-7.

36. Masaru Tanaka, Tadahiro Motomura, Miho Kawada, Takao Anzai, Yuu Kasori, Toshifumi Shiroya, Kenichi Shimura, Makoto Onishi, Akira Mochizuki. Blood compatible aspects of poly(2-methoxyethylacrylate) (PMEA)-relationship between protein adsorption and platelet adhesion on PMEA surface Biomaterials 21 **2000** 1471-1481

37. M. Kocakulak, C. Kocum, R. Saber, H. Ayhan, S. Gunaydin, T. Sari and Y. Zorlutuna, N. Bingol. Journal of Bioactive and compatible polymers, **2002**, 17:343-356.

38. U. Demirkilic, E. Kuralay, Y H. Tatar, M. Kocakulak, C. Kocum, H. Ayhan. Investigation of Blood Compatibility and Determination of Clinical Performance of PMEA Coated and Flow Optimized Oxygenator. Journal of Bioactive and compatible polymers, **2002**, 19:395-408.

39. Joseph Noora, Andre Lamy, Kelly M Smith, Rosanne Kent, Dianne Batt, John Fedoryshyn and Xiaoyin Wang. The effect of oxygenator membranes on blood: a comparison of two oxygenators in open-heart surgery. Perfusion **2003**,18: 313-320.

40. Jeanette M van den Goor, Willem van Oeveren, Peter M Rutten, Jan G Tijssen and Len Eijsman. Adhesion of thrombotic components to the surface of a clinically used oxygenator is not affected by Trillium coating Perfusion **2006**, 21: 165-172

41. F De Somer, Y Van Belleghem, F Caes, K Franois, J Arnout, X Bossuyt, Y Taeymans and G Van Nooten. Phosphorylcholine coating offers natural platelet preservation during cardiopulmonary bypass. Perfusion **2002** 17: 39-44

42. PA Farneti, S Sbrana, D Spiller, AG Cerillo, F Santarelli, D Di Dario, PA Del Sarto and M Glauber. Extracorporeal circulation system (Synergy) in coronary artery bypass grafting (CABG) Reduction of blood coagulation and monocyte-platelet interaction following the use of a minimal. Perfusion **2008**; 23: 4956

43. E De Stefano, D Delay, J Horisberger and LK von Segesser. Initial clinical experience with the admiral oxygenator combined with separated suction. Perfusion **2008**; 23: 209213

44. Jean-Olivier Defraigne, Joe l Pincemail, Guy Dekoster, Robert Larbuisson, Myriam Dujardin, Francine Blaffart, Jean-Louis David, and Raymond Limet. SMA circuits reduce patelet consumption and platelet factor release during cardiac surgery. Ann Thorac Surg **2000**;70:2075 81

45. T Nishinaka, E Tatsumi, N Katagiri, T Mizuno, T Tsukiya, S Kashiwabara and M Sato. Up to 151 days of continuous animal perfusion with trivial heparin infusion by the application of a long-term durable antithrombogenic coating to a combination of a seal-less centrifugal pump and a diffusion membrane oxygenator. J Artif Organ **2007**;10:240-244.

46. David A Palanzo, Debra L Zarro, Norman J Manley, Ralph M Montesano, Michael Quinn, Barbara-Anne Elmore, Patricia A Gustafson and Joseph M Castagna. Effect of Carmeda BioActive Surface coating versus Trillium Biopassive Surface coating of the oxygenator on circulating platelet count drop during cardiopulmonary bypass Perfusion **2001**; 16: 279-283

47. Hoel TM, Videm V, Baksaas ST, Mollnes TE, Brosstad F, and Svennevig JL. Comparison of a Duraflo II - coated cardiopulmonary bypass circuit and a trillium-coated oxygenator during open-heart surgery. Perfusion **2004**; 19:177-184

48. Douglas F Larson, David Arzouman, Leigh Kleinert, Vangie Patula and Stuart Williams. Comparison of Sarns 3M heparin bonded to Duraflo II and control circuits in a porcine model: macro- and microanalysis of thrombi accumulation in circuit arterial filters Perfusion **2000**; 15:13-20

49. AS Thiara, VY Andersen, V. Videm, TE Mollnes, K. Svennevig, TN Hoel and

AE Fiane. by the inflammatory response Comparable biocompatibility of Phisio- and Bioline-coated cardiopulmonary bypass circuits indicated. Perfusion **2010**; 25: 9-16

50. S Jacobs, F De Somer, G Vandenplas, Y Van Belleghem, Y Taeymans and G Van Nooten. Active or passive bio-coating: does it matters in extra-corporeal circulation? Perfusion 2011; 20: 1-7

51. AS Thiara, TE Mollnes, V. Videm, VY Andersen, K. Svennevig, SO Kolset and AE Fiane. Biocompatibility and pathways of initial complement pathway activation with Phisio- and PMEA-coated cardiopulmonary bypass circuits during open-heart surgery. Perfusion **2011**; 26: 107-114

52. Serdar Gunaydin. Clinical significance of coated extracorporeal circuits: a review of novel technologies. Perfusion **2004**; 19: S33-S41

53. J. Marcoux, N. Sohn, E. McNair, M. Rosin, G. Smith, H. Lim, T. Mycyk and Q. Meng. of patients undergoing cardiac surgery Outcomes comparison of 5 coated cardiopulmonary bypass circuits versus an uncoated control group. Perfusion **2009**, 24;307-315

54. Bader E. Hussaini, Patrick R. Treanor, Nancy A. Healey, Daniel Tilahun, Rithy Srey, Xiu-Gui Lu, Shukri F. Khuri and Hemant S. Thatte. Evaluation of blood components exposed to coated arterial filters in extracorporeal circuits. Perfusion **2009** 24: 317-323

55. Nojiri C, Hagiwara K, Yokoyama K et al. Evaluation of a New Heparin Bond-

ing Process in Prolonged Extracorporeal Membrane Oxygenation. ASAIO. 1995; 41: M561-M567

56. Matsuwaka R, Matsuda H, Kaneko M et al. Experimental evaluation of a heparin coated ECMO system simplified with a centrifugal pump. ASAIO Trans. 1990; 36: M473-M475

57. Palmer K, Ehren H, Benz R, Frenckner B. Carmeda surface heparinization in neonatal ECMO systems: long-term experiments in a sheep model. Perfusion. 1995; 10: 307-13

58. Stenach N, Korn RL, Fisher CA, Jeevanandam V, Addonizio VP. The effects of heparin bound surface modification (Carmeda Bioactive Surface) on human platelet alterations during simulated extracorporeal circulation. J Extra-Corpor Technol **1992**, 24: 97-102

.

59. Hatori N, Yoshizu H, Haga Y et al. Biocompatibility of heparin-coated membrane oxygenator during cardiopulmonary bypass. Artif Organs **1994**, 18: 904-910

60. Spiess BD, Vocelka C, Cochran RP, Soltow L, Chandler WL. Heparin-coated bypass circuits (Carmeda) suppress the release of tissue plasminogen activator during normothermic coronary artery bypass graft surgery. J Cardiothorac Vasc Anesth **1998**, 12: 299-304

61. Zhang Z, Zhang M, Chen S, Horbert TH, Ratner BD and Jiang S. Blood compatibility of surfaces with superlow protein adsorption Biomaterials **2008**, 29:42854291

62. Rodrigues SN, Goncalvesa IC, Martinsa MCL, Barbosa MA, Ratner BD. Fibrinogen adsorption, platelet adhesion and activation on mixed hydroxyl-methyl-terminated self-assembled monolayers. Biomaterials **2006**, 27:5357-5367

63. Lai BFL, Creagh AL, Janzen J, Haynes CA, Brooks DE, Kizhakkedathu JN. The induction of thrombus generation on nanostructured neutral polymer brush surfaces. Biomaterials **2006**, 31(26): 6710-6718

64. Gao G, Lange D, Hilpert K, Kindrachuk J, Zou Y, Cheng JTJ, Kazemzadeh-Narbat M, Yu K, Wang R, Straus SK, Brooks DE, Chew BH, Hancock REW and Kizhakkedathu JN. The biocompatibility and biofilm resistance of implant coatings based on hydrophilic polymer brushes conjugated with antimicrobial peptides. Biomaterials **2011**, 32(16): 3899-3909

65. Hartmann A, Nordal KP, Svennevig JL. Successful use of artificial lung (ECMO) and kidney in the treatment of a 20-year-old female with Wegeners syndrome. Nephrol Dial Transplant **1994**, 9: 316-19

66. Zwischenberger JB, Anderson CM, Cook KE, Lick SD, Mockros LF and Bartlett RH. Development of an Implantable Artificial Lung: Challenges and Progress. ASAIO **2001**, 47(4) 316-320

67. Angelica Oung (2008-01-31). "Patient recovers after 117 days of ECMO treatment". Taipei Times. Retrieved 05-29-2011

68. Gaylor JDS, Hickey S, Bell G and Pei JM. Membrane oxygenators: influence

of design on performance. Perfusion **1994**, 9: 173-80

69. Puis L, Ampe L and Hertleer R. Case report: plasma leakage in a polymethylpentene oxygenator during extracorporeal life support. Perfusion **2009**, 24:51-52

70. Nathan CF, Hibbs JB Jr. Role of nitric oxide synthesis in macrophage antimicrobial activity. Curr Opin Immunol **1991**, 3:65-70

71. Xu WM, Liu LZ. Nitric oxide: from a mysterious labile factor to the molecule of the Nobel Prize. Recent progress in nitric oxide research. Cell Res. **1998**, 8(4):251-258

72. Stuehr DJ, Kwon NS, Nathan CF, Griffith OW, Feldman PL, Wisean J. N omega-hydroxy-L-arginine is an intermediate in the biosynthesis of nitric oxide from L-arginine. J Biol Chem **1991**, 266: 6259-263

73. Gnarro IJ. Biosynthesis and metabolism of endothelium-derived nitric oxide. Annu Rev Pharmacol Toxicol **1990**, 30:535-560

74. Rapoport RM, Draznin MB, Murad F. Endothelium-dependent relaxation in rat aorta may be mediated through cyclic GMP-depedent protein phospharylation. Nature **1983**, 306:174-176

75. Palmer RM, Ferrige AG, Moncada S. Nitric oxide release accounts for the biological activity of endothelium-derived relaxing factor. Nature **1987**, 337:524-526

76. Howlett R. Nobel award stirs up debate on nitric oxide breakthrough. Nature **1998**, 395:625-626

77. Stamler S J, Singel J D, Loscalzo J. Biochemistry of nitric oxide and its redox-activated forms. Science, New Series **1992**, 258(5090): 1898-1902

78. Samuel TK. And Gitlin JD. Copper and nitric oxide meet in the plasma. Nature Chemical Biology **2006**, 2:452-453

79. Shiva S, Wang X, Ringwood LA, Xu X, Yuditskaya S, Annavajjhala V, Miyajima J, Hogg N, Harris ZL, and Gladwin MT. Ceruloplasmin is a NO oxidase and nitrite synthase that determines endocrine NO hemeostasis. Nature Chemical Biology **2006**; 2:486-93

80. Gow AJ, Luchsinger BP, Pawloski JR, Singel DJ, Stamler JS. **1999**. Proc Natl Acad Sci USA 96:v9027-9032

81. Jia L, Bonaventura C, Bonaventura J, Stamler J S. **1996** Nature (London) 380: 221-226

82. Gow, A. J. & Stamler, J. S. **1998** Nature (London) 391, 169-173

83. Stamler, J. S., Jia, L., Eu, J. P., McMahon, T. J., Demchenko, I. T.,Bonaventura, J., Gernert, K. & Piantadosi, C. A. **1997** Science, 276: 2034-2037

84. Smith DJ, Chakravarthy D, Pulfer S, Simmons ML, Hrabie JA, Citro ML, Saavedra JE, Davies KM, Hutsell TC, Mooradian DL, Hanson SR, Keefer LK. Nitric oxide

releasing polymers containing the NONO Group. J MedChem 1996;39:1148-56

85. Mowery KA, Schoenfsch MH, Saavedra JE, Keefer LK and Meyerhoff ME. Preparation and characterization of hydrophobic polymeric films that are thromboresistant via nitric oxide releas. Biomaterials 21 **2000**; 9-21

86. Reynolds MM, Frost MC, and Meyerhoff ME. Mechanisms and Novel Directions in the Biological Applications of Nitric Oxide Donors. Free Radical Biology & Medicine **2004**; 37: 926-936

87. Bohl KS and West JL. Nitric oxide-generating polymers reduce platelet adhesion and smooth muscle cell proliferation. Biomaterials **2000**;21:2273-2278

88. Major TC, Brant DO, Reynolds MM, Bartlett RH, Meyerhoff ME, Handa H, and Annich GM. The attenuation of platelet and monocyte activation in a rabbit model of extracorporeal circulation by a nitric oxide releasing polymer. Biomaterials **2010**; 31:2736-2745

89. Seabra AB and De Oliveira G. Poly(vinyl alcohol) and poly(vinyl pyrrolidone) blended films for local nitric oxide release. Biomaterials **2004**; 25:37733782

90. Riccio DA, Dobmeier KP, Hetrick EM, Preivett BJ, Paul HS, and Schoenfisch MH. Nitric oxide-releasing S-nitrosothiol-modified xerogels. Biomaterials **2009**;30: 4494-4502

91. Coneski PN, Nash JA, and Schoenfisch MH. Nitric Oxide-Releasing Electrospun Polymer Microfibers. ACS Appl. Mater. Interfaces **2011**;3: 426-432

92. Regev-shoshani G, Ko M, Miller C and Av-Gay Y. Slow Release of Nitric Oxide from Charged Catheters and Its Effect on Biofilm Formation by Escherichia coli. Antimicrobial agents and chemotherapy, **2010**; 54:273-279

93. Riccio DA, Nugent JL, and Schoenfisch MH. Stober Synthesis of Nitric Oxide-Releasing S-Nitrosothiol-Modified Silica Particles. Chem. Mater. **2011**; 23: 1727-1735

94. Stasko NA and Schoenfisch MH. Dendrimers as a Scaffold for Nitric Oxide Release. J. AM. CHEM. SOC. **2006**; 128: 8265-8271

95. Zhang H, Annich GM, Miskulin J, Osterholzer K, Merz SI, Bartlett RH, and Meyerhoff ME. Nitric oxide releasing silicone rubbers with improved blood compatibility: preparation, characterization, and in vivo evaluation. Biomaterials **2002**;23:1485-1494

96. Robbins ME and Mark H. Schoenfisch MH. Surface-Localized Release of Nitric Oxide via Sol-Gel Chemistry. J. AM. CHEM. SOC. **2003**; 125: 6068-6069

97. Oh BK and Mark E. Meyerhoff ME. Catalytic generation of nitric oxide from nitrite at the interface of polymeric films doped with lipophilic Cu(II)-complex: a potential route to the preparation of thromboresistant coatings. Biomaterials **2004**; 25: 283-293

98. Cha W and Meyerhoff ME. Catalytic generation of nitric oxide from S-nitrosothiols using immobilized organoselenium species. Biomaterials **2007**;28: 19-27

99. Hwang S and Meyerhoff ME. Polyurethane with tethered copper(II)ecyclen com-

plex: Preparation, characterization and catalytic generation of nitric oxide from S-nitrosothiols. Biomaterials 29 **2008**;29: 2443-2452

100. Major TC, Brant DO, Burney CP, Amoako KA, Annich GM, Meyerhoff ME, Handa H, and Bartlett RH. The hemocompatibility of a nitric oxide generating polymer that catalyzes S-nitrosothiol decomposition in an extracorporeal circulation model. Biomaterials **2011**;32: 5957-5969

101. Duan X and Lewis RS. Improved haemocompatibility of cysteine-modified polymers via endogenous nitric oxide. Biomaterials **2002**;23: 1197-1203

102. Meenakshi Kushwaha M, Anderson JM, Bosworth CA, Andukuri A, Minor WP, Lancaster JR, Anderson JE, Brott BC, and Jun H. A nitric oxide releasing, self assembled peptide amphiphile matrix that mimics native endothelium for coating implantable cardiovascular devices. Biomaterials **2010**;31: 1502-1508

103. Zhou Z and Meyerhoff ME. Preparation and characterization of polymeric coatings with combined nitric oxide release and immobilized active heparin. Biomaterials **2005**; 26:6506-6517

104 Reynolds M, Frost MC, and Meyerhoff ME. Nitric oxide-releasing hydrophobic polymers: preparation,characterization, and potential biomedical applications. Free Radical Biology & Medicine, **2004**; 37: 926-936

105. Mellgren K, Friberg LG, Mellgren G, Hedner T, Wennmalm A, and Wadenvik H., Nitric oxide in the oxygenator sweep gas reduces platelet activation during experimental perfusion. The Annals of Thoracic Surgery.**1996**;6:1194-8

106. Keh D, Gerlach M, Kurer I et al. Nitric oxide diffusion across membrane lungs protectsplatelets during simulated extracorporeal circulation. European Journal of Clinical Investigation 1999; 29: 344350

107. Tevaearai HT, Mueller XM, Tepic S, Cotting J, Boone Y, P.M. Montavon PM, and Von Segesser LK., Nitric Oxide Added to the Sweep Gas Infusion Reduces Local Clotting Formation in Adult Blood Oxygenators. ASAIO., 2000 46: p. 719-22

108. Mellgren K, Mellgren G, Lundin S, Wennmalm A, and Wadenvik H., Effect of Nitric Oxide Gas on Platelets During Open Heart Operations. Ann Thorac Surg., 1998 65: p.1335 41

109. Lowson SM, Hassan HM, and Rich GF., The Effect of Nitric Oxide on Platelets When Delivered to the Cardiopulmonary Bypass Circuit. Anesth Analg.**1999**;89:136-5

110. Sly MK, Prager MD, Li J, Harris FB, Shastri P, Bhujle R, Chao R, Kulkarni PV, Constantinescu A, Jessen ME, and Eberhart RC. Platelet and Neutrophil Distributions in Pump Oxygenator Circuits: Influence of Nitric Oxide Gas Infusion. ASAIO journal **1996**; 42: 494-99

CHAPTER II

SYNTHESIS AND CHARACTERIZATION OF NITRIC OXIDE-GENERATING SILICONE FOR USE AS A BLOOD-CONTACTING BIOMATERIAL

2.1 Abstract

Coagulation upon blood-contacting biomaterials remains a problem for clinical applications lasting anywhere from hours to years. The following study examined the ability of copper(II)-doped silicone surfaces to generate nitric oxide (NO) and inhibit coagulation at the biomaterial surface. Silicone was doped with 3-micron elemental copper (Cu) particles yielding 3, 5, 8, and 10 weight percent (wt%) Cu in 70 μm thick Cu/Silicone polymeric matrix composites (Cu/Si Polymetric matrice composite (PMC)s). At 3, 5, 8 and 10 wt% Cu doping, the surface expression of Cu was 12.1 $\pm$ 2.8%, 19.7 $\pm$ 5.4%, 29.0 $\pm$ 3.8%, and 33.8 $\pm$ 6.5% respectively. Cu expressed on the PMCs surfaces was observed to primarily coalesced into dendrites. After oxidizing elemental Cu to Cu(II) by spontaneous corrosion the surface NO flux, J_{NO} (mol cm^{-2} min^{-1}), as measured by gas-phase chemiluminescence, increased with surface Cu expression according to the relationship J_{NO} =(1.63 %SACu - 0.81)

x10^{-11}, R^2 = 0.98 where %SACu is the percentage of the surface occupied by Cu. The maximum flux measured at 10 wt% Cu was 5.35 ± 0.74 x10^{-10} mol cm^{-2} min^{-1}. Clotting time of sheep blood exposed to these surfaces increased with Cu content from 80 ± 13 seconds with pure silicone to 339 ± 44 seconds with 10 wt% Cu(II) added. SEMs of NO-generating coatings showed clots occurred away from exposed Cu-dendrites. Cu/Si PMCs inhibit coagulation in a dose-dependent fashion related to the extent of copper exposure on the coated surface.

Keywords: Nitric oxide, Cu(II), silicone, platelets, coagulation

2.2 Introduction

Over 200 million blood-contacting biomaterials are presently used in clinical applications such as catheters, vascular grafts, heart valves, extracorporeal membrane oxygenation (ECMO), cardiopulmonary bypass circuits, artificial kidneys, ventricular assist devices, glucose sensors, and stents [1]. In all these applications, it is important to reduce surface-induced blood activation in order to increase the useful life of the device and reduce thromboembolic complications. Thrombosis is especially problematic in long-term clinical applications such as artificial lungs (arteriovenous CO_2 removal, ECMO, thoracic artificial lungs) where the need for efficient gas transfer requires a larger surface area [2]. Currently, the administration of conventional systemic anticoagulants such as heparin, low-molecular-weight heparin, warfarin, aspirin, and clopidogrel is standard clinical practice to inhibit blood coagulation. Usage of newer Glycoprotein (GP)IIb/IIIa blockers like reopro, aggrastat and integrilin to achieve the same goal are also on the rise [3]. Unfortunately, these anticoagulants act systemically and have long half-lives. Thus, they limit coagulation at the artificial surface, at surgical sites, and within native blood vessels. The result is longer device lifespan but also increased risk of bleeding complications [3 - 5].

A relatively new approach to reduce clot formation on biomaterials is through

surface release or generation of NO [6,7]. NO is a free radical gas produced by the endothelium to maintain hemostasis [8 -11]. The gas reduces platelet activation by inhibiting agonist binding to their surface receptors. It freely diffuses into platelets to initiate the NO/cyclic guanosine monophosphate (cGMP) [10,11] pathway that in turn phosphorylates G protein-coupled surface receptors, changing their conformation to decrease binding affinities of agonists. Commonly known G protein-coupled receptors on the platelet include thrombin, thromboxane A2, and adenosine diphosphate receptors. The gas also reduces secondary activation of circulating platelets by inhibiting the release of platelets intracellular granules. This is achieved by blocking the release of their calcium stores needed for actin-myosin interaction that is required for platelets to change their shape and release their granules. Unlike other platelet inhibitors, NO has a very short half-life (milliseconds), as it is quickly taken up by RBCs, platelets, and other NO scavengers. Thus, the anticoagulant effect occurs near the surface that releases or generates NO and has no effect on coagulation downstream.

NO generation from polymeric materials impregnated with Cu and other transition metal particles has been described [6,7]. In brief, these metallic particles catalyze the release of NO from NO-donors in blood. In the case of Cu, the metal exists mostly as Cu(II) on the surface of the polymer after oxidation. Reducing agents convert Cu(II) to Cu(I), which then interacts with NO-donors(Figure 2.1) to produce thiolate ions, Cu(II), and NO gas. The thiolate ions then combine to form disulfides by reducing Cu(II) back to Cu(I). The entire reaction repeats to continuously generate NO. As shown also in Figure 2.1, numerous reactions affect the concentration of NO in blood. In addition to binding and inhibiting platelets, NO can form nitrites by oxidative species, including ceruloplasmin,[12 ,13] and bind to hemoglobin and form methemoglobin. Plasma deoxyhemoglobin can also reduce NO_2^- back to NO. Plasma deoxyhemoglobin is normally associated with blood trauma caused by extracorporeal

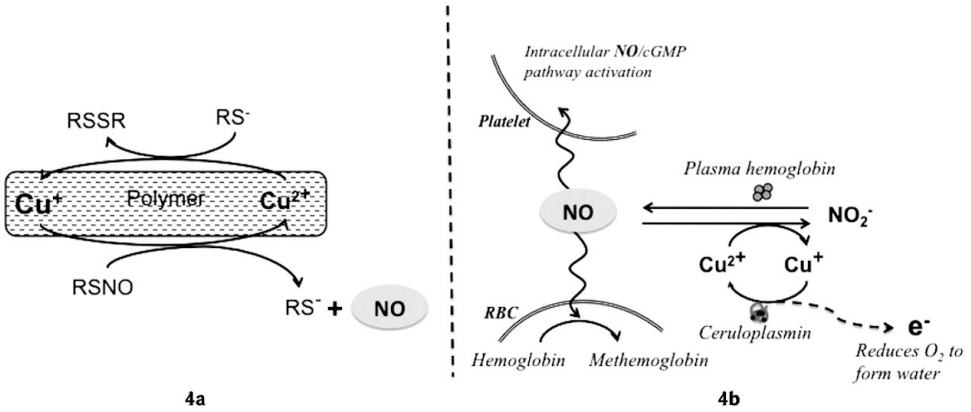

Figure 2.1: Cu-mediated NO generation model (6). The in vitro NO generation from these surfaces, (2.1a), can be measured accurately however the amount of NO generated in vivo from these surface still remains in question. Ceruloplasmin, a multicopper oxidase synthesized and secreted by the liver into plasma catalyzes the oxidation of NO into NO_2 concomitantly with cupric (Cu^{2+}) to cuprous (Cu^{+}) reduction (13, 14). Perhaps, with other NO scavengers in plasma, only a fraction of the NO generated diffuses into platelets to activate the NO/cGMP pathway to inhibit platelet activation, (2.1b).

circulation during CPB or ECMO.

These modified polymers could be used to coat blood contacting surfaces or the blood-contacting device could be constructed wholly out of NO-generating materials. For example, the artificial lung's gas exchange membrane could be made wholly from silicone that is doped with Cu. To this end, the following study characterizes the relationship between the surface exposure of Cu surface NO flux, and the resultant anticoagulant effect from a silicone-Cu polymeric matrix composite (Cu/Si PMC). The aim is to provide a guide to their future use in any device with significant blood-biomaterial interactions.

2.3 Materials and Methods

2.3.1 In vitro Test System

An in vitro test system was created by coating standard Hemochron tubes (P214 flip-top, ITC, Edison, NJ) with PMC at various weight percents of Cu. The tubes were emptied of their kaolin activator, rinsed with deionized water, and dried before coating. Three micron particles of elemental Cu (Sigma Aldrich Chemical Co. St. Louis, MO) were blended into part A of a two-part R21-2615 silicone resin (Nusil Silicone Technology,CA). An equal volume of silicone resin Part B was added followed by one mL of acetone per two mL of blend. The mixture was then stirred and sonicated (Branson 5510 Sonicator Bath, Norwich NY) for 60 minutes to create a uniform suspension. Cu microparticles were then added to create 0, 3, 5, 8, and 10 weight percent (wt%) Cu/Si PMCs. Cu/Si PMCs. The hemochron tubes were loaded with 0.3 mL of the mixture and rolled over a flat surface to eliminate uncoated patches. The tubes were then loaded horizontally into a rotisserie (Figure 2.2) and cured by rotating the tubes in the x-y plane at 1.5 rev min^{-1} for 24 hours at ambient temperature.

The resulting coatings had thicknesses of 70 m approximately. All cured coats were later oxidized at 37° C for 24 hours by bathing them in PBS at pH 7.4 using the Innova 4000 incubator shaker. Bathing in PBS oxidizes Cu to Cu(II) by spontaneous corrosion of metallic copper [6], thus creating a Cu/Si PMC. The hemochron tubes were then rinsed for approximately 2 minutes with deionized water and dried for testing.

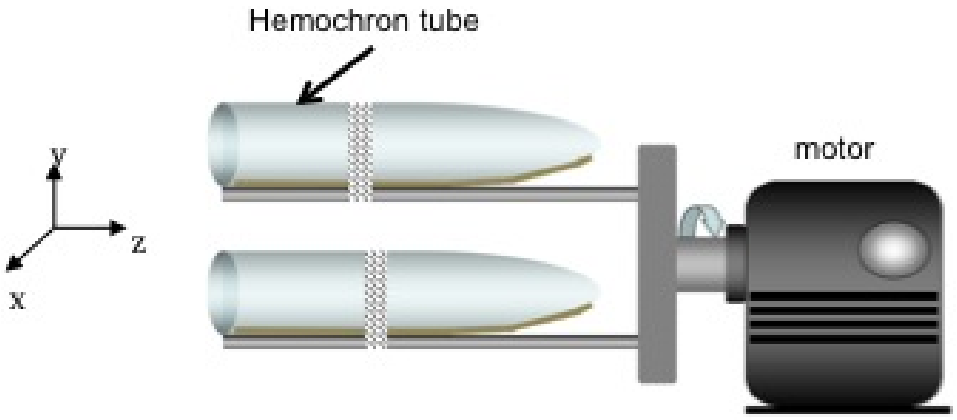

Figure 2.2: 24hr curing of coated hemochron tubes in ambient temperature at 1.5 rev min^{-1}. The slow curing speed allows resin to uniformly coat the lumen. All tubes ware capped with their flip tops during curing.

2.3.2 PMC Surface Analysis

The presence of Cu on the Cu/Si PMC was verified with energy dispersive x-ray spectroscopyenergy dispersive x-ray spectroscopy (EDS) (EDAX Inc. Mahwah NJ). The Cu/Si PMC layer was coated on to tubes as described above, but peeled and sectioned into two cm^2 pieces prior to oxidation and further testing. Twelve surface locations per wt% were then analyzed with EDS. The following settings were used: input count rate = 1000cps, energy resolution = 135eV, peak/background = 100, and the scanned surface area = 4 mm^2. SEMs of surfaces analyzed with EDS were then imported into Image J (NIH, Bethesda, MD) for quantifying the percentage of Cu exposed on the surface. The images were converted into a two-dimensional black and white binary map and then processed using the particle analysis package to quantify the percentage of total surface area occupied by Cu.

2.3.3 Measurement of NO flux and Clotting Times

NO generation from 0, 3, 5, 8, and 10 wt% PMC-coated tubes (N = 6 each) was measured by gas-phase chemiluminescence. Specifically, 2.75 ± 0.5 cm^2 coated pieces of the hemochron tube wall were introduced into a 1 μM S-nitrosoglutathione (S nitrosoglutathione (GSNO)) to activate a chemiluminescence reaction in a standard setup as shown in Figure 2.3. The NO generation profiles are decaying, left-skewed Gaussian curves (See Figure 2.7). A peak NO flux is reached initially; thereafter the GSNO concentration decreases and NO flux decreases. NO generation was measured for at least 30 minutes from each sample, and the peak flux was recorded for presentation. Clotting times of sheep blood were measured for the 0, 3, 5, 8, and 10 wt% Cu-doped PMC-coated tubes (N = 6 each) using the coated hemochron tubes. Non-heparinized sheep blood (0.4ml) was dispensed into the tubes immediately after being drawn. Unlike typical activated clotting time assays, the tubes did not contain any procoagulant activator. Thus, the artificial surface was the only activator present. All other methods, including detection of a formed clot, followed standard Hemochron activated clotting time protocols. Thus, clotting time was measured as the time elapsed between loading the Hemochron tube with blood and when the Hemochron detected solid clot. All in vitro clotting time experiments were performed in atmospheric level of PO_2, or approximately PO_2 = 150 mmHg

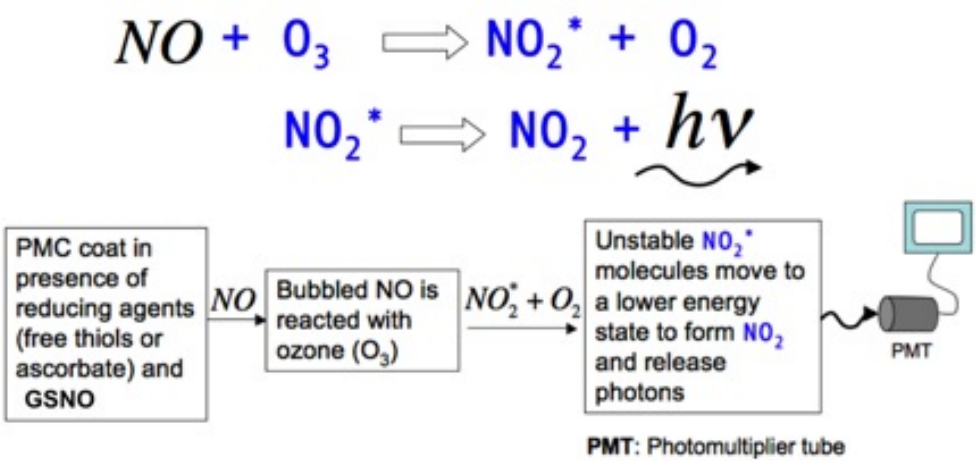

Figure 2.3: Chemiluminescence reaction and reaction setup.

2.3.4 Clot Distribution on NO-generating Cu(II)/Si PMCs

To examine the mechanism of anticoagulation, Hemochron tubes were coated with 0 or 10 wt% Cu-doped silicone and filled with approximately 5 ml of blood. The tubes were placed on an Eberbach model EL687 shaker (Eberbach Labtools, Ann Arbor, MI) at 50 cycles/min within a 37◦ C incubator for 30, 60, 90, 240, 360, and 480 seconds. After incubation, the surfaces were gently rinsed with saline solution until the effluent was clear and fixed with 2% gluteraldehyde (Sigma Aldrich Chemical Co. ST. Louis, MO). The samples were imaged with a Philips XL30 FEG SEM to examine protein adsorption and platelet adhesion to the surface.

2.3.5 Statistical Analysis

One-way analysis of variance (ANOVA) with Tukey's post hoc tests was performed to compare the dependent variables NO flux, clotting times and surface area of Cu using the weight percent of copper as the independent variable. A p-value < 0.05 is regarded as significant. All data is expressed as mean $\pm$ standard deviation.

2.4 Results

2.4.1 PMC's Surface Microstructure and Composition

In Figure 2.4, the surfaces of control and Cu(II)/Si coatings show different surface morphologies. As expected particle aggregates are not present on control surfaces, whereas dendrites of Cu microparticles are present on the non-control surfaces. The presence of Cu dendrites, as verified by EDS microanalysis, is shown in Figure 2.5. SEMs of the Cu/Si PMC showing Cu dendrites were first analyzed with energy dispersive spectroscopy. The result showed a mapping of Cu in Figures 4.4B and 4.4C similar to the Cu dendrite pattern of the SEM in Figure 4.4A. The energy spectra in Figure 4D also shows the corresponding Cu peaks.

The percentage of the surface area of membranes occupied by Cu was quantified with image J (NIH, Bethesda MD) to be 12.1 ± 2.8%, 19.7 ± 5.4%, 29.0 ± 3.8% and 33.8 ± 6.5% at 3, 5, 8 and 10 wt% Cu doping respectively (see Figure 2.6). These results are significantly different from 0 wt% group and from each other ($p < 0.05$). The only exception is that the percentage of Cu/Si surface area occupied by Cu on the 10 wt% Cu surface was not significantly difference from that of the 8 wt% Cu group.

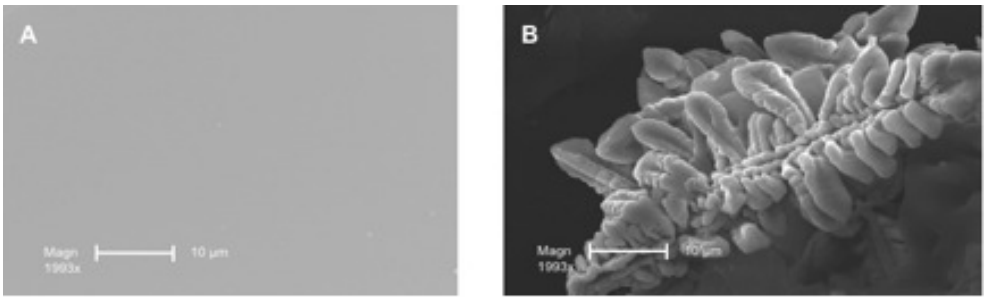

Figure 2.4: Surface of silicone coated control (A) and surface of Cu(II)/Si PMC coating showing Cu dendrites necessary for nitric oxide generation (B).

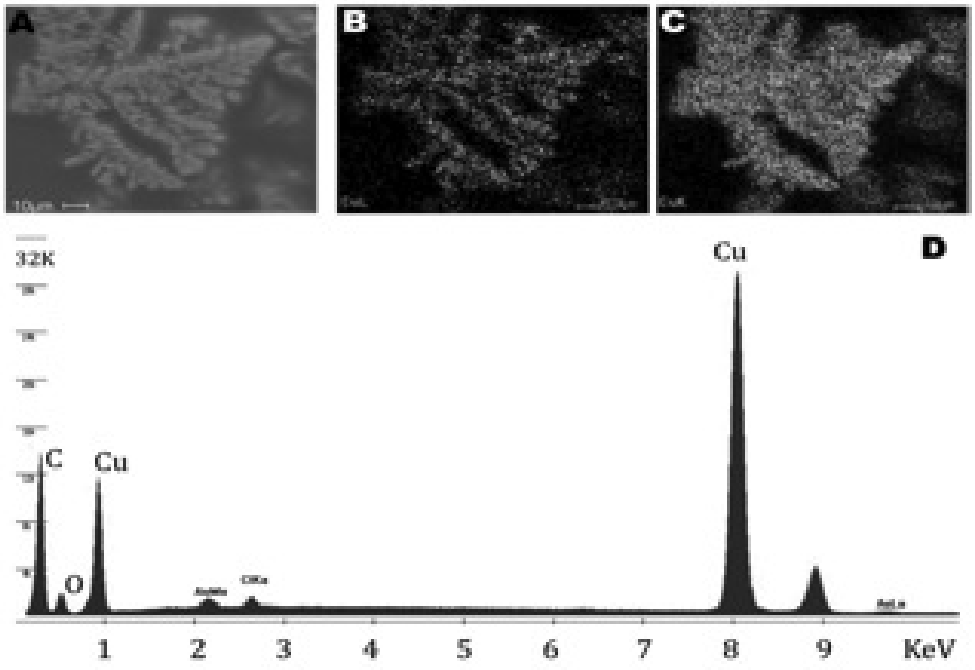

Figure 2.5: Energy dispersive X-ray microanalysis results confirming the presence of Cu on Cu/SI PMC coated surfaces: SEM of Cu/Si PMC showing Cu dendrites (A) were analyzed with energy dispersive spectroscopy. The result showed a mapping of Cu in the L (B), and K (C) shells similar to the Cu dendrite pattern of the SEM. The energy spectra in D) also shows the corresponding Cu peaks.

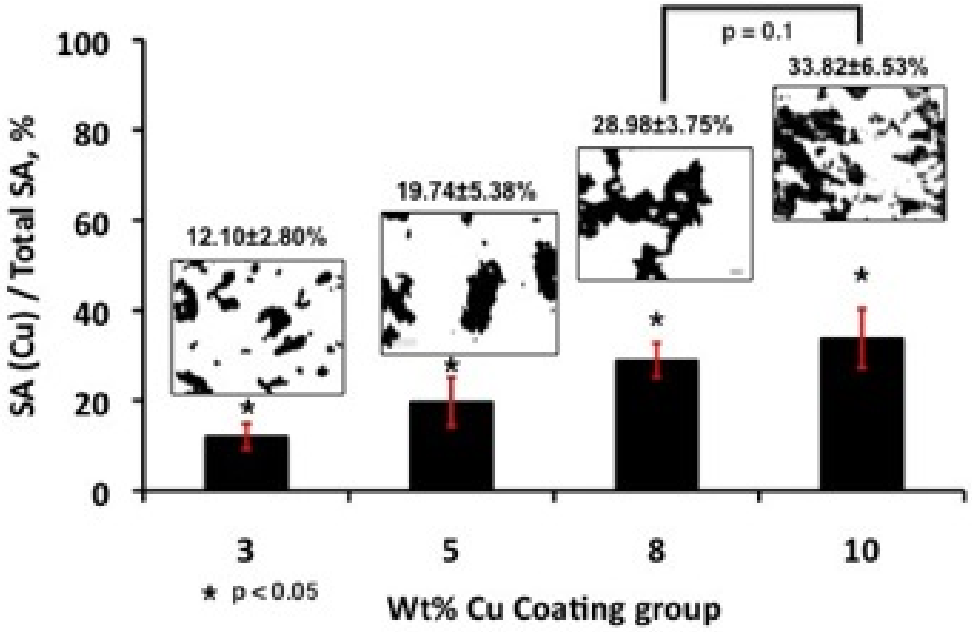

Figure 2.6: The percentage of silicone surface-Cu as function of wt% Cu increased from 12.90% at 3wt% Cu to 33.82% at 10wt%Cu. The percentage of surface Cu in each wt% Cu coating group was significantly different from control and from the each other ($p < 0.05$). The only exception was that the 10 wt% Cu group was not significantly different from the 8 wt% Cu ($\alpha = 0.05$).

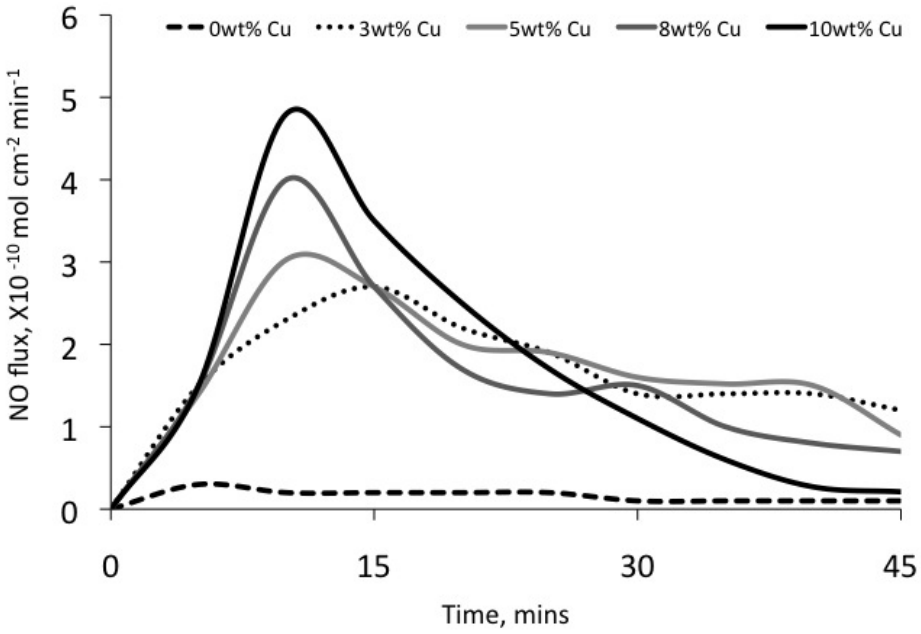

Figure 2.7: Representative NO generation profiles for 0 (Control), 3, 5, 8, and 10 wt% Cu PMC coated surface.

2.4.2 Relationships among wt% Cu, Surface Expression of Cu and NO Flux and Clotting Times of PMCs

The peak NO flux increased with surface expression of Cu from 2.13 x 10^{-10} ± 0.38x 10^{-10} mol cm^{-12} min^{-1} at 3 w% to 5.35 x10^{-10} ± 0.73x 10^{-10} mol cm^{-2} min^{-1} at 10 wt% (Figure 2.8). The average peak flux of each group is significantly different from control and from each other ($p < 0.05$). The one exception is that flux from the 10wt% Cu group was not significantly different from that of the 8wt% Cu group ($p = 0.4$). These fluxes were all greater than published human endothelial NO flux in the range of (0.5 - 4) x10^{-10} mol cm^{-2} min^{-1} [12]. A linear fit of the relationship between NO flux and wt% Cu yielded J_{NO} = (-0.15wt%^{2} + 6.3wt% + 4.5) x 10^{-11}, $R^2 = 0.99$.

Accordingly, clotting times increased with wt% Cu from 80 ± 13 seconds at 0 wt% Cu to 339 ± 44.5 seconds at 10 wt% Cu (Figure 2.8). The average clotting time of each group is significantly different from control and from each other ($p < 0.05$).

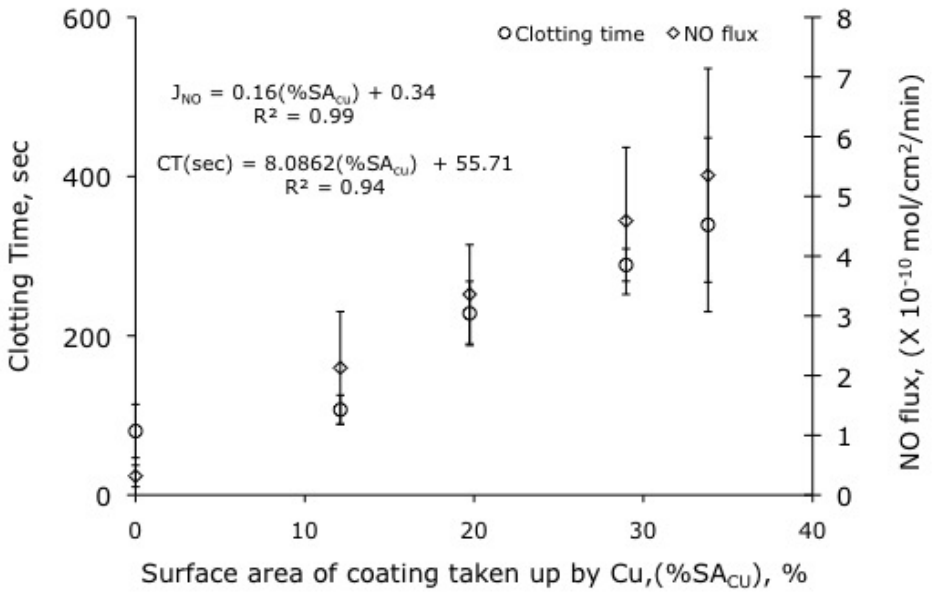

Figure 2.8: Average clotting time and NO flux from PMC coated surfaces for 0 (Control), 3, 5, 8, and 10 wt% Cu polymeric matrix composites. The average clotting time and average peak NO flux of each group is significantly different from control and from each other ($p < 0.05$). However the clotting time and peak flux of the 10wt% Cu group was not significantly different from that of the 8wt% Cu group ($p = 0.29$ and $p = 0.4$ respectively).

However the clotting time of the 33.8 ± 6.5% Cu surface expression group was not significantly different from that of the 28.9 ± 3.7% Cu surface expression group ($p = 0.29$). A linear fit of the relationship between clotting time in seconds (CT) and surface expression yielded CT = 8.08(%SA_{CU}) + 55.71, $R^2 = 0.94$.

2.4.3 Clots on Coated Surfaces

Scanning electron micrographs of clots on control and NO-releasing surfaces are shown in Figure 2.9. Following exposure to blood for different durations, an adsorbed protein layer was present at all times, indicating that NO had no significant effect on total protein adsorption. However, Cu-doped surfaces had a smaller number of adhered platelets. In particular, it can be seen that areas around exposed Cu dendrites are free from platelets. Thus, the effect of NO on coagulation appears to be primarily

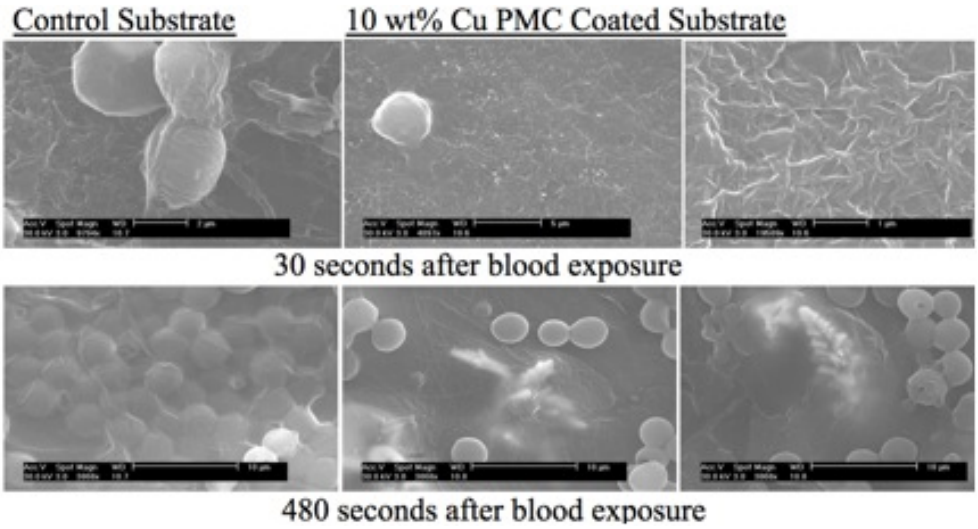

Figure 2.9: SEMs of Cu/Si polymeric matrix composite surfaces (PMCs), demonstrating platelet adherence to control (0 wt% Cu) and 10 wt% Cu materials after 30 and 480 seconds. It appears that the adsorbed protein layer was present at all times, indicating that NO had no effect on protein adsorption. In addition the Cu-doped surfaces had less adhered platelets and the area around exposed Cu dendrites are free from platelets. Thus, the effect of NO on coagulation appears to be primarily keeping platelets from adhering and perhaps keeping platelets that adhere from activating.

keeping platelets from adhering to the adsorbed protein layer and perhaps keeping platelets that adhere from activating.

2.5 Discussion

Overall, these results indicate that Cu catalyzes NO formation effectively in these Cu/Si composites, and the NO formation leads to significant inhibition of clotting. Clotting times were 1.33 and 4.24 times longer at 3 and 10 wt%, respectively, than without Cu. Furthermore, the NO flux and resultant increase in clotting time is dependent primarily on the amount of copper exposed on the surface of silicone. At higher Cu weight percents, however, there are diminishing returns to adding more copper. The surface concentration of copper does not increase significantly between 8 and 10 wt% (Figure 2.6), as increasing amounts of Cu get trapped inside the bulk

material. Thus, there is little improvement in NO flux and clotting time at higher Cu concentrations. Thus, at greater than 8%, a significant amount of copper is buried within the bulk material and not assisting in NO generation. If greater NO generation were desired, surface processing would be necessary. A base layer of pure silicone could be laid down first, followed by a second, far thinner layer with a high Cu concentration. The thin layer would keep Cu from being subsumed within the bulk material. In the case of artificial lung membranes, this technique would reduce overall copper content and might better maintain the gas permeability of the membrane.

These results also indicate that each wt% surface was capable of NO fluxes on the same order as endothelial cells [14]. However, in vivo NO flux will depend on the concentration of a variety of NO-donors in present in blood and the reaction rate between each donor and Cu(I). In blood, the total concentration of GSNO and other low molecular weight NO donors such as S-Nitrosocysteine (CysNO), S-nitrosohomocysteine (HCysNO), and S-nitrosocysteinylglycine (CysGlyNO) in healthy subjects ranges across several orders of magnitude, from nanomolar to micromolar concentrations [15,16]. Thus, predicting NO fluxes in blood are difficult. In this study, 1μ M of GSNO was used as the substrate for in vitro studies. The concentration of GSNO in blood is about one-third of that used here, 320 ± 60 nM, but this is augmented by the presence of the low molecular weight NO donors. In addition, the rate of reaction between Cu(I) and these donors is faster than between Cu(I) and GSNO [17]. Thus, NO generation and the rate of clot formation may be different in vivo and vary across test subjects. Generation of NO will also vary with time. If not supplemented, concentrations of NO donors will decrease as these molecules are cleaved to generate NO. In situations in which small surface area devices such as stents and arterial and venous lines are used, consumption would be minimal. In large surface area devices such as artificial lungs, consumption would be rapid, as there will be more catalytic sites for NO generation and widely studied synthetic RSNOs supplements such as

S-Nitrosoglutathione and S-Nitroso-N-acetylpenicillamine (SNAP) would likely have to be infused into the device inlet to maximize the local NO generation. SNAP will be better suited for infusion, as it has been shown to be more stable than other S-nitrosothiols that lead to inconsistency due to their highly unstable nature[18, 19].

Ultimately, choosing an appropriate level of copper for a biomaterial depends greatly on the application. First, the minimum amount of Cu should be used to avoid any potential risk of high blood Cu concentrations. The amount of leached copper was not calculated here because of the short blood exposure times. In this study, at 10 wt%, 60 mg of copper was used per coating over a surface area of 33 cm^2. If a similar coating were applied to a stent (surface area = 6 cm^2) and adult sized oxygenators (surface area up to 25,000 cm^2), the total amount of Cu that could potentially leach would be 10 mg and 45,000 mg respectively. Thus, even if all of the Cu leached from stents, the amount would be negligible compared to the recommended daily intake. The amount that could leach from adult size oxygenators is higher than the tolerable daily intake, but this amount would leach slowly over the devices lifespan. Moreover, it is likely that only surface exposed copper would leach in significant amounts.

The rate Cu leaching into plasma has been studied in a 4 h, rabbit model of extracorporeal life support [20]. There, a 10 wt% Cu circuit with a surface area of 0.02 m^2 was used in 2-3 kg rabbits. The long term Cu leaching of these surfaces was also addressed by measuring the Cu content over seven days in a similar, saline filled extracorporeal circuit. There was a two-fold increase in plasma Cu to 5.9 $\pm$ 0.2 μg/dl after 4h. After 7 days, Cu levels in saline was 23.4 $\pm$ 8 μg/dl. This indicates a very slow rate of copper corrosion to copper ions within the coatings containing copper nanoparticles.

Additionally, the level of Cu that should be used will depend on the application and its duration. Large bore cannulae with relatively small surface area to volume ratios and high blood flow velocities will require lesser amounts of NO release, whereas

artificial lung surfaces, with high surface area to volume ratios and low blood flow velocities will require far more NO release. Moreover, the longer the application, the greater anticoagulation required. This study indicates that weight percents between 5% and 8% would be the most likely therapeutic range if the copper were in the bulk polymer. Despite these positive results, this study is limited by the short periods of blood biomaterial contact and the relatively static setting. Future long-term in vivo studies are needed to determine the effectiveness of the Cu/Si PMC on coagulation for periods of hours to days under blood flow. The hemochron tube wall velocity is 0.08 m*min^{-1}, whereas the average blood flow velocity is anywhere from 0.4 m*min^{-1} in an artificial lung [21] to 35 m*min^{-1} in an ECMO cannula [22]. The static setting of this study results in pooling of reactants, including activated procoagulant molecules and possibly Cu leaching from the surface into the bulk fluid. In a dynamic system, both would be washed into circulation, reducing their effect at the biomaterial surface.

2.6 Conclusion

Results from this study indicate that Cu catalyzes NO formation effectively in silicone-Cu composites, and the NO formation leads to significant inhibition of clotting. Both the NO flux and clotting time depend on the surface copper exposure. At 10 wt%, the clotting time is 4.24 times greater than with pure silicone. Additional Cu will have diminishing returns, as the surface concentration of copper does not increase markedly with increasing wt% in this range. Currently we are developing artificial lungs whose hollow fibers are completely composed of Cu-doped silicone. These devices will be tested for gas-transfer and for their biocompatibility in vitro and in vivo respectively.

2.7 References

1. Ratner DB. The catastrophy revisited: Blood compatibility in the 21st century. Biomaterials 28: 5144-5147, 2007.

2. Bartlett RH. Extracorporeal life support registry report 1995. ASAIO Journal 43:104-107, 1997.

3. Rapaport SI and Rao VM. Initiation and regulation of the tissue factor-dependent blood coagulation. Arterioscler Thromb 12: 1111-21, 1992.

4. LaBan MM, Whitmore CE, Taylor RS. Bilateral adrenal hemorrhage after anti-coagulation prophylaxis for bilateral knee arthroplasty. Am J Phys Med Rehabil 82: 418-420, 2003.

5. Ereth MH, Nuttall GA, Clarke SH, Dearani JA, Fiechtner BK, Rishavy CR, Buda DA, Shaw TA, Orszulak TA, and Oliver WC. Biocompatibility of Trillium Biopassive Surface-Coated Oxygenator versus Uncoated Oxygenator During CBP. Journal of Cardiothoracic and Vascular Anesthesia 15: 545-550, 2001.

6. Wu Y, Rojas AP, Grifth GW, Skrzypchak AM, Lafayette N, Bartlett RH and Meyerhoff ME. Improving blood compatibility of intravascular oxygen sensors via catalytic decomposition of S-nitrosothiols to generate nitric oxide in situ. Sensors and Actuators B: Chemical121: 36-46, 2007.

7. Oh BK, Meyerhoff ME. Catalytic generation of nitric oxide from nitrite at the interface of polymeric films doped with lipophilic Cu(II)-complex: a potential route to the preparation of thromboresistant coatings. Biomaterials 25: 283-293, 2004.

8. Boudko DY. Bioanalytical profile of the L-arginine/nitric oxide pathway and its evaluation by capillary electrophoresis. Journal of Chromatography B 851:186-210, 2007.

9. Murad F. Discovery of Some of the Biological Effects of Nitric Oxide and its Role in Cell Signaling. Bioscience Reports 19: 453-474, 1999.

10. Napoli C, De Nigris F, Williams-Ignarro S, Pignalosa O, Sica V and Ignarro L J. Nitric oxide and atherosclerosis: An update. Nitric Oxide15: 265-279, 2006.

11. Rabelink TJ and Luscher TF. Endothelial Nitric Oxide Synthase, Host Defense Enzyme of the Endothelium? Arterioscler Thromb Vasc Biol 26: 267-271, 2006.

12. Zhang Z, Zhang M, Chen S, Horbett TA, Ratner BD, and Jiang S. Blood compatibility of surfaces with super low protein adsorption. Biomaterials 29: 4285-4291, 2008.

13. Samuel TK. And Gitlin JD. Cpper and nitric oxide meet in the plasma. Nature Chemical Biology 2:452-453, 2006.

14. Shiva S. Wang X., Ringwood LA., Xu X., Yuditskaya S., Annavajjhala V., Miyajima J., Hogg N, Harris ZL., and Gladwin MT. Ceruloplasmin is a NO oxidase and nitrite synthase that determines endocrine NO hemeostasis. Nature Chemical Biology 2:486-93, 2006.

15. Singh RJ, Hogg N, Joseph J, Kalyanaraman B. Mechanism of nitric oxide release

from S-nitrosothiols. J Biol Chem 271: 1859-6603, 1996.

16. Hwang S and Meyerhoff ME. Polyurethane with tethered copper(II)-cyclen complex: Preparation, characterization and catalytic generation of nitric oxide from S-nitrosothiols. Biomaterials 29 (16):2443-52, 2008.

17. Bramanti E, Jacovozzi K, DUlivo L, Vecoli C, Zamboni R, Mester Z, and DUlivo A. Determination of S-nitrosoglutathione and other nitrosothiols by p-hydroxymercurybenzoate derivatization and reverse phase chromatography coupled with chemical vapor generation atomic fluorescence detection. Talanta 77: 684 -694, 2008.

18. Radomski, MW, REss DD, Dutra A, Moncada S. S-Nitrosoglutathione inhibits platelet activation in vitro and in vivo. Br. J. Pharmacol 107:745-749, 1992.

19. Stern BR. Essentiality and toxicity in copper health risk assessment: overview, update and regulatory considerations. J Toxicol Environ Health A 73: 114-127, 2010.

20. Major TC, Brant DO, Burney CP, Amoako KA et al, The hemocompatibility of a nitric oxide generating polymer that catalyzes S-nitrosothiol decomposition in an extracorporeal circulation model, Biomaterials (2011), doi:10.1016/j.biomaterials.2011.03.036

21. Cook KE, Perlman CE, Backer CL, Mavroudis C and Mockros LF. Hemodynamic and gas transfer properties of a compliant thoracic artificial lung. ASAIO Journal 51:404-411, 2005.

22. Haft J. The University of Michigan medical centers critical care protocol for

ECMO [University of Michigan medical school web site]. Available at: http://www.med.umich.edu/anescriticalcare/Documents/Protocol%20Manual/Critical%20Care%20Protocol%207%20ECMO%20Section%20legal.pdf. Accessed October 10, 2010.

CHAPTER III

FABRICATION AND FLUX OPTIMIZATION OF NITRIC OXIDE-GENERATING HOLLOW SILICONE FIBERS

3.1 Abstract

Gas exchange fibers represent the majority of the surface area of gas exchange devices and are thus the primary source of clot generation. In this study silicone hollow fibers were fabricated to incorporate copper (Cu) particles randomly dispersed or localized in their walls and evaluated for their ability to produce endothelial levels of Nitric oxide (NO) flux. Different Cu particle sizes (25 nm, 50 nm, and 3 μm) at 10 wt% were dispersed into fiber walls and the presence of Cu on the fibers' surfaces were examined using (Phillips XL30FEG) and energy-dispersive X-ray spectroscopy (EDS) as surface expression of Cu in silicone is necessary for NO generation. Fiber NO generation via NO donor decomposition were then examined as a function of Cu particle size. NO generation from 1 cm long fibers (N=5 fibers/ Cu particle size group) was measured by chemiluminescence with a 280i NO analyzer (Sievers 280i NOA GE, Boulder, CO) using a 1μM S-nitrosoglutathione as the NO-donor in an aqueous medium (pH = 7.38, 37°C). The wall thickness of fibers averaged 90 $\pm$ 4.4 μm with an average outside diameter of 335 $\pm$ 2.1 μm. SEM analysis of fibers'

surfaces showed the expression of dendritic features that were confirmed to be Cu by the chemical spectra of EDS. Fibers with 25 nm, 50 nm, and 3 μm Cu particles randomly dispersed in their walls produced an average peak NO flux of 5.9 $\pm$ 0.89, 15.5 $\pm$ 3.3, and 3.2 $\pm$ 0.5 (x 10^{-10}mol min^{-1} cm^{-2}) respectively. Those with their Cu particles localized/concentrated near their outer surfaces produced significantly higher NO fluxes (9.8 $\pm$ 6.8, 29 $\pm$ 6, and 48.9 $\pm$ 4.3 (x 10^{-10}mol min^{-1} cm^{-2})) at the respective particle sizes ($p<0.05$). These results indicate that gas exchange fiber can be modified to generate tunable concentrations of NO at levels comparable to that produced by the endothelium.

Keywords: Gas exchange fibers, Nitric oxide, Cu(II), and Silicone

3.2 Introduction

The results of work conducted in Chapter II allowed the relationships between the physical and chemical surface properties of flat silicone membrane and their NO generation and clotting time to be established. The next logical question was weather that knowledge can be translated to fibricating gas exchange hollow fibers of artificial lungs that generates NO? Artificial lungs are used in various respiratory strategies including extracorporeal membrane oxygenation, arteriovenous CO_2 removal, total artificial lungs, and also in cardiopulmonary bypass (CPB) during cardiac surgery. Their gas exchange fibers make up the majority of the device surface area and are made up of polypropylene, polymethylpentene, or silicone. None of these materials are non-thrombogenic so upon blood contact they adsorb blood proteins, activate platelets and clot blood leading to increased resistance to blood flow, reduced gas transfer and thromboembolic complications.

Current methods used to control clotting in gas exchange devices either cause life-threatening side effects or do not show any clinical benefit in terms of reducing clotting. Systemic anticoagulation cause bleeding in many patients [1-3] and fiber

surface coatings such as heparin, trillium, and phosphrylcholine have generally not shown reduced clotting even during short-term (up to 4h) use in CPB [4-7]. As the gas exchange fibers represent the majority of device surface area, it's prudent that alternative methods for improving device biocompatibility be focused on fibers.

One such alternative that could be applied to gas exchange fibers to improve their biocompatibility is imparting endothelial-like properties to the fiber's surface. Nitric oxide(NO) secretion by endothelial cells is understood as one of the mechanisms that the endothelium uses to control clotting [8]. NO secretion rate by the endothelium has been reported to be in the range (1-5) x 10^{-10}mol min^{-1} cm^{-2} [9]. Because NO is lipophilic, the gas can freely cross the lipid bilayer of platelets to indirectly activate a series of intracellular reactions leading to inhibition of platelet activation [10,11].

Several groups have therefore investigated the functionalization of biomaterials for either controlled release or generation of NO at physiological fluxes. Both NO releasing and generation approaches do show positive outcomes in terms of *in vivo* inhibition of platelet activation [12]. In a long-term respiratory support however, NO generation by catalytic decomposition of NO donors will be more suitable for maintaining better gas exchange as the fiber's NO production will not be limited by a finite NO storage capacity. NO production via this approach will continuously occur for as long as supplied NO donors can interact with catalysts (eg Cu(II)) on fibers. The catalytic mechanism of NO generation via the decomposition of NO donors by Cu(II) has already been described in Chapter II.

In this study, hollow silicone fibers are fabricated to incorporate different copper particle sizes as catalysts for generating NO from NO donors. NO flux is evaluated as a function of particle size. The effect of particle distribution on NO flux and gas transfer is also presented.

3.3 Materials and Methods

3.3.1 Preparation of Hollow Fiber Material

The NO-generating polymer was synthesized from a two-part R21-2615 silicone resin (Nusil Silicone Technology,CA), acetone, and 25 nm, 50 nm, 3 μm copper particles (Sigma Aldrich Chemical Co. St. Louis, MO). Resins A, B, and acetone solvent at a ratio of 1:1:0.3 and 10 wt% of Cu at each particle size were systematically mixed for extruding fibers. To prevent premature cross-linking of resins that may lead to non-uniform suspension of Cu particles, two separate mixtures were prepared. Resin A was dissolved into the solvent and Cu particles were suspended in resin B as shown in Figure 3.1. The two mixtures were separately sonicated for 30 minutes, combined and sonicated again for 60 minutes to break down aggregates of Cu particles and to attain a uniform suspension. This step was taken to ensure a uniform distribution of Cu on the surfaces of fibers. The final mixture was allowed to cross-link under room temperature for another 60 minutes to increase its viscosity before beginning fiber fabrication.

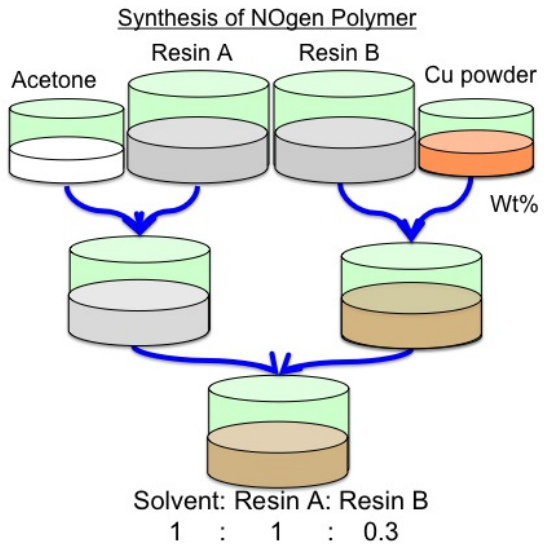

Figure 3.1: Synthesis of nitric oxide generating silicone

3.3.2 Fabrication of NO-generating Hollow Silicone Fibers

Three groups of hollow silicone fibers were evaluated for NO generation. The first group had randomly distributed particles, the second group of fibers had their Cu particles concentrated close to their outer surface and the third group did not contain Cu particles (controls). The fabrication process of the fibers shown in Figure 3.2 centered on incorporating a water soluble polyvinyl alcohol (PVA) supporting rods (150 μm OD) over which the fibers were extruded. PVA is a non-toxic and environmentally safe polymer that is easily extruded much like polypropylene, and has been engineered to dissolve in water at any desired temperature. This polymer is used in applications ranging from pharmaceuticals, food processing, to disposable surgical gowns. The core adds strength and rigidity to the Cu-doped silicone fibers during fabrication and subsequent oxygenator manufacturing. In finished oxygenators however, this core support would be purged out leaving behind hollow fibers.

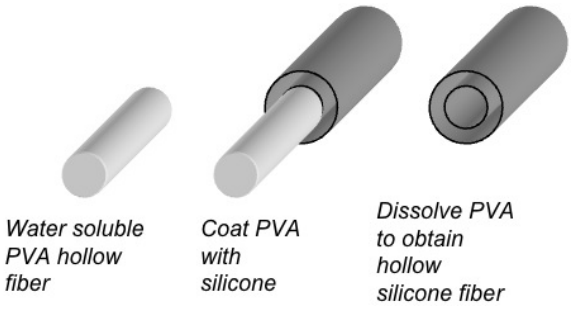

Figure 3.2: Fabrication process for nitric oxide generating hollow silicone fibers

The fiber fabrication setup shown in Figure 3.3 consisted of a top guide plate with a 150 μm aperture (not shown) placed on top of the die to help feed PVA rods vertically down during extrusion, a 2.5mm-aperture die containing a reservoir into which coating materials are loaded, and a bottom guide plate (aperture size = 350 μm) placed beneath the die to regulate the final outside diameter of fibers. This fabrication setup is a modified benchtop replica of that used by Medarray Inc. PVA rods were hand-fed at 12 inches/min and emerged coated at the opposite end of the

die. Coated rods were immediately cured at 500°F.

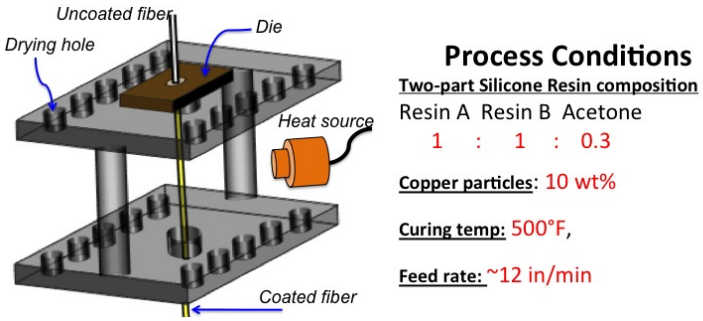

Figure 3.3: Extrusion setup for nitric oxide generating hollow silicone fibers

Control fibers and fibers with randomly dispersed Cu particles were fabricated by passing naked PVA rods through the die once. Fibers with particles localized close to the outside walls were fabricated to have a double layered (DL) structure. The PVA rods were first coated with pure silicone to a finite thickness using a bottom guide plate with a 250 μm aperture. After curing, a second 50 μm silicone layer containing appropriate Cu amounts was coated over the first and then cured.

3.3.3 Characterization of Fiber Structure and Wall Surface

To examine fiber-to-fiber cross section and wall thickness uniformity, all fibers were imaged with a Philips XL30 FEG scanning electron microscope. As NO generation from Cu-doped silicone depends on surface Cu, the extruded fibers were characterized for the presence of Cu on their surfaces. The presence of Cu on the fibers was verified with energy dispersive x-ray spectroscopy (EDS) (EDAX Inc. Mahwah NJ). Specifically, sections of the extruded fibers (N=5, 1 cm long per fiber group) were analyzed with EDS. The following settings were used during the EDS analysis: input count rate = 1000cps, energy resolution = 135eV, peak/background = 100, and the scanned surface area = 4 mm^2.

3.3.4 Measurement of Nitric Oxide Generation from Fibers

NO generation from fibers were measured by gas-phase chemiluminescence as described in Chapter II. Specifically fibers (N = 5/1 cm long per fiber group) were introduced into a 1 μM S-nitrosoglutathione (GSNO) to activate a chemiluminescence reaction and the peak NO flux was measured with a nitric oxide analyzer (Sievers 280i NOA GE, Boulder, CO). NO generation was measured for at least 30 minutes from each sample.

3.3.5 Statistical Analysis

One-way ANOVA was performed to compare the dependent variable, NO flux, using the weight percent of copper and copper distribution inside fiber wall as the independent variables. A p-value < 0.05 is regarded as significant. All data is expressed as mean $\pm$ standard deviation.

3.4 Results

3.4.1 Structure and Surface of Hollow Silicone Fibers

All fibers tested in this study showed uniform cross section and and wall thicknesse. As shown in Figures 3.4A and 3.4B, their wall thickness averaged 90 $\pm$ 4.4 μm and outside diameter averaged 335 $\pm$ 2.1 μm. Also the cross section of fibers fabricated to concentrate their Cu particles close to their outer surface is shown in Figure 3.4C. The area between the broken concentric circles (t = 50 $\pm$ 10 μm) is the first layer void of copper particles and the outer layer (t = 55 $\pm$ 15 μm) contained Cu particles.

The surface morphology of Cu-doped fibers were similar to that of Cu-doped silicone membranes presented in Chapter II. As shown in Figure 3.5 their surface morphology showed dendritic structures that were evenly distributed on their outer surfaces. Figure 3.5A is a low magnification view representative of 10 wt% Cu-doped

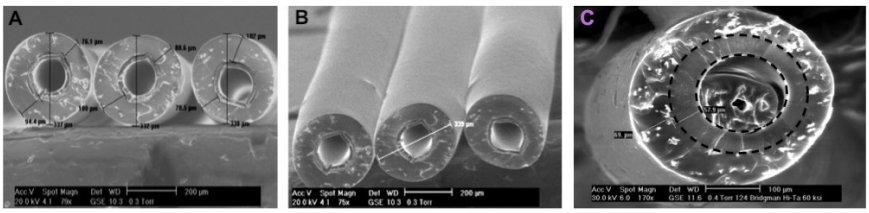

Figure 3.4: Extruded NOgen fibers showing cross section A)and outer surface of fibers B) of fibers with randomly distributed Cu, and cross section of fibers with their Cu concentrated towards their outer surface C).

fibers. Close inspection of fibers (Figure 3.5B) by magnifying the area highlighted in Figure 3.5A, revealed features similar to those found in previous studies where Cu particles were doped into silicone membranes. The chemical map of the fibers' surface shown in Figure 3.5C and the chemical spectra in Figure 3.5D confirmed the dendritic features to be Cu particles. The presence of carbon, oxygen, and silicone which make up the base polymer were also confirmed.

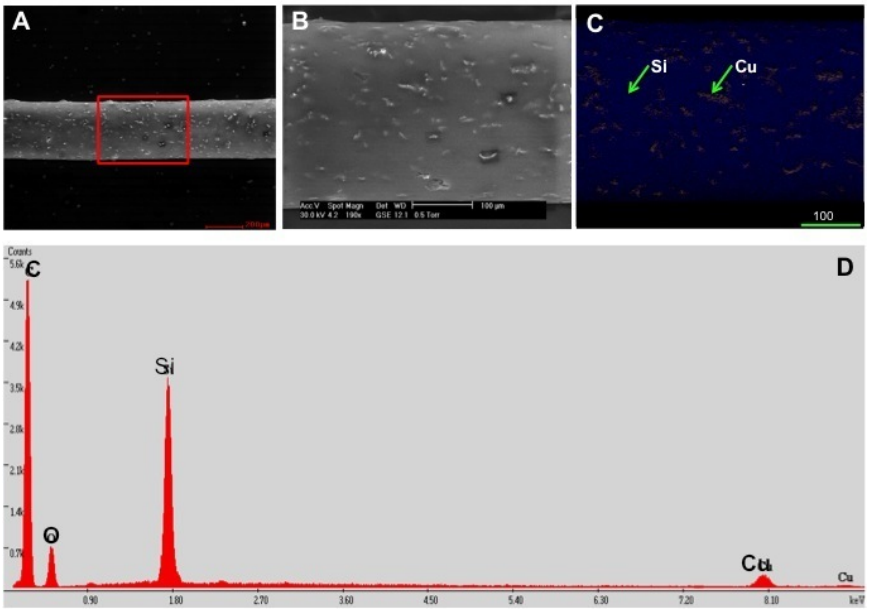

Figure 3.5: A representative surface morphorlogy and chemical composition of NOgen hollow silicone fibers. The SEMs of the fiber is shown in a) and in b) at a higher magnification. The elemental map on the surface of the fiber showing Cu dendrite expression on silicone is shown in c) and the elemental spectra in d).

3.4.2 NO Generation from Hollow Silicone Fibers

A representative nitric oxide generation profile from fibers using methods described in section 3.3.4 is shown in Figure 3.6. All fibers tested showed a similar profile where NO generation only began after the fiber was introduced into the GSNO solution. The level of NO flux return back to pre-sample introduction levels after GSNO was consumed. The average peak NO flux from randomly distributed 25 nm, 50 nm and 3 μm Cu fibers is shown in Figure 3.7.

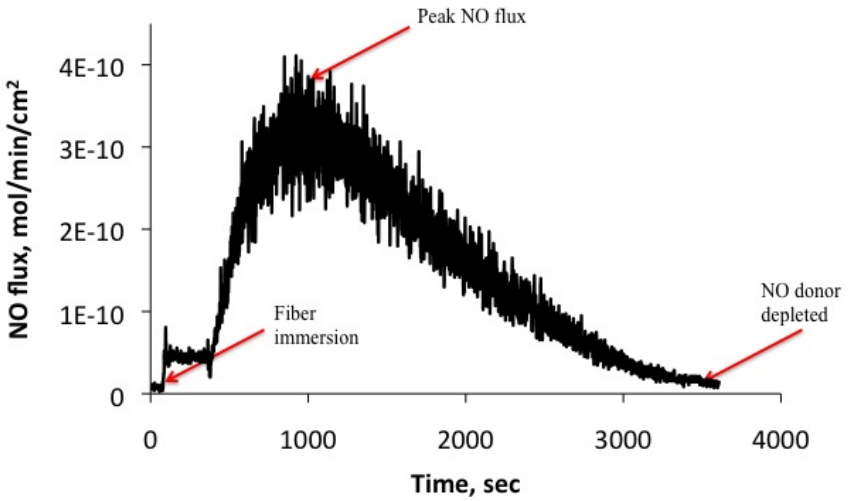

Figure 3.6: Representative profile of nitric oxide generation from Cu-impregnated silicone hollow fibers. Fibers were bathed in 1 μM GSNO at 37°C for NO detection by chemiluminescence

As summarized in Table 3.1, all the fibers produced NO fluxes comparable to physiological levels. NO flux produced from the 50 nm Cu particle fibers (15 $\pm$ 4 x 10^{-10} mol cm^{-2} min^{-1}) was significantly higher than those produced from the 25 nm Cu particle fibers (6 $\pm$ 1 x 10^{-10} mol min^{-1} cm^{-2}) and the 3 μm Cu particle fibers (3 $\pm$ 0.6 x 10^{-10} mol min^{-1} cm^{-2}), $p<0.01$.

Table 3.1: Nitric oxide (NO) flux levels from hollow silicone fibers

Copper particle size (average diameter)	**Fiber structure (Single/Double layer)**	**Peak NO flux (x10^{-10} mol min^{-1} cm^{-2})**
—	Single	0
25 nm	Single	5.9 ± 0.89*
√	Double	9.8 ± 6.8*
50 μm	Single	15.5 ± 3.3**
√	Double	29 ± 6**
3 μm	Single	3.2 ± 0.5*
√	Double	48.9 ± 4.3***

* : p<0.05, ** : p<0.01, *** : p<0.001 significance from control

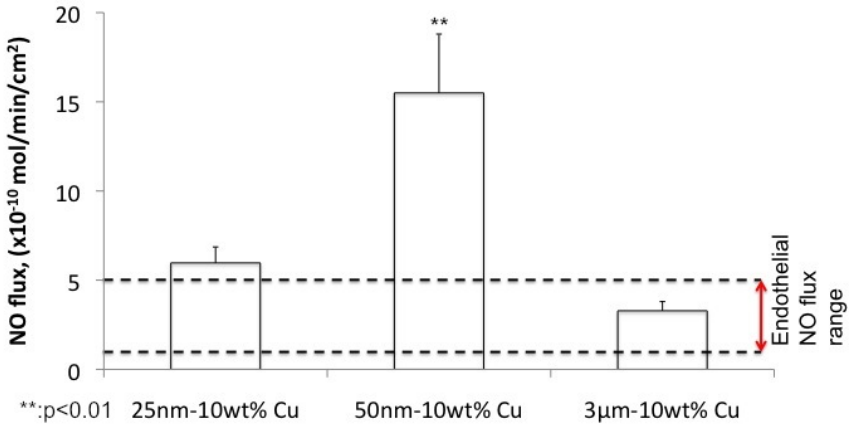

Figure 3.7: Peak nitric oxide flux from hollow silicone fibers impregnated with different sizes of Cu particles

NO flux from DL fibers having wall structures similar to that shown in Figure 3.5C further increased significantly compared to fibers with random dispersion of Cu. Their peak flux levels are shown in Figure 3.8. The clear bars are the same data shown in Figure 3.7 which represent the NO flux levels from single layer fibers and the dark bars are flux levels from double layer fibers. The dark bars show significantly larger

($p < 0.05$) NO flux levels than their clear counterparts in the 3 μm and 50 nm Cu particle groups. Such significance level was however not seen between the double and single layer fibers of the 25 nm Cu particle group. In general fibers with random dispersion of Cu showed higher fluxes with smaller Cu particles.

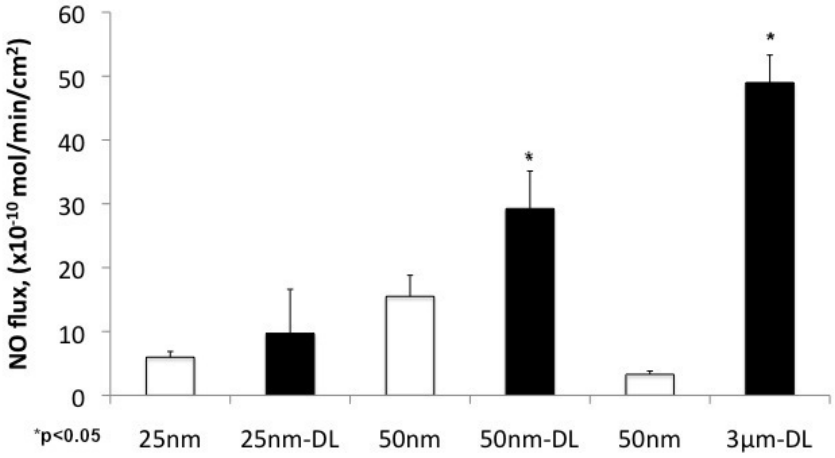

Figure 3.8: Peak nitric oxide flux from hollow silicone fibers with different Cu distribution and particle sizes

3.5 Discussion

The results show that Cu particles can be incorporated into hollow silicone fibers during fabrication to impart NO generating property to the fibers. NO fluxes produced by these fibers were greater than physiological production levels. Fibers that had randomly dispersed Cu particles showed flux levels ranging from (3 ± 0.6 to 15.5 ± 3.3) x 10^{-10} mol min^{-1} cm^{-2}. When the Cu particles were localized at fibers' surface, even higher NO fluxes were observed. Their NO flux ranged from (9.8 ± 6.8 to 48.9 ± 4.3) x10^{-10} mol min^{-1} cm^{-2}. As discussed in Chapter II, greater NO production was possible in the double layer fibers because all the Cu particles were dispersed in the second layer of the fibers allowing for a higher concentration of Cu close to their surfaces. Essentially, the amount of Cu in the second layer was 10 wt%.

However, with respect to the total fiber composition, the amount of constituent Cu equals 5 wt%. Therefore the amount of total Cu in the double layer fiber could be as small as half of that in the double layer fibers. Yet, greater amounts of NO production was measured in the single layer fiber group indicating that lesser wt% Cu is capable of generating physiological levels of NO flux and might better maintain the gas permeability of the membrane.

NO generation from these fibers during blood flow through gas exchange devices will depend on availability of NO donors. Physiological NO donor concentrations range from nanomolar to micromolar levels [13] and maybe inadequate for sustained NO production. Exogenous NO donors may have to be supplemented into blood in order to sustain NO production. In fact this method of sustaining continued generation of NO has been published in work involving NO generation via Cu mediated nitrosothiol decomposition from Cu-coated extracorporeal circulation (ECC) circuits [14].

The problem of leaching in blood-contacting surfaces coated with commercial anticlotting agents during blood flow is also present in membranes impregnated with Cu particles. Leached Cu from Cu-coated ECC circuits after 4hrs of blood flow has been reported to rise from normal serum copper concentration of 134.7 $\pm$22.5 μg/dl by two fold. This level of leaching is still well below the food and drug administration's acceptable serum copper concentration of 750 μg/dl. Leaching levels from NO generating fibers is unknown and can be better evaluated when they are incorporated into gas exchange devices.

The inclusion of Cu particles in fibers may also influence their gas transfer to a magnitude corresponding to the finite amount of fiber's surface area taken up by Cu. Secondary flows due to fibers' orientations inside fiber bundles of gas exchange devices may counter any diminutive effect that Cu particles might have on gas transfer. The gas transfer of NO generating fibers must be determined and will be best evaluated

after incorporating them into gas exchange devices.

3.6 Conclusion

Incorporation of Cu particles into hollow silicone fibers during fabrication imparts NO generating property to the fibers. These fibers containing 10 wt% Cu either randomly dispersed in their wall or concentrated in their outer half of their walls showed higher than physiological levels of NO flux. Concentrating Cu particles in the outer half of the fiber's wall at least doubles NO production.

3.7 References

1. Rapaport SI and Rao VM. Initiation and regulation of the tissue factor-dependent blood coagulation. Arterioscler Thromb 1992,12:1111-1121

2. LaBan MM, Whitmore CE, Taylor RS. Bilateral adrenal hemorrhage after anticoagulation prophylaxis for bilateral knee arthroplasty. Am J Phys Med Rehabil 2003, 82:418-420

3. Campbell BT, Braun T, Schumacher R, Bartlett RH, Hirschl RB. Impact of ECMO on neonatal mortality in Michigan (1980-1999). J Ped Surg 2003, 38(3):290-295

4. Yoshinari Niimi, Fumito Ichinose, Yoshiki Ishiguro, Katsuo Terui, Shoichi Uezono, Shigeho Morita,and Shingo Yamane. The Effects of Heparin Coating of Oxygenator Fibers on Platelet Adhesion and Protein Adsorption. Anesth Analg 1999, 89:573-9

5. I Fluger, K Maderov, M Simek, R Hjek, J Zapletalov and V Lonsk? . The effect of a cardiopulmonary bypass system with biocompatible coating on fibrinogen levels determined by the TEG - functional fibrinogen method: preliminary results. Perfusion 2001, 20(10): 1-7

6. Joseph Noora, Andre Lamy, Kelly M Smith, Rosanne Kent, Dianne Batt, John Fedoryshyn and Xiaoyin Wang. The effect of oxygenator membranes on blood: a comparison of two oxygenators in open-heart surgery. Perfusion 2003,18: 313-320

7. F De Somer, Y Van Belleghem, F Caes, K Franois, J Arnout, X Bossuyt, Y

Taey- mans and G Van Nooten. Phosphorylcholine coating offers natural platelet preserva- tion during cardiopulmonary bypass. Perfusion 2002 17: 39-44

8. Zhang H, Annich GM, Miskulin J, Osterholzer K, Merz SI, Bartlett RH, and Meyerhoff ME. Nitric oxide releasing silicone rubbers with improved blood compatibility: preparation, characterization, and in vivo evaluation. Biomaterials 2002;23:1485-1494

9. Wu Y, Rojas AP, Grifth GW, Skrzypchak AM, Lafayette N, Bartlett RH and Meyerhoff ME. Improving blood compatibility of intravascular oxygen sensors via catalytic decomposition of S-nitrosothiols to generate nitric oxide in situ. Sensors and Actuators B: Chemical121: 36-46, 2007

10. Napoli C, De Nigris F, Williams-Ignarro S, Pignalosa O, Sica V and Ignarro L J. Nitric oxide and atherosclerosis: An update. Nitric Oxide15: 265-279, 2006

11. Rabelink TJ and Luscher TF. Endothelial Nitric Oxide Synthase, Host Defense Enzyme of the Endothelium? Arterioscler Thromb Vasc Biol 26: 267-271, 2006

12. Reynolds M, Frost MC, and Meyerhoff ME. Nitric oxide-releasing hydrophobic polymers: preparation,characterization, and potential biomedical applications. Free Radical Biology & Medicine, 2004; 37: 926-936

13. Singh RJ, Hogg N, Joseph J, Kalyanaraman B. Mechanism of nitric oxide release from S-nitrosothiols. J Biol Chem 271: 1859-6603, 1996

14. Major TC, Brant DO, Burney CP, Amoako KA, Annich GM, Meyerhoff ME,

Handa H, and Bartlett RH. The hemocompatibility of a nitric oxide generating polymer that catalyzes S-nitrosothiol decomposition in an extracorporeal circulation model. Biomaterials 2011;32: 5957-5969

CHAPTER IV

DEVELOPMENT AND BIOCOMPATIBILITY TESTING OF NITRIC OXIDE-GENERATING HOLLOW FIBER ARTIFICIAL LUNG

4.1 Introduction

In Chapter III, we learned the following: Cu incorporation into gas exchange fiber walls lead to NO generation, smaller particle sizes of Cu at the same wt% yield higher NO flux levels, and localization of Cu particles close to outer surface of fibers increases NO flux levels. This knowledge was applied to the development of the first NO-generating artificial lung. Thrombogenicity testing of NO generating surfaces has been studied in the past, but only in large-bore high-flow and low surface area ECC circuits and never in artificial lungs with low flows and high surface areas. A single-layer fiber structure and 50 nm Cu particles were employed for developing the artificial lung because of manufacturability and the fact that the highest NO generation from fibers fabricated in the previous chapter was observed in single layer fiber group containing 50 nm Cu particles.

NO generating artificial lungs require evaluation in terms of their inhibition of clot formation as current artificial lung solutions for clot reduction, although decades old, have not worked without some form of clotting complication or bleeding in patients

requiring respiratory support for reasons including lung diseases. About 400,000 Americans die from lung diseases such as acute respiratory distress syndrom (ARDS), chronic obstructive pulmonary disease (COPD), cystic fibrosis and bronchopulmonary dysplasia every year [1]. Mortality rates in ARDS patients alone range from 25 - 40% of 190,000 Americans afflicted with the disease each year. Also 4.2% COPD patients in America do not survive the disease per year. The only treatment for these diseases in their end-stage conditions is transplantation, but unfortunately the limited pool of available donor lungs makes it impossible to treat all patients. As a result about 300 patients waitlisted for lung transplantation loose their lives before treatment every year [2]. Bridge-to-lung transplantation strategies like total artificial lung (TAL), arteriovenous CO_2 removal ($AVCO_2R$) and extracorporeal membrane oxygenation (ECMO) are able to provide respiratory support for these patient population only for a couple of weeks without replacement of their gas exchange devices. New methods intended for reducing clot formation inside artificial lungs may lead to fewer device replacement, and thus extend the functional lifespan of the artificial lung. Patient populations given short-term respiratory support, without systemic anticoagulation or with a limited use of it, can also benefit from devices that remain clot-free during long-term use.

The gas exchange materials of these respiratory support devices are capable of modifying venous blood to arterial conditions by providing oxygen and removing CO2 [3-6]. However, none of these fibers are sufficiently biocompatible to allow a single device to be used for more than two weeks to one month. Their contact with blood can lead to clotting complications, and poor gas exchange [7-10]. For example, the MC3 Biolung when used as a TAL showed a 300% increase in resistance from baseline, and warranted device repalcement, on average, every 9.5 ± 2.1 days [11]. In addition, clot shedding led to ischemic regions in the kidney. Membrane lungs with antithrombotic coatings are available,[12-16] but unfortunately the coatings have not

worked well enough to eliminate the frequent device replacement due to clot formation or eliminate the need for systemic anticoagulation.

In this work NO generation artificial lungs were fabricated by modifying their gas exchange silicone fibers with Copper. Copper (Cu) particles dispersed in their gas exchange fiber walls catalyze circulating s-nitrosothiols to generate NO locally as shown in Figure 4.1 [17-19]. The NO generating artificial lung was inserted into an extracorporeal circulation (ECC) circuit that was similarly coated with the NO generating material, and the circuit was evaluated for their thrombogenicity during a 4 h ECC in rabbits

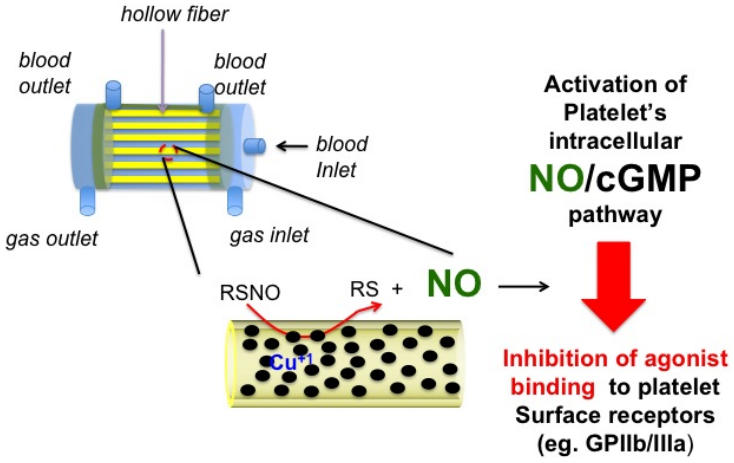

Figure 4.1: Model of Cu-mediated NO generation from circulating S-nitrosothiols by hollow fiber membrane lungs for platelet inhibition

4.2 Materials and Methods

4.2.1 Design of NO-Generating Hollow Silicone Fiber Oxygenator

A radial flow artificial lung design was constructed with NO generating or non-NO generating silicone hollow fibers. NO generating fibers were doped with 50 nm Cu particles at 10 wt% and non-NO generating fiber had no Cu. In the radial flow design, blood flows through an annular hollow fiber bundle (see Figure 4.2). This

design constraints blood to flow radially outward through the fiber bundle thereby reducing shunting or channelling across the bundle, thus ensuring blood perfusion throughout. Blood enters the device through the bottom inlet and flows within a 1/4" polyester bundle core serving as a central passageway oriented along the axis of the fiber bundle. Blood is then directed radially outward through the bundle driven by a pressure difference between the central core and an outer passageway or gap between the outside of the bundle and the oxygenator housing. Blood is collected and oriented toward the oxygenator outlet(s) at one side of the oxygenator. The fiber bundle porosity of all NOgen prototypes (% of volume occupied by blood in the bundle over total volume of the bundle) were fixed at 10%.

Standard hollow fiber oxygenator fabrication methods were used to manufacture the NO-generating lungs at Medarray Inc.

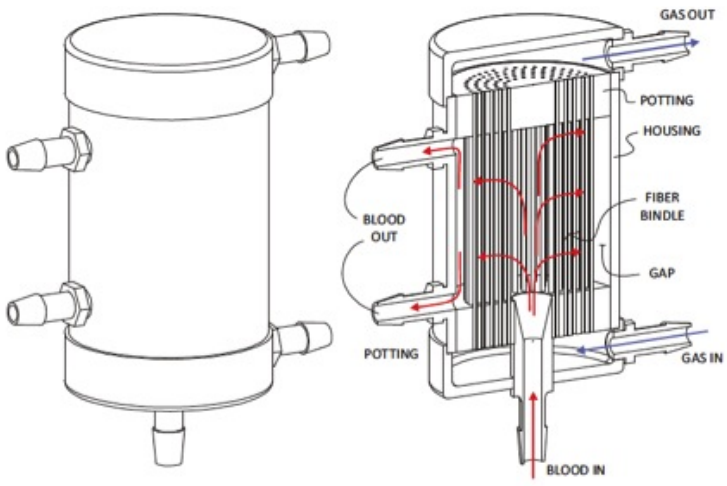

Figure 4.2: Design of radial flow ECMO oxygenator (Borrowed with permision from Medarray Inc).

In brief, a spool of NO generating and non-NO generating fibers were woven into a mat with an industrial capacity knitter. The fiber mats were then rolled over the meshed cylindrical polyester bundle core. This bundle assembly was potted within a polycarbonate housing inside an 80 Gs centripetal force centrifuge. The potted

devices were then purged of their PVC fiber cores using a constant flow of water jet (25 Psi, 70 °C). All devices were then leak teasted as they underwent an aggressive purging process during PVA core romval. Defective fibers demonstrating water leaks were plugged at both ends with polyurethane. Gas flow end caps were then attached at the ends of each device (see Figure 4.2) to have them ready to be incorporated into extracorporeal circulation circuits (ECCs).

4.2.2 ECC Circuit Components

The ECC circuit is an arterio-venous (AV) shunt shown in Figure 4.3. From the inlet to the outlet, it consisted of a 16 gauge angiocath, 1/4" luer lock PVC connector, 3" long 1/4" ID tygon tubing, a 1/4" - 1/4" luer lock straight polycarbonate connector, 3" long 1/4" ID tygon tubing, the artificial lung (SA = 0.09 m^2), and 1" and 2" long 1/4" ID tygon tubings connecting to a 1/4" - 1/4" - 1/4" Y polycarbonate connector, 3" long 1/4" ID tygon tubing, a 1/4" - 1/4" leur lock straight polycarbonate connector, 1/4" leur-lock PVC connector, and a 14 gauge angiocath all connected in series. The NO generating shunts were coated tip-to-tip with our NO-generating material (50 nm Cu particles in silicone) following the same synthesis procedure described in Figure 3.1. The tygon tubing were however difficult to coat with silicone. Therefore, small pieces of tubing were dissolved in THF (1g per 3mL THF), and then the Cu nano particles were blended into the dissolved material. The resin were then coated onto the tubing. All coated tubing sections were cured under ambient temperature for 48 hours. The NO-generating and control shunts are shown in Figures 4.3B and 4.3A respectively.

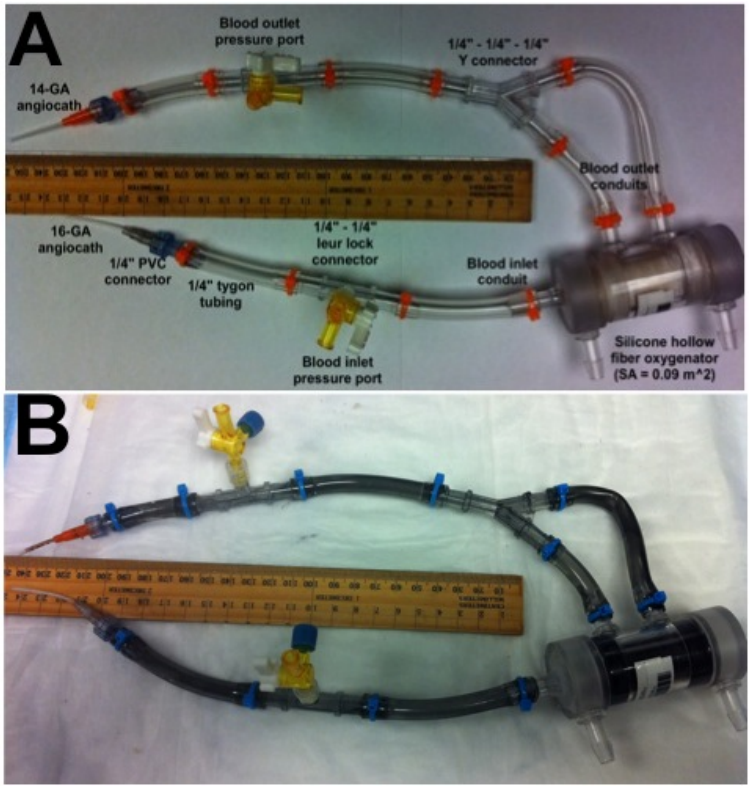

Figure 4.3: Extracorporeal circulation circuits: Control (clear) and NO-generating (bottom)

4.2.3 Measurement of NO Flux from Fibers

NO generation were measured from 1 cm long tubing samples (N = 5/NO generating and non-NO generating surfaces), and from 1 cm long fibers (N=5/NO generating and non-NO generating type) using the same NO measurement techniques described in section 3.3.4 of Chapter III. In brief, NO released from the surface was measured through a chemiluminescence reaction using a Seivers nitric oxide analyzer (NOA), model 280 (Boulder, CO). A nitric oxide donor, S-nitrosoglutathione (GSNO) was first prepared by reacting equimolar glutathione (GSH) and $NaNO_2$ in 0.06 M H_2SO_4. Next, the GSNO (1 μM), 30 mM GSH and 5 mM EDTA were added to an amber reaction vessel containing phosphate-buffered saline (PBS, pH= 7.34) at 37 °C. EDTA was used to chelate any trace metal ions that may be present in the solution. The

solution was then purged with nitrogen gas and the output gas was swept to the NOA through an air-tight sampling line at 200 ml/min. Baseline measurements were taken for 5 minutes before samples were introduced into the GSNO rich solution. The NO generated from the reaction between Cu ions and GSNO was continuously swept to the NOA and recorded over time. Inside the NOA, the NO content in the output gas is reacted with ozone to produce oxygen and a high energy unstable NO gas. To achieve a thermodynamically stable state, each unstable NO molecule releases a photon which is counted to measure the concentration of NO produced by the samples. NO concentration was continuously measured, and a peak NO flux was calculated by dividing the sample surface area into the peak rate of NO generation.

4.2.4 Rabbit Thrombogenecity Model for Testing ECC Circuits

The animal handling and surgical procedures were approved by the University Committee on the Use and Care of Animals in accordance with university and federal regulations. A total of 10 ECC circuits (N=5/group) were tested for thrombogenecity using 10 adult New Zealand male rabbits (Myrtle's Rabbitry, Thompson's Station, TN). All rabbits (2.5-3.5 kg) were initially anesthetized with intramuscular injections of 5 mg/kg xylazine injectable (AnaSed Lloyd Laboratories Shenandoah, Iowa) and 30 mg/kg ketamine hydrochloride (Hospira, Inc. Lake Forest, IL). Maintenance anesthesia was administered via a diluted intravenous (IV) infusion of ketamine (2 mg/ml) at a rate of 1.53 mg/kg/hr. In order to maintain normal blood pressure, Lactated Ringers solution was given at a rate of 33 ml/kg/hr. A tracheotomy was performed with a 5mm OD trach tube, and the rabbit was placed on a Sechrist Infant Ventilator Model IV-100 (Anaheim, CA). The paralytic, pancuronium bromide (0.33 mg/kg, IV), was then administered to ensure that the rabbit would not over-breathe the ventilator. For monitoring blood pressure and collecting blood samples, the rabbit right carotid artery was cannulated using a 16-gauge IV angiocatheter (Jelco®, Johnson

and Johnson, Cincinnati, OH).

Blood pressure and derived heart rate were monitored with a Series 7000 Monitor (Marquette Electronics Milwaukee, WI). Body temperature was monitored with a rectal probe and maintained at 37°C using a water-jacketed heating blanket. Prior to placement of the AV ECC shunt, the rabbit left carotid artery and right external jugular vein were isolated, and hemodynamic data was recorded. Arterial blood pH, pCO_2, pO_2, total hemoglobin and methemoglobin were then measured using an ABL 725 blood gas analyzer and OSM3 Hemoximeter (Radiometer Copenhagen Copenhagen, DK). In addition, baseline blood samples were collected for platelet and total white blood cell (WBC) counts utilizing a Coulter Counter Z1 (Coulter Electronics Hialeah, FL), plasma fibrinogen levels measured by a Dade Behring BCS Coagulation Analyzer (Siemans Deerfield, IL), activated clotting time (ACT) using a Hemochron Blood Coagulation System Model 801 (International Technidyne Corp. Edison, NJ) and platelet aggregation using a Chrono-Log optical aggregometer model 490 (Havertown, PA).

The ECC was primed with saline solution and 6U/ml of heparin sulfate and placed into position by cannulating the left carotid artery for ECC inflow and the right external jugular vein for ECC outflow. Blood flow through the ECC was started by unclamping the arterial and venous sides of ECC and blood flow in circuit was monitored with an ultrasonic flow probe (1/4" ME6PXN) and flow meter (Transonic HT207 Ithaca, NY). The rabbits were then given a heparin bolus (300U/kg, IV) followed by a 10U/kg/hr heparin infusion to maintain ACTs between 350-400 seconds. In addition, 0.1182 μmol/kg/min infusion of the NO donor, S-Nitroso-N-acetylpenicillamine (SNAP), was started immediately after the ECC blood flow was initiated. After four hours on ECC plus either saline or SNAP infusion, the circuits were clamped, removed from animal, gently rinsed with 60 ml of saline and drained. Any residual thrombus in the larger tubing of ECC (i.e., thrombogenicity chamber)

was photographed. All rabbits then received a dose of 400 U/kg sodium heparin to prevent necrotic thrombosis, were euthanized with Fatal Plus (130 mg/kg sodium pentobarbital; Vortech Pharmaceuticals Dearborn, MI), and underwent gross necropsy to examine the lungs, heart, liver and spleen for any signs of thromboembolic events.

4.2.5 Blood sampling

Rabbit whole blood samples were collected in non-anticoagulated 1 cc syringes for ACT, 10% anticoagulant containing sodium citrate, sodium phosphate and dextrose (ACD) (Hospira,Inc. Lake Forest, IL) in 3 cc syringes for cell counts, aggregometry and FACS analysis and 1 cc syringes containing 40 U/ml of sodium heparin (APP Pharmaceuticals, LLC Schaumburg, IL) for blood gas analysis. Every hour up to 4 hours, following the initiation of ECC blood flow, blood samples were collected for in vitro measurements. Samples were used within 2 hours of collection to avoid any artifactual activation of platelets, monocytes or plasma fibrinogen.

4.2.6 Plasma Fibrinogen

Plasma fibrinogen plays an important role in clot formation as it forms interconnecting bridges for platelet adhesion. Soluble fibrinogen concentration in control and NOgen ECC circuits plasma samples were measured at baseline and every hour for 4 hours using a BCS XP System hemostasis analyzer (Siemens Healthcare Diagnostics, Deerfield, IL). Briefly, lyophilized bovine thrombin (Dade Behring, Deerfield, IL) was prepared according to Dade thrombin reagent kit instructions and added to plasma samples. The clotting time of plasma (time taken to convert soluble fibrinogen into insoluble fibrin), inversely proportional to fibrinogen concentration, was measured with the BCS XP System and then compared to that of standardized fibrinogen concentrations of human plasma (Chrono-Log Corp. Havertown, PA).

4.2.7 Platelet aggregometry

Rabbit platelet aggregation was assayed based on Born's turbidimetric method using a Chrono-Log optical aggregometer. The method used was previously described [**23**]. Briefly, citrated blood (1:10 blood to ACD) was collected (6 mls) and platelet-rich plasma (PRP) was obtained by centrifugation at 110 x g for 15 min. Platelet-poor plasma (PPP) was obtained by another centrifugation of the PRP-removed blood sample at 2730 x g for 15 min and was used as the blank for aggregation. PRP was incubated for 10 min at 37°C and then 40 mg/ml collagen (Chrono-PAR #385 Havertown, PA) was added. The percentage of aggregation was determined 3 min after the addition of collagen using Chrono-Log Aggrolink software.

4.2.8 Measurement Plasma Copper

The in vitro plasma copper assay (DICU-250, Gentaur, Accurate Chemical & Scientific Corporation New York, NY) was performed in a 96-well format to determine the amount of copper leaching from the ECC over the 4 hour experimental period. Briefly, both baseline and 4 hour plasma samples were treated with 30% trichloroacetic acid. Samples were centrifuged at 14,000 RPM for 5 minutes and 100 μl of the supernatant was collected. Each sample was diluted 1 : 2 with deionized water and 100 μl placed in a 96-well plate. A copper standard (1.5 mg/dl CuSO4) was serial diluted and 100 μl of each concentration, ranging from 0-300 μg/dl, was placed in separate wells. A working reagent mix containing 0.9% ascorbic acid, 0.1% 4,4-Dicarboxy-2,2-biquinoline, 2% NaOH and 8% Hepes-free acid was then added to each well of the 96-well plate and then mixed. After a 5 minute incubation, absorbance measurement of the plate was performed at 359 nm on a Synergy 2 microplate reader (Biotek Winooski, VT). All measurements were done in duplicate. Using a linear regression curve from a copper standard (0-300 μg/dl), sample copper concentrations were calculated.

4.2.9 Measurement of Blood Flow Resistance

To monitor blood flow resistance inside artificial lung prototypes, real time pressure drop across the devices was measured with a Biopac MP150 data acquisition system (Linton Instrumentation, UK). Briefly, primed line pressure transducers (Hospira Inc. Lake Forest, IL) were connected to the device's inlet and outlet stopcocks (see Figure 4.3). The pressures were recorded at the onset of blood flow, at every 5 minutes during the first hour of flow, and at every 30 minutes for the 4 h test duration. Resistance to blood flow inside the device was calculated as the pressure drop (mmHg) across the device devided by blood flow rate (ml/min).

4.2.10 Statistical Analysis

The statistical program, SPSS, was used to analyze significance in means of outcomes data. Mixed model analysis with repeated measures was used to compare dependent dependent variables (platelet count, plasma fibrinogen, and blood flow resistance) between subjects (10 wt% of NOGen and control ECC circuits). Time effects on dependent variables were analyzed within groups. A p-value < 0.05 is regarded as significant.

4.3 Results

4.3.1 NO generating Artificial Lung Prototype and their NO generation

The prototype of nitric oxide generating hollow silicone fiber oxygenator is shown in Figure 4.4. As briefly described in oxygenator design phase (section 4.2.1), blood enters the device through the blood inlet conduit, radially flows around the NO-generating hollow fibers and exits through the two outlet conduits on the side of the device. Gas also flows into the device through the gas inlet, then through the hollow fibers and exits through the gas outlet. Its path length is about 1.1 cm and the axial

length is about 2.7 cm. The fiber packing fraction is 0.33. All NO-generating lungs as well as controls had a prime volume of 20 cc and a total membrane surface area of 0.09 m^2. The gas exchange silicone fibers of the NO-generating lung, as opposed controls, appear dark due to the copper nanoparticles incorporated into their walls.

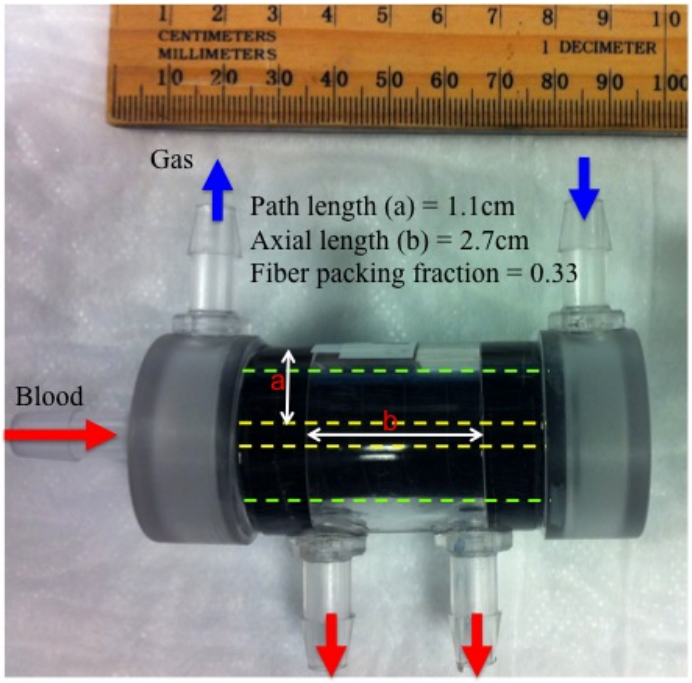

Figure 4.4: Prototype of nitric oxide generating hollow silicone fiber oxygenator

4.3.2 NO Flux from Fibers

The NO flux from 10 wt% 50 nm Cu particle doped fibers and coated ECC tubing were (12 ± 4 and 14.7 ± 2.5) x 10^{-10} mol cm^{-2} min^{-1} respectively. Their control counterparts showed no NO release.

4.3.3 Survival of NOgen and Control ECCs

The Kaplan-Meier survival for flow in control and NOgen ECC circuits is shown in Figure 4.5. All NOgen ECC circuits stayed patent for the entire test duration. In contrast, after 30 minutes of blood flow initiation, 2 control ECC circuits totally

occluded stopping flow and thus ending their thrombogencity test. Another control ECC circuit occluded after 60 minutes. On the other hand, all N = 5 NOgen ECC circuits were stayed patent at the during the 4-hour test period.

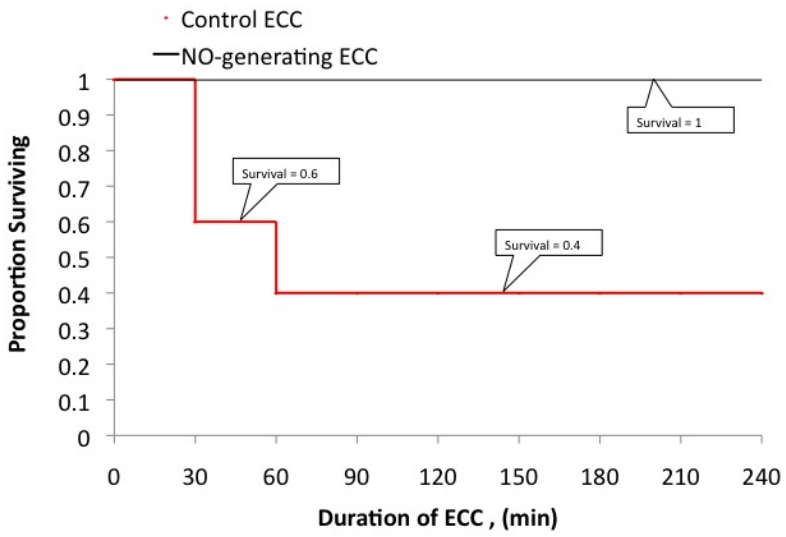

Figure 4.5: Survival of control and experimental ECC circuits after flow initiation.

During ECC, the resistances within the circuits were monitored to further evaluate thrombogenic differences in NOgen and control groups. The in-vivo average resistance results of control and NOgen ECC circuits are discussed in detail in section 4.3.6.

4.3.4 Thrombogenecity Outcomes

Platelet consumption, plasma fibrinogen concentration, and copper leached into plasma over the course of the experiment is shown in Figures 4.6, 4.7 and 4.9 respectively.

Platelet consumption: The preservation of platelets during any blood-contact application is one of the evaluational parameters for determining the overall thrombogenecity of the application/biomaterial. Platelet preservation as measured with a Coulter counter in terms of the concentration of platelets in circulation on an hourly

basis showed a general decline. This method of evaluating platelet preservation basically compared baseline to post-baseline platelet concentrations to determine how many platelets were lost to adhesion and adsorption. This method is insensitive to the state of aggregation and location of adsorption.

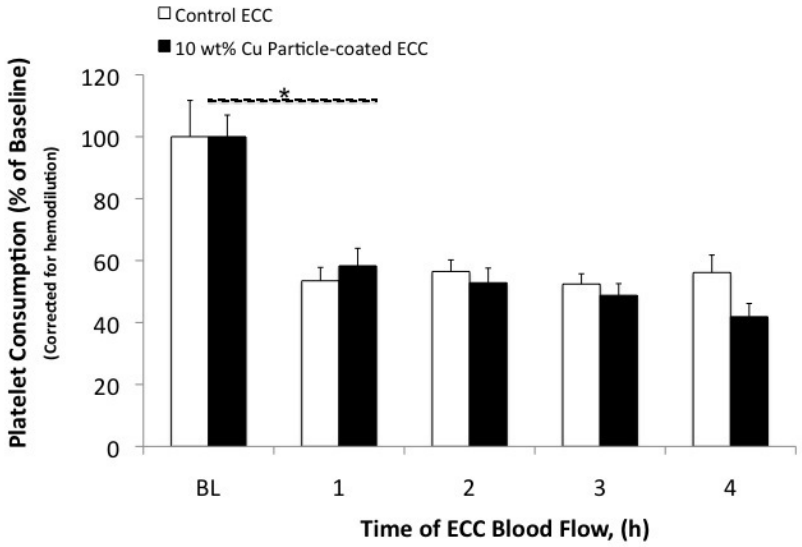

Figure 4.6: ECC circuits' platelet consumption during blood flow.

It is important to note in Figure 4.6 that only an N=2 control ECC circuits survived the 4 h test duration. The remaining 3 circuits clotted off within an hour. Hence the use of mixed model analysis to better determine significance in outcomes. In both control and NOgen ECC groups, platelet counts dropped significantly ($p < 0.05$) from baseline to 58.3 $\pm$ 5.6% and 53.5 $\pm$ 4.3% respectively after an hour of extracorporeal circulation. The effect of wt%Cu on platelet count approached significance ($p=0.055$), but a larger N size (>5) may reveal it's true effect. In the test duration, there was no time effect, as a function of wt%Cu, on platelet count within groups ($p>0.05$).

Plasma fibrinogen: The time-course concentration of plasma fibrinogen as shown in Figure 4.7 indicate the conversion of fibrinogen into fibrin. After 1 hour on ECC,

there was a significant reduction in plasma fibrinogen from baseline in both control and NOgen circuits ($p < 0.01$). The intra-group time-dependent fibrinogen level remained unchanged after an hour ($p < 0.01$) in both groups. However there was a significant difference between the inter-group time-dependent fibrinogen levels ($p < 0.05$). In the NOgen ECC circuits more fibrinogen was polymerized than in controls perhaps due to increased fibrinogen attraction to and activation at a more charged and irregular surface. No time effect, as a function of wt%Cu, on plasma fibrinogen concentration was observed (p=0.24).

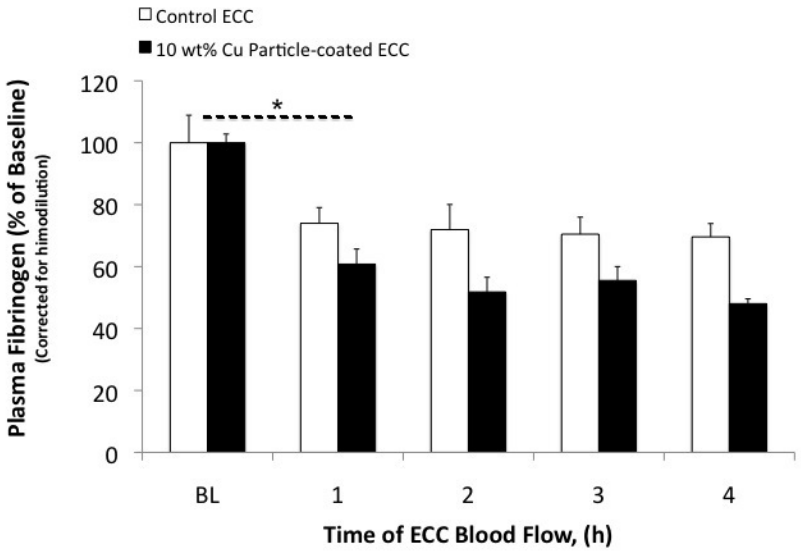

Figure 4.7: Levels of plasma fibrinogen concentration during extracorporeal circulation

The total surface area contacted by blood is also a relevant assessment parameter for thrombogenecity of ECC circuits because 1) blood activation and coagulation is both time and surface sensitive and 2) a fair comparison can still be made between different ECC groups regardless of group survival. As shown in Figure 4.8 there was a drastic difference in total surface area contacted by blood in the control and NOgen ECC groups. The total blood-contacted surface area in control group is significantly

smaller than the NOgen group after 30 minutes of ECC ($p < 0.05$).

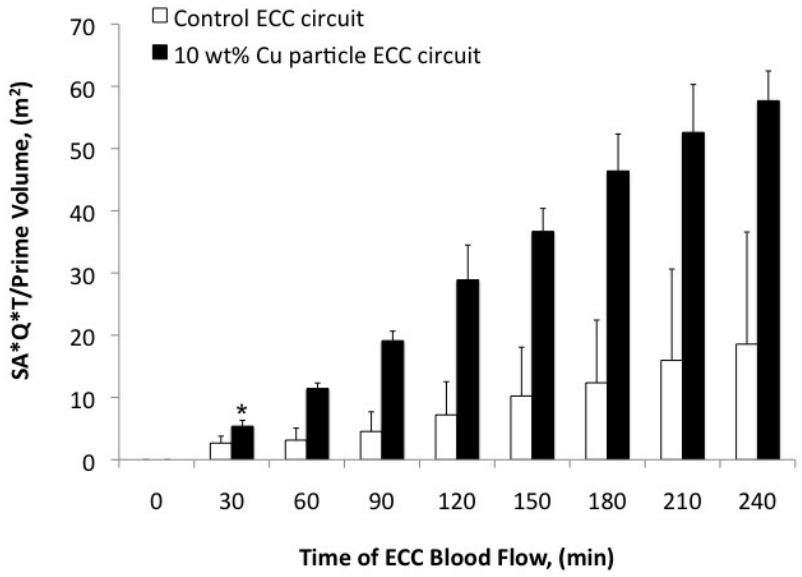

Figure 4.8: Time course of blood flow

The difference was even more significant ($p < 0.001$) at 4 hours of circulation since all 5 NOgen and only 2 control ECC circuits maintained flow. Taken together, the Kaplan-Meier survival, platelet consumption and total-blood-contacted surface area data indicate worse thromboses in the control ECC circuits. In general, less blood contact with a biomaterial due to clotting leading to stopage of blood flow through an ECC circuit also implies no platelet consumption. Therefore for the control and NOgen ECCs to have comparable platelet consumption but significantly different total-blood-contacted surface area due to increased resistance and stopage of flow in controls means the state of platelet activation/aggregation was different in both groups.

4.3.5 Plasma Copper Concentration:

Plasma copper concentrations measured during extracorporeal circulation through the NOgen circuits is shown in Figure 4.9). Serum copper levels at the onset of blood

flow in control group (132.8 ± 4.5 μg/dl) and NOgen group (134.7 ± 22.5 μg/dl) were not significantly different ($p < 0.01$). They were also about 6 fold lower than the acceptable daily copper intake for adults. As expected baseline copper levels was maintained after 4 hours ($p < 0.01$) in the control group. However, plasma copper levels in the NOgen group significantly ($p < 0.001$) increased from baseline by 2.8 folds.

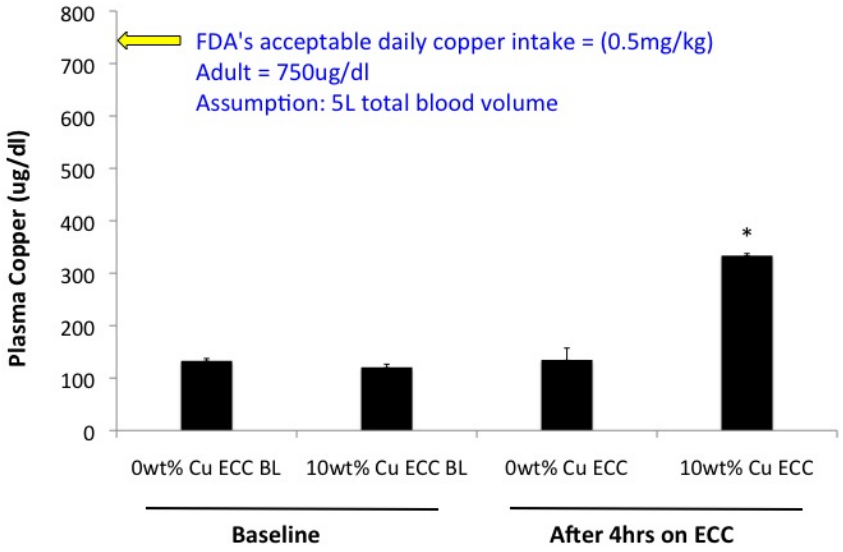

Figure 4.9: Levels of plasma copper at baseline and at the end of extracorporeal circulation

4.3.6 ECC Blood Flow and Artificial Lung Resistance

Comparisons of the intra-group and inter-group time-dependent average resistance were made to determine differences between ECC circuit groups and within groups. The resistance in the NOgen circuits (black bars) and control circuits (white bars) is shown in Figure 4.10. At the onset of ECC blood flow, the resistances in the controls (0.08 ± 0.06 mmHg min/mL) and NOgen ECC circuit (0.05 ± 0.02 mmHg min/mL) were not different ($p < 0.05$). These values were consistent with pre-ECC resistance measurements with water flow. Also, there was no difference in the time-dependent

resistance from baseline within the NOgen group after 4 hours of ECC ($p < 0.01$). In the Control group, post baseline resistance were all significantly higher than baseline resistance ($p < 0.01$). After 30 minutes of ECC, the resistance of the control group was significantly higher (21 ± 9 mmHg min/mL, $p < 0.01$) than that of the NOgen group (0.07 ± 0.02 mmHg min/mL). This difference in significance is also maintained through out the rest of the experimental time.

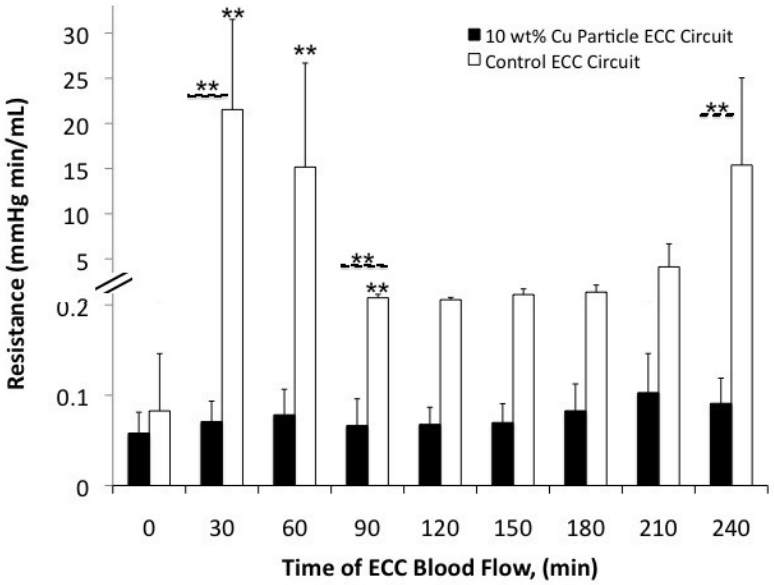

Figure 4.10: Time course of control ECC resistance to blood flow

As shown in Figure 4.11, there was no difference between baseline blood flow in control (63.6 ± 8.04 mL/min) and in NOgen (70.2 ± 28.1 mL/min) circuits at baseline ($p = 0.62$) indicating similar cardiac function in rabbit populations used in both groups. The dramatic differences seen after baseline is a not a function of cardiac output but rather the differences in inter-group ECC resistance represented in Figure 4.10. In the NOgen group, flow was stable during the entire experiment. There was no significant difference in baseline and post-baseline flows within the NOgen ECC group ($p = 0.07$). However in the control group, post-baseline flow were significantly lower than baseline flow ($p < 0.01$).

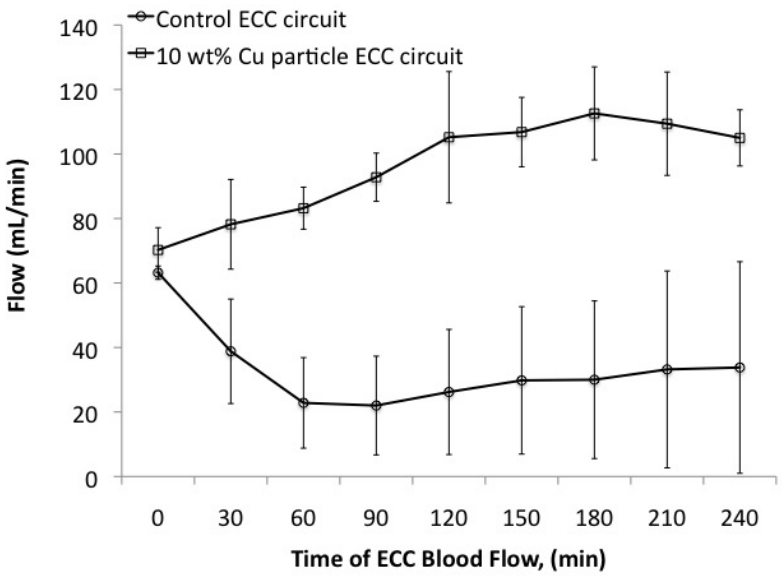

Figure 4.11: Time course of blood flow

The time-course ECC resistance and flow clearly show a dramatic difference between the NOgen circuit group and the control group. The NOgen group maintained baseline flows and resistance during the 4 hour study. These parameters have an important effect on organ perfusion and heart function during extracorporeal membrane oxygenation in general. In pulmonary artery - left ventricle ECMO attatchment mode for instance, the right heart can failure due to loading from highly resistive circuits. In addition limited blood flow to organs can cause hypoxia and irreversible organ damage.

4.4 Discussion

The aim of this study was to develop a copper mediated NO-generating hollow fiber membrane lung and evaluate its non-thrombogenicity in an extracorporeal circulation set up. The results indicate that the NO-generating ECC circuits were less thrombogenic than their non NO-generating controls.

Nitric oxide generation from NOgen circuits was controlled against non-NO gen-

erating circuits. The NO flux from 10 wt% Cu NOgen fibers and 10 wt% Cu coated PVC tubings making up the NOgen circuit were 12 ± 4 x 10^{-10} mol cm^{-2} min^{-1} and 14.7 ± 2.5 x 10^{-10} mol cm^{-2} min^{-1} respectively. These levels of NO flux produced by the NOgen ECC circuits have been previously shown to reduce thrombogenecity [24], and are also higher than levels produced by the endothelium. The importance of copper expression on the surface of silicone for efficient NO generation has already been described in section 3.5. Briefly, Cu-mediated NO generation at the surface of silicone requires a physical interaction between RSNOs and Cu ions produced by Cu corrosion at the polymer's surface. The effect of surface exposure of copper on NO flux is demonstrated in Chapter II, and was important for NO generation from Cu-doped silicone fibers.

NO generating ECC circuits group were patent for the duration of the study while the survival of control circuits dropped to 40% after an hour of circulation. The modified ECC circuits also showed significantly lower resistance compared to the control group. Resistance in control circuits were, on average, almost two orders of magnitude larger (x 87.4) than that in the NO generating group. Accordingly, flows in the control group was significantly lower than the NOgen group after baseline. Larger clot formation in the control increased their resistance to flow and subsequently occluded the devices. Platelet consumption in the ECC groups as measured with a coulter counter interestingly showed insignificant differences between the groups. This piece of data is contradictory to the global thrombogenicity differences observed between the groups. This contradiction is due to the fact that the coulter counter method for measuring platelet proved insensitive to the degree of platelet aggregation. It measures platelet concentration by counting flowing platelets through a 3 - 4 μm gated channel specific to the size of a single platelet. Any body bigger in diameter is not counted. It is therefore possible to measure a 50% drop in platelet count for two different samples; one with aggregates of two platelets per aggregate and the other

with massive aggregates. However these two states of aggregation will have very different physiological effect as low levels of activation lead to more transient responses. This insensitivity in detecting low level aggregation can obscure differences in aggregation degrees and thrombogenecity evaluation as evident in the control and NOgen groups. In the NOgen ECC group, these platelet microaggregates are prevented from growing into macroaggregates because of the anesthetic effect of nitric oxide being generated at the blood/polymer interface. That was why their circuit resistance and flow remained at baseline levels through out the experiment.

The results also indicate that plasma fibrinogen is lost to the NOgen environment more than in controls. The decrease in fibrinogen adsorption perhaps is due to a rougher blood/NOgen polymer interface owing to surface copper particles or due to a stronger charge interaction between the polymer surface, where an oxidation-reduction reaction is constantly taking place, and the polar terminals of plasma fibrinogen in flowing blood. The mechanisms of interaction among the NOgen surface, NO generation and fibrinogen activation is however still not clear [24].

Blood activation and subsequent coagulation on biomaterials depends on duration of exposure and other factors. When the duration of exposure is expressed in terms of total blood contacted surface area in ECC circuits, the inter-group thrombogenicity difference can be further evaluated. As shown in Figure 4.8, blood essentially resided on a surface area 3.10 x larger in the NOgen group than in the control group (18.02 $\pm$ 4.78 m^2). For surfaces with stark differences in thrombogenecity, this evaluational parameter further characterizes blood coagulation in flow conditions as shown in this study. It is however not helpful when evaluating the non-thrombogenecity of ECC circuits with equal flow rates and survivals.

Although copper is an essential trace element present in normal diet, excess of it in serum can be toxic and can have detrimental health effects. Since the entire surface of the NOgen group is coated with 10 wt% Cu nanoparticles to mediate NO

generation from circulating RNSOs, it was therefore important to monitor the amount of copper that may leach into blood. At the blood/polymer interface, it is free copper ions at the polymer surface that undergo oxidation/reduction reaction to catalyze NO generation and therefore leaching of copper. According to the food and drug administration (FDA), about 2mg copper per day is required by the average adult with an acceptable daily intake of 0.5mg per kg body weight. This implies that in a 75kg man with say 5L total blood volume, the acceptable daily total Cu intake is 37mg. This will yield a blood copper concentration of 750 μg/dl. The amount of leached copper at 4 hours was 333 $\pm$ 3.9 μg/dl. This plasma copper level is still 2.25 times lower than the acceptable daily intake.

The purpose of heparin administration in the form of a bolus and infusion was to target ACTs between 350 - 400 seconds. This level of ACT is comparable to the ACT regiment ($>$ 400 seconds) during cardiopulmonary bypass but greater than normal range of ACTs (180 - 200 seconds) during ECMO. Earlier in the protocol development of this study it was observed that not using systemic anticoagulation to increase ACTs above 300 seconds in addition to local NO generation from NOgen ECC circuits, all test ECC circuit groups clotted off. This was, perhaps, due to the fact that the NOgen ECC circuits had a rougher surface from the presence of copper particles. We currently do not know if that observation was entirely because of surface roughness effects or because the fiber bundle housing and core was not coated with the NO generation material. This must be further investigated by top-coating the NOgen fibers and NOgen tubings with a thin layer of hydrophilic polymer to smoothen the fibers' surface. This top coat must be thin enough to allow hydration, corrosion, and ionization of copper at the blood/polymer interface. Coatable housings and bundle cores must also be used for further studies so that NO is generated from tip-to-tip of the test circuit.

Finally the inclusion of copper particles in the gas exchange fibers changes the

original material properties of silicone. The most pertinent material property for oxygenators is the gas transfer. Although the ECC devices were not used for oxygenation in this study, their gas transfer were evaluated by flowing nitrogen gas on blood side and nitric oxide in nitrogen sweep gas on the gas side. NO transferred across the membrane to the blood side was swept into a nitric oxide analyzer where the NO concentration was measured. NOgen lung gas transfer was reduced by 32% compared to silicone control lungs. This reduction in gas transfer due to a change in material property may not significantly affect gas transfer due to secondary flow design of hollow silicone fiber oxygenators. However further testing using blood is necessary to determine the gas transfer performance of NOgen lungs.

4.5 Conclusion

This study evaluated the first Cu-mediated NO generating hollow silicone fiber lung in an extracorporeal circulation setup. The results indicate that NO-generating hollow fiber lung significantly reduces blood coagulation compared to their nonNO-generating controls. Blood flow in controls was significantly lower and their resistance was higher than the NOgen ECC circuit group due to massive and occlusive blood clots in contol circuits. Futhermore the amount of copper leached into plasma over the course of the experiment was 2.25 x less than the acceptable daily intake of copper.

4.6 References

1. American Lung Association: Lung Disease Data 2008.

2. www.transplantliving.org, 2009

3. Toomasian JM, Schreiner RJ, Meyer DE, Schmidt ME, Hagan SE, Griffith GW, Bartlett RH and Cook KE. A polymethylpentene fiber gas exchange for long-term extracorporeal life support. ASAIO Journal 51: 390-397, 2005.

4. Bartlett RH. Extracorporeal life support registry report 1995. ASAIO Journal 43:104-107,1997.

5. Fischer S, Hoeper MM, Tomaszek S, Simon A, Gottlib J, Welte T, Haverich A and Strueber M. Bridge to lung transplantation with the extracorporeal membrane ventilator Novalung in the veno-venous mode: The initial Hannover experience. ASAIO Journal 53:168-170, 2007.

6. Wang D, Lick SD, Campbell KM, Loran DB, Alpard SK, Zwischenberger JB and Chamberst SD. Development of ambulatory arterior-venous carbon dioxide removal (AVCO2R): the downsized gas exchange prototype for ambulation removes enough CO2 with low blood resistance. ASAIO Journal 51:385-389, 2005.

7. Conrad SA, Zwischenberger Grier LR, Alpard SK and Bidani A. Total extracorporeal arteriovenous carbon dioxide removal in acute respiratory failure: a phase I clinical study, Intensive Care Med 2001;27: 1340-1351

8. Vaslef SN Implantable artificial lungs: fantasy or feasibility. Landes Biosciences 2001; 116-126

9. Zwischenberger JB, Conrad SA, Alpard SK, Grier LR, Bidani A. Percutaneous extracorporeal arteriovenous CO2 removal for severe respiratory failure. Ann Thorac Surg. 1999; 68:181-7

10. Wang D, Lick SD, Zhou X, Liu X, Benkowski RJ, Zwischenberger JB. Ambulatory Oxygenator Right Ventricular Assist Device for Total Right Heart and Respiratory Support. The Annals of Thoracic Surgery, 2007: (84);1699-1703

11. Sato H, Hall C, Lafayette NG, Pohlmann JR, Padiya N, Toomasian JM, Haft JW and Cook KE. Thirty-day in-parallel artificial lung testing in sheep. The Annals of Thoracic Surgery 84:1136-1143, 2007.

12. Larson DF, Arzouman D, Kleinert L, Patula V and Williams S. Comparison of Sarns 3M heparin bonded to Duraflo II and control circuits in a porcine model: macro- and microanalysis of thrombi accumulation in circuit arterial filters. Perfusion 2000, 15:13-20

13. Larm O, Larsson R, Olsson P. Biomater. Med. Devices Artif. Organs 1983, 11: 161-173

14. Tayama E, Hayashida N, Akasu K, Kosuga T, Fukunaga S, Akashi H, Kawara T, Aoyagi S. Artif. Organs 2000, 24:618-623

15. Engbers GH, Feijen J. Int. J. Artif. Organs 1991, 14:199-215

16. Palanzo DA, Zarro DL, Manley NJ, Montesano RM, Quinn M, Elmore BA, Gustafson PA, Castagna JM. Effect of Carmeda-BioActive surface coating versus TrilliumTM Biopassive surface coating Bypass coating of the oxygenator on circulating platelet count drop during cardiopulmonary bypass. Perfusion 2001; 16; 279-283

17. Colman RW, Hirsh J, Marder VJ, Clowes AW, and George NJ. (2001) Hemostasis and Thrombosis: Basic Principles & clinical Practice, 4th Edition: Lippincott Williams & Wilkins, Philadelphia, PA, USA.

18. Wu Y, Rojas AP, Grifth GW, Skrzypchak AM, Lafayette N, Bartlett RH and Meyerhoff ME. Improving blood compatibility of intravascular oxygen sensors via catalytic decomposition of S-nitrosothiols to generate nitric oxide in situ. Sensors and Actuators B: Chemical121: 36-46, 2007

19. Oh BK, Meyerhoff ME. Catalytic generation of nitric oxide from nitrite at the interface of polymeric films doped with lipophilic Cu(II)-complex: a potential route to the preparation of thromboresistant coatings. Biomaterials 25: 283-293, 2004

20. Napoli C, De Nigris F, Williams-Ignarro S, Pignalosa O, Sica V and Ignarro L J. Nitric oxide and atherosclerosis: An update. Nitric Oxide15: 265-279, 2006

21. Rabelink TJ and Luscher TF. Endothelial Nitric Oxide Synthase, Host Defense Enzyme of the Endothelium? Arterioscler Thromb Vasc Biol 26: 267-271, 2006

22. Major TC, Brant DO, Reynolds MM, Bartlett RH, Meyerhoff ME, Handa H, Annich GM. The attenuation of platelet and monocyte activation in a rabbit

model of extracorporeal circulation by a nitric oxide releasing polymer. Biomaterials 2010;31:2736-2745

23. Major TC, et al., The hemocompatibility of a nitric oxide generating polymer that catalyzes S-nitrosothiol decomposition in an extracorporeal circulation model, Biomaterials (2011), doi:10.1016/j.biomaterials.2011.03.036

24. Grunkemeier JM, Tsai WB, McFarland CD, Horbett TA. The effect of adsorbed fibrinogen, fibronectin, von Willebrand factor and vitronectin on the procoagulant state of adherent platelets. Biomaterials 2000;21:2243-2252.

CHAPTER V

NON-THROMBOGENIC CHARACTERIZATION OF EXTRUDED NITRIC OXIDE RELEASING SILICONE CATHETERS

5.1 Abstract

Intravascular catheters used in clinical practice can activate platelets, leading to thrombus formation and stagnation of blood flow. Nitric oxide (NO) releasing polymers have been shown previously to reduce clot formation on a number of blood contacting devices. In this work, trilaminar NO-releasing silicone catheters were fabricated and tested for their thrombogenecity. All catheters had specifications of L = 6 cm, inner diameter = 21-gauge (0.0723 cm), outer diameter = 12-gauge (0.2052 cm), and NO-releasing layer thickness = 200 ± 11 m. Control and NO-releasing catheters were characterized in vitro for their NO flux and NO release duration by gas phase chemiluminescence measurements. The catheters were then implanted in the right and left internal jugular veins of (N=6, avg. weight = 3kg) adult male rabbits for 4h thrombogenicity testing. Platelet counts and function, methemoglobin (metHb), hemoglobin (Hb), white cell counts and functional time (defined as patency

time of catheter) were monitored as measured outcomes. NO-releasing catheters (N=6) maintained an average flux above (2 0.5) x 10 $^{-10}$ mol min^{-1} cm^{-2} for over 24 h whereas controls showed no NO release. MetHb, Hb, white cell and platelet counts and platelet function at 4h were not significantly different from baseline (α = 0.05). However clots on controls were visibly larger and prevented blood draws at a significantly ($p<0.05$) earlier time (2.3 $\pm$ 0.7 h) into the experiment whereas all NO-releasing catheters survived the entire 4h test period. Results indicate that catheter NO flux levels attenuated thrombus formation in a short-term animal model.

5.2 Introduction

There are 500,000 admissions to neonatal intensive care units in the U.S. each year. Most of these babies require management through central venous, umbilical venous or umbilical artery catheter access for the administration of either one or a combination of the following: total parenteral nutrition, chemotherapy, fluid, blood products, and life-saving medications [1]. These catheters are commonly made up of poly(vinyl chloride) (PVC), polyurethane, or silicone rubber. Despite best practices, these catheters are often compromised because of infection, thrombosis, complications leading to an increase in morbidity, extended hospital stay, and mortality, in some cases [2 - 5]. The risk of complication associated with catheterization is even higher in population of predominantly premature neonates [6] whose haemostatic system is not yet matured [7 - 8]. The overall rate of catheter occlusion is estimated to be 2.0 per 1,000 catheter days [9]

Current attempts in clinical practice to prevent clot formation involve heparin flushing through indwelling catheters. Although its use can be appreciated, heparin is a systemic-acting anticoagulation agent associated with bleeding in patients [10]. Its effect can be especially problematic in infants because of the potential risk of inadvertent overdose. Occluded catheters that cant be cleared with heparin are locked

with thrombolytics like urokinase to break down clots. The catheters are locked for hours [11] before flushing, and thereby interrupt vascular access for as long as it takes to flush out clots from indwelling catheters if they are simply not removed. Despite the relatively high potency of thrombolytics, there are still cases where catheters remain partially occluded after 2h of thrombolytic locking [11].

Our attempt to improving antithrombotic properties of catheters is through surface release of nitric oxide (NO). NO is a free radical gas produced by the endothelium to maintain hemostasis [12 - 15]. Because the gas is both lipophilic and small it freely diffuses into the platelet across its bilipid membranes to initiate several inhibitions of enzymatic reactions necessary for platelet activation[16 -20]. It activates the NO/cGMP pathway that, in turn, phosphorylates G protein-coupled surface receptors, changing their conformation to decrease binding affinities of agonists. Commonly known G protein-coupled receptors on platelets include thrombin, thromboxane A2, and adenosine diphosphate receptors. The gas also reduces secondary activation of circulating platelets by inhibiting the release of platelets of intracellular granules. This is achieved by blocking the release of calcium stores needed for actin-myosin interaction required for platelets to change shape and release their granules. Unlike other platelet inhibitors, NO has a very short halflife (milliseconds), as it is quickly taken up by RBCs, platelets, and other NO scavengers. Thus, the anticoagulant effect occurs near the NO releasing/generating surface and elicits no effect on coagulation downstream.

The property of NO release has been imparted to catheters through surface coatings. This can be problematic in terms of the duration of NO release especially in pediatric catheters with small diameters. In this case only a thin layer of the NO releasing material can be coated onto pediatric commercial catheters, and therefore NO release will last for short durations. In this work, the NO releasing material was incorporated into the wall of small diameter silicone rubber catheters for prolonged

release. Specifically, the catheters were extruded with chemistry incorporated within that enables post-extrusion charging with NO to create NO releasing dizeniumdiolate structures within the walls of the extrude catheter. The controlled NO release from the catheters was measured in vitro by chemiluminescence and finally a 4h biocompatibility testing of NO-secreting catheters and controls was conducted using a rabbit model of thrombogenecity without systemic anticoagulation.

5.3 Materials and Methods

N-(6-aminohexyl) aminopropyl trimethoxysiloxane (N-(6-aminohexyl) aminopropyl-trimethoxysiloxane (DACA-6)), potassium tetrakis(4-chlorophenyl) borate, phosphate buffer saline, and tetrahydrofuran (THF) were purchased from Sigma Aldrich (St Louis, MO). The two part silicone resin was purchased from nuSil Silicone Tech (Carpinteria, CA). The fumed silica particles were purchased from Sigma Aldrich (St Louis, MO) and the stainless steel mandrel was a product of Small Parts Inc. (Marimar, FL). The 21-gauge angiocaths that were bonded to the extruded catheters were purchased from Infusion Therapy Systems Inc. (Sandy, Utah).

5.3.1 Structure and Composition of NO-releasing Catheters

All extruded catheters had a trilayer structure; a base-layer, an active-layer, and a top-layer. The active layer, where NO molecules are immobilized, is sandwiched between the base and top layers as shown in Figure 5.1. The compositions of the base, active and top layers are shown in Table 5.1. The base layer consisted of silicone resin oligomers A and B in a 1:1 ratio and 5 wt% fumed silica to add stiffness to the catheters. The active layer contained 1:1 silicone resin A to B, 15 wt% DACA-6 and 11 wt% by mole of DACA-6 of potassium tetrakis(4-chlorophenyl) borate. Only silicone (1:1 resin A to B) was used as the top-coating material.

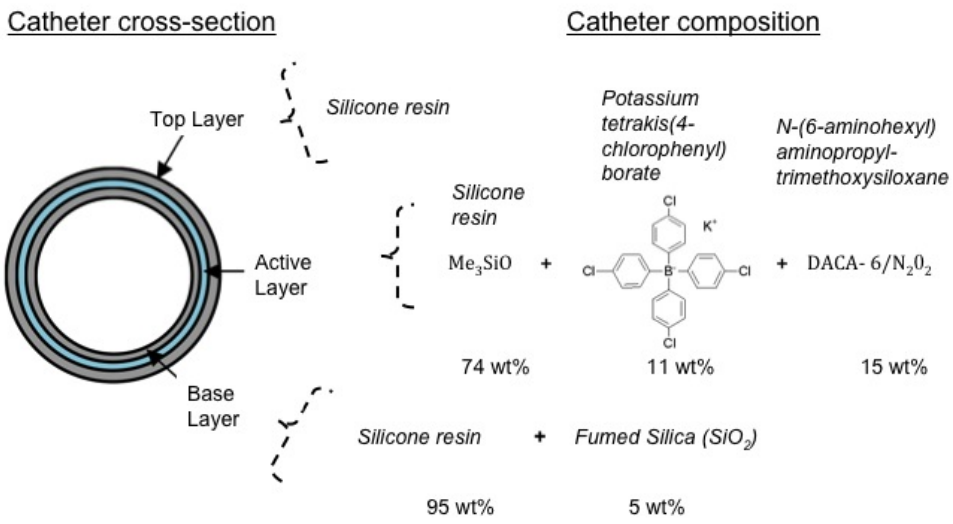

Figure 5.1: Cross sectional composition of nitric-oxide-releasing catheters

Table 5.1: Chemical composition of base, active and top layers of nitric oxide releasing catheter

Catheter Layer	Resin A	Resin B	Fumed Silica	DACA-6	Borate
Base Layer	**1 part**	**1 part**	**5 wt%**	**-**	**-**
Active Layer	**1 part**	**1 part**	**-**	**15 wt%**	**11 wt% by mole of DACA-6**
Top Layer	**1 part**	**1 part**	**-**	**-**	**-**

The base, active and top layers were sequentially extruded during fabrication of the catheters. The catheter fabrication process is shown in Figure 5.2. Stainless steel mandrels (21 gauge) were used as cores over which catheter material was extruded using a setup with a fixed aperture size through which mandrels are passed. After extrusion and curing, the stainless steel cores were removed leaving behind the experimental catheters. For extrusion of the base layer, 10 cm long stainless steel mandrels were hand-fed through the catheter fabrication setup. After three passes, a uniform coat over the mandrels was achieved. The mandrels are then stationed vertically and cured at 500 F for 30 min. The cured base layers were then slid off the mandrels

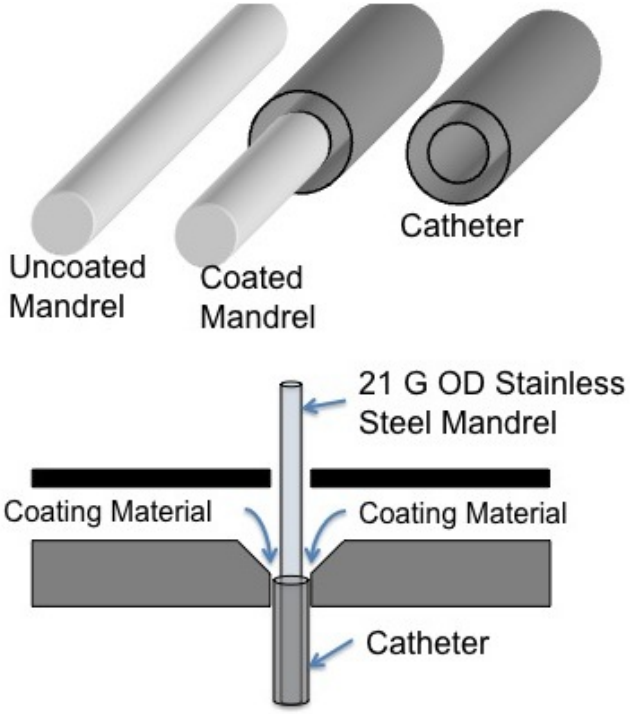

Figure 5.2: Setup for Extruding Nitric Oxide Releasing Silicone Catheters.

after immersion in water for 2 h. The newly formed catheter base layers were left to dry in a drying hood for 30 min before the active layer was extruded over the base-layer. The thickness of the active layer was achieved after 2 passes through the extruder. The 2 layers were dried in ambient temperature for 24 h. Finally, to remove any surface irregularities, the top layer was added with a single pass. The extruded catheters were then dried in a fume hood for 48 h before charging the NOreleasing group with nitric oxide.

5.3.2 Nitric Oxide Charging of Catheters and NO-release Testing

The method used to charge the active layers with NO has been previously described [21]. In brief, the NO-releasing catheter group were charged with NO using a NO reactor (80 psi of $NO_{(g)}$) whereas the control group, having the same structure and composition as the NO-releasing group, were not charged with NO. Catheters were kept in the reactor for 72 h to allow the NO molecules to react with DACA-6.

The catheters were then immediately tested for their NO release by chemiluminescence. NO release testing by chemiluminesence has also been described in [22]. In brief, 1 cm long sections of the NO-reacted catheters were bathed in a chelex-treated PBS, pH 7.34, at 37°C. NO released was then measured with a Sievers Nitric Oxide Analyzer 280i (GE instruments Boulder, CO). The NO release signal was integrated over a given time, and knowing the surface area of the catheter, the flux of NO from the surface can be readily calculated as NO concentration per unit time divided by the total surface area of the catheters. Since all catheters were implanted 24h after charging, their NO release after 24h of dry storage in -20°C environment was also tested. To test whether DACA-6 is essential for immobilizing NO molecules during charging, catheters without DACA-6 (N=3) were charged and tested for their NO release. In addition, to test whether borate was needed to stabilize NO release, catheters prepared with active layers of 5% and 15% DACA-6 without borate (N=3 each) were also charged and tested for NO release.

5.3.3 Preparing Catheters for Non-thrombogencity Evaluation

All catheters, controls and NO-releasing, were cut to 6 cm long sections and connected to a 21-gauge angiocatheter. Part of the commercial catheter was dipped in THF and inserted into one end of the extruded catheter to bond the interface. This assembly process was necessary for controlled and leak-free blood draws and infusions using luer-lock syringes. The catheters were then stored in a -20°C fridge to reduce spontaneous NO loses.

5.3.4 Rabbit Thrombogenicity Model for Testing of Catheters

The animal handling and surgical procedures were approved by the University Committee on the Use and Care of Animals in accordance with university and federal regulations. A total of 6 New Zealand white rabbits (Myrtle's Rabbitry, Thomp-

sons Station, TN) were used in this study. All rabbits (2.5-3.5 kg) were initially anesthetized with intramuscular injections of 5 mg/kg xylazine injectable (AnaSed Lloyd Laboratories Shenandoah, Iowa) and 30 mg/kg ketamine hydrochloride (Hospira, Inc. Lake Forest, IL). Maintenance anesthesia was administered via a diluted intravenous (IV) infusion of ketamine at a rate of 15 mg/kg/h. In order to maintain blood pressure stability, intravenous (IV) Lactated Ringers solution was given at a rate of 10 ml/kg/h. The paralytic, pancuronium bromide (0.2 mg/kg, IV), was administered to have the animal totally dependent upon mechanical ventilation which was done via a tracheotomy and using a Sechrist Infant Ventilator Model IV-100 (Sechrist, Anaheim, CA). For monitoring blood pressure and collecting blood samples, the rabbit right carotid artery was cannulated using a 16-gauge IV angiocatheter (Jelco, Johnson & Johnson, Cincinnati, OH). Blood pressure and derived heart rate were monitored with a Series 7000 Monitor (Marquette Electronics Milwaukee, WI). Prior to placement of the catheters, the rabbits left and right internal jugular veins were isolated and baseline hemodynamics were recorded. Arterial blood pH, pCO_2, pO_2, total hemoglobin and methemoglobin were determined using an ABL 725 blood gas analyzer and OSM3 Hemoximeter (Radiometer Copenhagen Copenhagen, DK). In addition, baseline blood samples were collected for platelet and total white blood cell (WBC) counts utilizing a Coulter Counter Z1 (Coulter Elec- tronics Hialeah, FL), ACT was determined using a Hemochron Blood Coagulation System Model 801 (International Technidyne Corp. Edison, NJ), and platelet function was determined using a Chrono-Log optical aggregometer model 490 (Havertown, PA). Animals had no systemic anticoagulation throughout the experiment.

After baseline blood measurements, catheters were placed 1 cm distal to the bifurcation of the right and left jugular vein. A control and an NO releasing catheter were placed in each animal, and the placement was varied so that 3 animals had controls on the right internal jugular vein and 3 animals had controls in the left internal jugu-

lar vein. The catheters were locked with 0.9% saline (Hospira Inc, Lake Forest, IL). At 20 min intervals, each catheter was tested for its ability to allow blood draw and saline infusion using a 1cc luer-lock syringe. Each animal received a 400 U/kg sodium heparin dose prior to euthanasia to prevent necrotic thrombosis. The animals were euthanized using a dose of Fatal Plus (130 mg/kg sodium pentobarbital) (Vortech Pharmaceuticals Dearborn, MI). The internal jugular veins were dissected out from the site of catheter entry to approximately 1 cm below the end of the catheter. The jugular vein was cut parallel to the length of the catheter, and the catheter was removed. The catheters were photographed and a 1 cm section of the tip of the catheter was preserved in glutaraldehyde for obtaining a scanning electron micrograph (SEM).

5.3.5 Blood sampling

Rabbit whole blood samples were collected in non-anticoagulated 1 cc syringes for ACT, 10% anticoagulant containing sodium citrate, sodium phosphate and dextrose (ACD) (Hospira, Inc. Lake Forest, IL) by volume of blood collected in 3 cc syringes for cell counts, aggregometry and FACS analysis and 1 cc syringes containing 40 U/ml of sodium heparin (APP Pharmaceuticals, LLC Schaumburg, IL) for blood gas analysis. Every hour up to 4 h, following placement of the catheters, blood samples were collected for *in vitro* measurements. Samples were used within 2 h of collection to avoid any artifactual activation of platelets and monocytes. Also all data collected after baseline was corrected for the hemodilution effect of IV fluids.

5.3.6 Platelet Aggregometry

A previously published method [**21**] for platelet aggregometry was used to assess platelet function. In brief, rabbit platelet aggregation was assayed based on Borns turbidimetric method using a Chrono-Log optical aggregometer. Citrated blood (1:10 blood to ACD) was collected (6 mL) and platelet-rich plasma Platelet-Rich Plasma

(PRP) was obtained by centrifugation at 110 g for 15 min. Platelet-poor plasma Platelet-Poor Plasma (PPP) was obtained by another centrifugation of the PRP-removed blood sample at 2730 g for 15 min and was used as the blank for aggregation. PRP was incubated for 10 min at 37°C and then 40 mg/mL collagen (Chrono-PAR No 385 Havertown, PA) was added. The percentage of aggregation was determined 3 min after the addition of collagen using Chrono-Log Aggrolink software.

5.3.7 Statistical Analysis

One-way ANOVA with repeated comparison of the means using Tukeys post hoc tests were done to compare the dependent variables between the NO-releasing and control catheter groups. A p-value < 0.05 is regarded as significant.

5.4 Results

5.4.1 Extruded Catheter

The finished catheter shown in Figure 5.3A was partly filled with a mixture of water and blue food dye for perspective visualization. The extruded NO releasing portion of the catheter, left of the demarcation, was connected to a 21 ga angiocath. All implanted catheters had the following dimensions: L= 6 cm, ID = 21-guage (0.723 mm), and OD = 12-gauge (2.052 mm). A cross secitonal representative is shown in Figure 5.3B. The lumen is to the top left corner followed by the base, active, and top layers. Since the NO flux of the catheters is dependent on the amount of DACA-6 and subsequent in-situ diazeniumdiolation of the secondary amine site of this species, the thickness of the active layers was measured. The opaque active layer thickness averaged 200 ± 11 μm (N= 6 catheters).

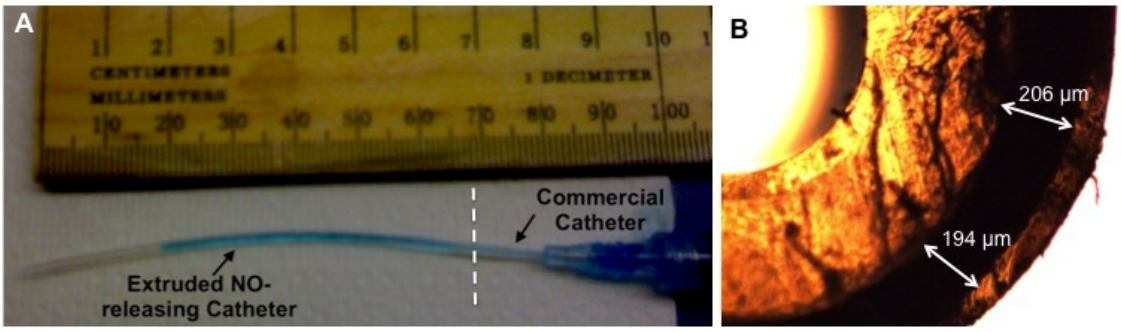

Figure 5.3: Extruded silicone-rubber nitric-oxide-releasing catheter, a) and cross section of catheter, b).

5.4.2 NO Release from DACA-6 Doped Silicone Catheters

NO release from control and NO-charged catheter groups is shown in Figure 5.4. As expected control catheters did not release NO whereas NO-charged catheter secreted NO for the test duration. On average (N = 6) NO releasing catheters released NO at a flux of ca. 6 ± 0.92 x 10^{-10} mol min^{-1} cm^{-2} steadily for first 4 h of testing.

After 24 h of dry storage in a -20 °C freezer, the flux levels dropped to ca. 2 ± 0.5 x 10^{-10} mol min^{-1} cm^{-2} on average (N=6). In brief, the NO flux from catheters increased for the first two hours until the release rate peaked. Thereafter, the NO stores within the walls of the catheters started to be depleted gradually for the remainder of the *in vitro* test period.

The outcomes of the effects of DACA-6 and borate on NO release are shown in Figures 5.6 and 5.5. Catheters without borate did release larger bursts of NO within an hour but thereafter released relatively lower flux levels of NO. The addition of borate helped reduce this burst for a more sustained NO release profile (Figure 5.4). The catheters prepared without DACA-6 did not release significant levels of NO after charging. Low levels of NO release were measured from these catheter types, likely because of NO gas has high solubility in silicone rubber materials. However, this temporary storage of NO dissipates very quickly during NO release testing. NO flux density (NO), (x 10 -8 mol/cm2), of catheters was function of wt% DACA-6 according to the relationship $NO = 0.38(\text{wt\% DACA-6}) + 0.21$, $R2 = 0.99$ (See Figure 6). Higher NO flux levels were sustained for over 24h at 40wt% borate inclusion compared to no borate.

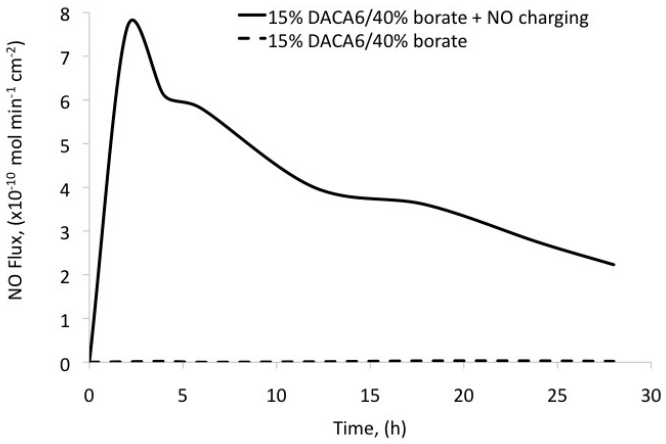

Figure 5.4: Nitric oxide release from control catheters (15%DACA-6, 40%borate by mole of DACA-6, uncharged) and NO releasing catheters (15%DACA-6, 40%borate by mole of DACA-6, NO charged) as measured by chemiluminescence. Control catheter samples were bathed in a chelex-treated phosphate buffer saline (pH 7.34, 37°C) medium and NO release was measured with a Nitric oxide analyzer

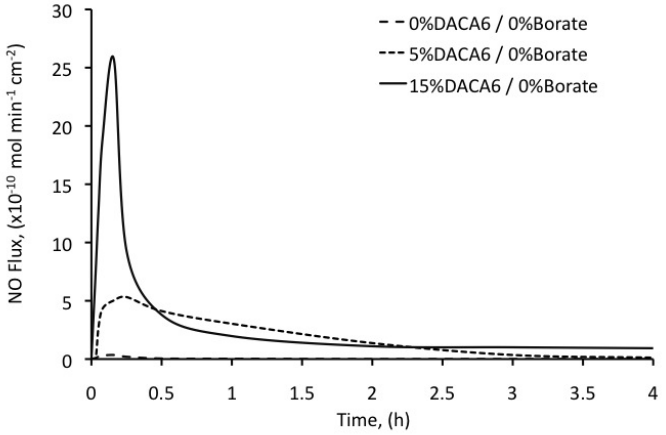

Figure 5.5: Nitric oxide release from catheters(0%DACA-6 and 0%borate, 5%DACA-6 and 0%borate, 15%DACA-6 and 0%borate) as measured by chemiluminescence. Catheter samples were bathed in a chelex-treated phosphate buffer saline (pH 7.34, 37°C) medium. NO released was measured with a Nitric oxide analyzer

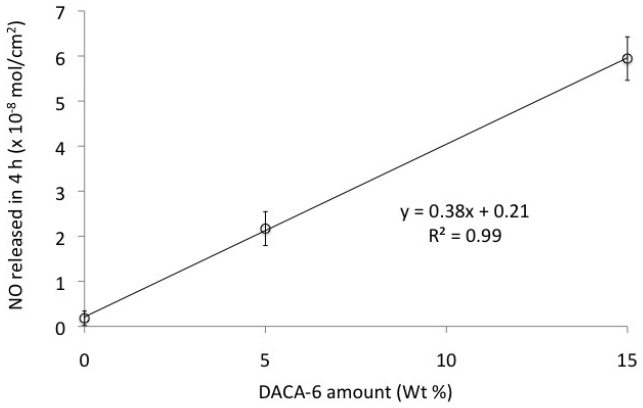

Figure 5.6: NO flux density of NO-releasing catheters as a function of their wt% of DACA-6 amounts

5.4.3 Thrombogenicity Testing Outcomes

All NO-releasing silicone catheters lasted the entire duration of the thrombogenecity testing. There were no blood-drawing or saline-infusion incidents with any of the NO-releasing catheters. However 4 out of 6 control catheters became occluded before the end of the in vivo testing experiments. Catheter occlusion was interpreted as the first time when blood draw was totally impeded. Further investigations for clots on the occluded catheters using SEMs and photography were also performed after carefully dissecting out the implanted catheters. Representative images of clots on implanted control catheters and explanted control and NO-releasing catheters are shown in Figures 5.7 and 5.8.

Biological markers such as metHb, Hb, WBC count, platelet count and platelet function, frequently used to measure NO toxicity, inflammation, and blood activation, were collectively used for a general evaluation of the biocompatibility of the catheters. MetHb ($p = 0.1$), WBC count ($p = 0.8$), platelet counts ($p = 0.2$) and platelet function ($p = 0.9$) at 4h were not significantly different from baseline ($\alpha = 0.05$). Basically the surface area (3.9 ± 0.4 cm^2) of the catheters are so small that 4 h of blood exposure is not long enough to effect significant changes in those biological markers.

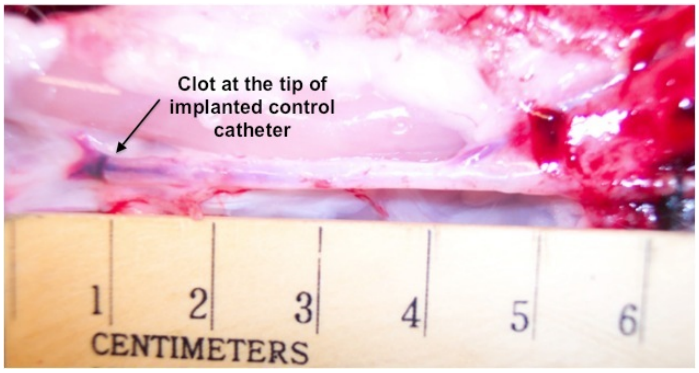

Figure 5.7: Clots on control catheters after 4hr - implantation in the jugular vein of adult New Zealand male rabbits

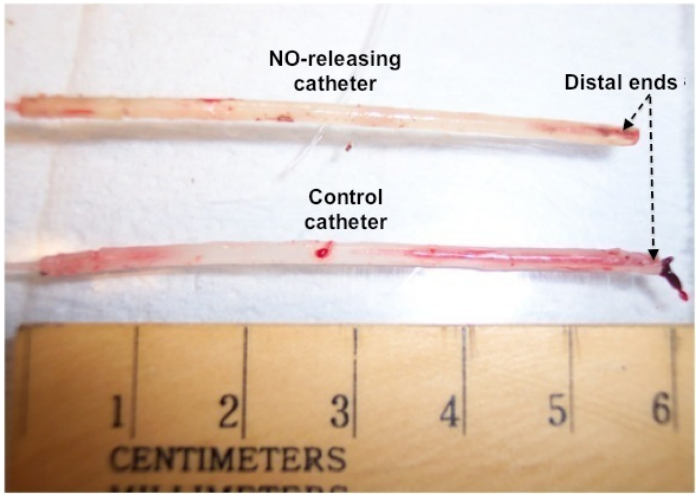

Figure 5.8: Clots on control and NO-releasing catheters. All NO-releasing catheters showed no occlusive clots at their tips after explantation (top) whereas control catheters (bottom) got completely occluded by clots before the end of the 4hr-experiments.

Hemoglobin, however, did decrease by a significant amount (14%, $p < 0.05$) after 4 h due to hemodilution.

An important evaluation parameter of any catheter is its ability to remain patent. In our study, the average time until the first blood draw incident occurred was termed the patency time. All NO-releasing catheters remained functional after 4 ± 0 h whereas the controls' functional time averaged 2.3 ± 0.7 h (Figure 5.9). There was a 100% survival in the NO-releasing group and 33.33% in the control group.

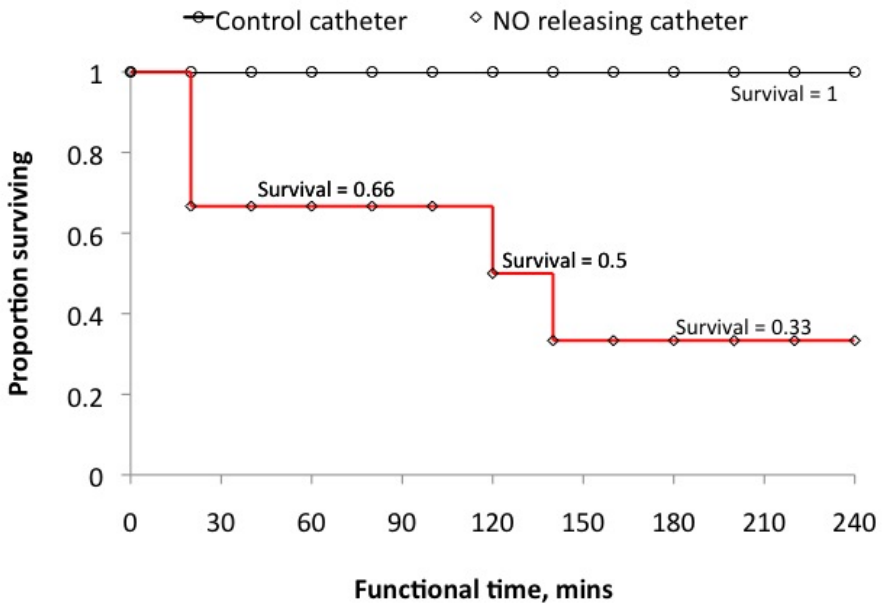

Figure 5.9: In vivo functional time of control and NO-releasing catheter groups. Functional time was interpreted as average time until first blood draw incident per catheter group

5.5 Discussion

Research is needed to develop small (21 to 24 gauge) intravascular catheters that function similar to vascular endothelium, producing nitric oxide locally, preventing development of biofilm, repelling platelets and preventing thrombus formation. The risks of clotting and infection with current catheters occur in all patients (including children and adults), but the problem is most serious in newborns because the vessels are so narrow that even a small thrombus can occlude the catheter, and because the newborns host response to bacterial infection is not fully developed.

Preventing these risks would have a major impact on neonatal care, and even greater impact on all patients who require intravascular catheters. It would decrease morbidity and mortality, and decrease costs by shortening hospital stay while increasing survival. Creating catheters from materials that are highly resistant to thrombus

and biofilm formation would solve these major problems. Current approaches do not eliminate these problems. Catheters with heparin bonded to the surfaces are available [23 25], but systemic heparin injections/infusions are still required. Catheters coated with antiseptics or antibiotics are available [26], and do decrease the risk of infection somewhat, but do not prevent biofilm formation on the outer surface of the catheter in contact with blood/tissue. Catheter-related sepsis (or the possibility of catheter sepsis requiring catheter removal) is still a major problem in the hospital setting [26].

The results of this study suggest that NO-releasing catheters attenuate thrombus formation in a short-term animal model, and that such catheters can be fabricated by extrusion with the precursors for NO release chemistry incorporated in to the walls of the catheters.

Key properties of the extruded catheters are the level of NO flux they secrete and the duration of the NO secretion. The levels of NO release from catheters (6 x10 $^{-10}$ mol min^{-1} cm^{-2}) after NO charging and (ca 2 x 10^{-10} mol min^{-1} cm^{-2}) after 24h of dry storage were comparable to endothelial level of NO flux. Although the catheters were stored dry and at a low temperature (-20°C) to reduce spontaneous release of NO, there was a 66.7% decrease in flux levels when tested after 24 h. Therefore such storage condition may not be ideal for long- term storage as most of the stored NO may be lost. In this study, however, the levels of NO release after 24 h storage proved adequate for maintaining catheter patency.

If further improvements in the NO release profile are necessary, they might be achieve by adjusting the thickness of the active layer, the availability of anionic borate sites in the active layer, and the NO charging conditions. The effect of catheter wall thickness is already explained above. The inclusion of anionic sites in the active layer sustains NO release by keeping the microenvironment of the catheters in a more acidic condition [27]. Anionic agents such as borate (used in this study), dibutyltin dilaurate (DBTDL), and the United States Food and Drug Administra-

tion approved poly(lactic-co-glycolic acid) (PLGA) are currently being investigated in detail to determine what levels allow sustained NO release from hydrophobic polymers doped with diazeniumdiolates for a 30 d period. Their stability may also be important in keeping the acidic conditions necessary for sustained release. For instance slow-degradation-rate PLGAs may serve as a better regulator of NO release than a faster-degradation-rate PLGA. Lastly, the optimal charging time of these catheters are, at this point, unknown and needs to be examined in detail. The method of loading NO into catheters was based on previous work on silicone membranes [21]. A combination of longer NO charging and high NO-payload amines with stable anionic sites may improve the longevity of NO release from catheters.

The short-term rabbit model used to test the biocompatibility of catheters is a well-developed model that allowed for monitoring an array of biological markers. There are however some improvements that can be made. For example, the 20-min blood withdrawal test interval may mask true differences between control and test catheters, as forming clots maybe broken up before they grow into larger occlusive masses. Blood draws could be done every hour, instead, such that clots have a greater duration to form. This methodology would be more aggressive in teasing out differences in performance between catheter test groups but would require an animal model with catheter placement lasting for a longer period of time (e.g., 8-24 h). Therefore, the next step in testing these extruded NO-releasing catheters should focus on longer-term outcomes using appropriate animal models. The longer term model would also allow for examination of the antimicrobial effects of the NO-releasing catheters. This measure will be added during the longer-term thrombogenicity testing.

5.6 Conclusion

The goals of this study were to investigate the following: fabrication of silicone catheters, NO charging of catheters to release endothelial levels of NO in a con-

trolled environment, characterization and investigation of how to control NO flux and non-thrombogenic evaluation of the NO-releasing catheters in vivo. The catheter fabrication process was adequate for the manufacturing of silicone catheters for non-thrombogenic evaluation. Quality controls built into the fabrication process ensured the manufacturing of 12 gauge OD catheters that could be implanted into the right and left internal jugular veins in adult rabbits. Since the catheters walls were fabricated in layers, chemistry could be incorporated into their active layers to allow loading of NO into their walls. NOcharged catheters also released endothelial levels ($> 2 \times 10^{-10}$ mol min^{-1} cm^{-2}) of NO upon stimulation in a PBS solution (37°C, pH = 7.34). Their NO flux, as measured by chemiluminescence, showed that 1) NO flux depended of DACA-6 concentration and 2) high levels of sustained NO release depended on borate inclusion. NO flux density (NO), ($\times 10^{-8}$ mol cm^{-2}), of catheters was function of wt% DACA-6 according to the relationship NO = 0.38(wt% DACA-6) + 0.21, $R^2 = 0.99$. In addition higher NO flux levels were sustained for over 24h at 40wt% borate inclusion compared to no borate. Overall, 100% of the NO-releasing catheters survived the 4h test duration compared to a 33% survival of the non-NO releasing controls. For NO-releasing catheters to find use in both pediatric and adult care, fabrication of NO-releasing catheters with ODs as small as 21 gauge should be investigated. The duration of NO release should also be studied in order to extend their patency up to 30 d and beyond. To get there, different NO immobilizing compounds and anionic sites must be investigated.

5.7 Reference

1. Bass J, Halton J, Drouet Y, Ni A, Barrowman N. Central venous catheter database: an important issue in quality assurance. Journal of Pediatric Surgery 2011; 46, 942945.

2. Wiener ES, McGuire P, Stolar JH, et al. The CCSG prospective study in venous access devices: an analysis of insertions and causes for removal. J Pediatr Surg 1992;27:155-64.

3. Hollyoak MA, Ong TH, Leditschke JF. Critical appraisal of surgical venous access in children. Pediatr Surg Int 1997;12:177-82.

4. Dillon PA, Foglia RP. Complication associated with an implantable vascular access device. J Pediatr Surg 2006;41:1582-7.

5. Male C, Chait P, Andrew M, et al. Central venous linerelated thrombosis in children: association with central venous line location and insertion technique. Blood 2003;101:4273-8.

noindent

6. Grisoni ER, Mehta SK, and Connors AF. Thrombosis and infection complicating central venous catheterization in neonates. Journal of Pediatric Surgery 1986; 21(9): 772-776.

7. Peters M, ten Cate JW, Koo LH, et al: Persistent antithrombin III deficiency: Risk factor for thromboembolic complications in neonates small for gestational age. J Pediatr 1984; 105:310-314.

8. Peters M, ten Cate JW, Jansen E, et al: Coagulation and fibrinolytic factors in the first week of life in healthy infants. J Pediatr 1985;106:292- 295.

9. Journeycake JM and Buchanan GR. Catheter-related deep venous thrombosis and other catheter complications in children with cancer. J Clin Oncol 24:4575-4580.

10. Bartlett RH. Extracorporeal life support registry report 1995. ASAIO Journal 1997;43:104-7.

11. Winthrop AL and Wesson DE. Urokinase in the Treatment of Occluded Central Venous Catheters in Children. Journal of Pediatric Surgery 1984; 19(5): 536-8.

12. Wu Y, Rojas AP, Griffith GW, Skrzypchak AM, Lafayette N, Bartlett RH, et al. Improving blood compatibility of intravascular oxygen sensors via catalytic decomposition of S-nitrosothiols to generate nitric oxide in situ. Sensors and Actuators B: Chemical 2007;21: 36-46.

14. Oh BK, Meyerhoff ME. Catalytic generation of nitric oxide from nitrite at the interface of polymeric films doped with lipophilic Cu(II)-complex: a potential route to the preparation of thromboresistant coatings. Biomaterials 2004;25: 283-93.

15. Boudko DY. Bioanalytical profile of the L-arginine/nitric oxide pathway and its evaluation by capillary electrophoresis. Journal of Chromatography B 2007; 851:186-210.

16. Murad F. Discovery of some of the biological effects of nitric oxide and its role in cell signaling. Bioscience Reports 1999; 9:453-74.

17. Bogdan C. Nitric Oxide and the Immune Response. Nature immunology 2 2001;10:907-16.

17. Ghaffari A, Miller CC, McMullin B, Ghahar A. Potential application of gaseous nitric oxide as a topical antimicrobial agent. Nitric Oxide 2006;14(1):21-9.

18. Yoo JW, Choe ES, Ahn SM, Lee CH. Pharmacological activity and protein phosphorylation caused by nitric oxide-releasing microparticles. Biomaterials 2010;31:552-8.

19. Kushwaha M, Anderson JM, Jun HW. A nitric oxide releasing, self assembled peptide amphiphile matrix that mimics native endothelium for coating implantable cardiovascular devices. Biomaterials 2010;31:1502-8.

20. Ramamurthi A, Robson SC, Lewis RS. Effects of nitric oxide (NO) and soluble nucleoside triphosphate diphosphohydrolase (NTPDase) on inhibition of platelet deposition in vitro. Thromb Res 2001;102:331-41.

21. Zhang HP, Annich GM, Miskulin J, Osterholzer K, Merz SI, Bartlett RH, et al. Nitric oxide releasing silicone rubbers with improved blood compatibility: preparation, characterization, and in vivo evaluations. Biomaterials 2002;23 (6):1485-94.

22. Major TC, Brant DO, Reynolds MM, Bartlett RH, Meyerhoff ME, Handa H, et al. The attenuation of platelet and monocyte activation in a rabbit model of extracorporeal circulation by a nitric oxide releasing polymer. Biomaterials 2010; 31:2736-45.

23. Anton N, Cox PN, Massicotte MP, Chait P, Yasui L, Dinyari PM, et al. Heparin-bonded central venous catheters do not reduce thrombosis in infants with congenital heart disease: A blinded randomized, con- trolled trial. Pediatrics 2009;123:453-8.

24. Krafte-Jacobs B, Sivit CJ, Mejia R, Pollack MM. Catheter related thrombosis in critically ill children: comparison of catheters with and without heparin bonding. J Pediatr 1995;126(1):5054-60.

25. Massicotte MP, Dix D, Monagle P, Adams M, Andrew M. Central venous catheter related thrombosis in children: analysis of the Canadian registry of venous thromboembolic complications. J Pediatr 1998;133(6):770-6.

26. Riley KD, Classen CD, Stevens LE, Burke JP. A large randomized clinical trial of a silver-impregnated urinary catheter: Lack of efficacy and staphylococcal superinfection. J Amer Med 1995;98:349-56.

27. Batchelor MM, Reoma SL, Fleser PS, Nuthakki VK, Callahan RE, Shanley CJ, et al, More lipophilic dialkyldiamine-based diazeniumdiolates: synthesis, characterization, and application in preparing thromboresistant nitric oxide release polymeric coatings. J of Medicinal Chemistry 2003;46:5153-61.

CHAPTER VI

NITRIC OXIDE IN SWEEP-GAS FOR LOCAL CLOT INHIBITION IN OXYGENATORS

6.1 Abstract

Studies have explored supplementation of nitric oxide Nitric Oxide (NO) in sweep gas to reduce platelet adhesion, activation, and coagulation within oxygenators with mixed results. The mixed results may be due to wide variations from study to study in NO concentrations, oxygenator types, blood flow rates, and in vitro and in vivo models. Each of these factors is likely to affect NO flux rates from the gas exchange membrane. However, these flux rates have never been measured or modeled, making interpretation of the results difficult. In this study, in vitro experiments were conducted to determine the flux rates through clinical oxygenators at a range of sweep gas NO concentrations.

Specifically, the Biolung and the Terumo Capiox RX25 (N = 3 each) were perfused with a liter of water circulating at 4 L/min while NO gas at 10, 100 and 1000 ppm concentrations in nitrogen were swept through the devices at 8 L/min. NO concentration in the water was measured at baseline prior to initiating NO flow and at 1,3 5, 10, 15, and 30 minutes after initiation. The NO concentration data were then used to calculate NO flux by dividing the change in the amount of dissolved

NO per unit time by the total surface area of the artificial lung. The flux data was used to calculate the mass transfer coefficient, k_c, by dividing the flux by the difference between the maximum NO concentration (NO concentration at its solubility at standard temperature and pressure) and NO concentration at time t. The flux rates of NO for each lung was then calculated as the product of their average k_c's and the maximum NO concentration.

The k_cs of the Biolung and the Capiox RX25 were 0.05 ± 0.001 cm/min and 0.025 ± 0.004 cm/min respectively. From these values, the calculated NO flux from the Biolung and the Capiox RX25 at 5000 ppm NO/N_2 sweep gas were 4.85 ± 0.1 and 2.43 ± 0.007 (x 10^{-10} mol/cm^2/min) respectively. These results indicate that the range of sweep gas NO concentrations previously tested were insufficient to generate flux rates that significantly limit platelet deposition, but that further increases are not warranted due to the high levels of mHb that are generated. Future studies should focus on passivating surfaces to platelet deposition such that lower NO flux rates may be sufficient to counteract platelet activation.

6.2 Introduction

In the previous chapters, surface functionalization with NO via chemical procedures have been evaluated in flat silicone membranes, hollow silicone fibers, artificial lung ECC circuits, and intravascular catheters. The chemical procedure employed for these applications modifies surfaces to either release of generate NO. In artificial lungs where the longevity of NO production is pertinent, NO generation shows more practicality than NO release. In the NO generation method however, Cu toxicity due to leaching of Cu particles from the surface of a biomaterial into blood is a real problem. This problem can be completely avoided by a relatively easier approach of functionalizing the gas exchange surfaces of artificial lungs with NO. In this approach, NO gas is supplementated into the sweep gas of artificial lungs, and the

NO gas continuously diffuses across the gas exchange fibers to provide a flux at the blood/polymer interface. Not only does this method avoid the problem of toxicity from metallic catalysts but also preserve the longevity of NO production afforded by the NO generation procedure.

NO gas has a long history for its capacity to inhibit platelet adhesion to gas exchange membranes of oxygenators [**1**]. Its utility in controlling clots via NO inhalation by patients during CPB surgery, through supplementation into sweep gas during extracorporeal membrane oxygenation of severe pulmonary hypertension patients, or for reducing biomaterial-induced clot formation *in vitro* experimentation has shown outcomes with little consensus. A wide range of sweep gas NO concentrations (15-1000 ppm) has been tested using different oxygenator types and membranes in CPB and extracorporeal membrane oxygenation ECMO since 1995. This range is reflective of the fact that there is no agreement on what NO concentration is optimal for: maintaining oxygen carrying capacity of red blood cell Red Blood Cell (RBC)s (by keeping methemoglobin Methemoglobin (MetHb) below 5%), inhibiting platelet activation, maintaining platelet function, maintaining good hemodynamics and hemocompatibility while remaining non-toxic to cells.

One of the earliest NO sweep gas work was conducted using 15, 40, and 75 ppm sweep gas NO concentration to study their effect of blood coagulation *in vitro*. Sweep gases (NO in nitrogen bled into 5%CO_2 in air) were flowed into oxygenators primed with heparin-treated blood recirculating at 0.6 L/min in an ECC for 24 hours [**2**]. Plasma nitrate, cyclic guanosine monophosphate levels, and platelet count were significantly higher in the NO circuits than in the control circuits ($p<0.01$). Beta thromboglobulin released from an activated platelet's alpha granules was observed at lower levels in the NO circuits ($p<0.01$). No difference was observed in platelet's serotonin content and membrane glycoprotein Ib density between circuits. There were no dose-response effects in all measured variables for the NO concentrations tested. Similar

positive results using low sweep gas NO concentration (20ppm) were also reported by Keh et al 1999 [**3**]. In their study, the NO gas was supplied into M18 Jostra oxygenators in a simulated ECMO circuit primed with 1IU/ml heparinized blood. Platelet count, betathromboglobulin, and methemoglobin concentrations were monitored in the circulating blood (0.6 L/min) for 4h. Platelet count and methemoglobin concentrations were significantly higher ($p<0.01$) in NO group than in controls. Betathromboglobulin was also significantly lower in the NO group ($p<0.05$). Due the positive effect of 40 ppm sweep gas NO seen *in vitro* by Mellgren et al 1996 [**2**], the same group investigated the effect of that concentration during CPB of twenty patients[**4**]. Unfortunately there was no significant differences in platelet count and function between control and NO groups. Platelet function, as measured by glycoprotein GP I/Ib and GP IIb/IIIa exposure, was preserved in both groups.

Based on previous outcomes of positive *in vitro* conclusions at a low sweep gas NO concentrations and disappointing *in vivo* conlcusions, several sweep gases with higher NO concentrations have thus been tested. In a study by Tevaearai et al 2000 [**5**], a slightly higher NO concentration (80ppm, in O_2 and N_2) was infused into oxygenators in ECC during a CPB procedure in calfs to determine the effect of NO on local clot formation. The surface area of the oxygenator covered with clots was significantly reduced from $5.78 \pm 3.80\%$ in the control group to $0.54 \pm 0.41\%$, ($p<0.05$), in the NO group. Interestingly platelet count dropped to 60% of basal value and its evolution during the 6-hour experiment was comparable in both groups [**5**]. In a different study, a 100ppm NO/N_2 was utilized for inhibiting platelet activation inside membrane oxygenators supporting 47 CBP patients. Methemoglobin remained below 4% and there was no significant difference in platelet count between NO and control groups ($p< 0.05$). Furthermore, NO had no detectable effect on the levels of beta thromboglobulin and did not affect bleeding. Methemoglobin levels also remained in the safe range (up to 4%) during the entire 3-hour procedures [**6**]. Due to yet

undesirable outcomes, other research groups ventured for higher concentrations. Two sweep gas NO concentrations (100 and 200ppm NO/N_2) were infused into hollow fiber oxygenators to test for their ability to inhibit platelet activation. Platelet count decreased with 100ppm NO concentration during the first hour and platelet factor 4 (PF4) increased also in this time frame. At 200 ppm sweep gas NO concentration, there was significant reduction in platelet adhesion in the NO group, and no difference was observed in PF4 levels between the NO and non-NO groups after 1 h. Plasma PF4 however, increased after an hour regardless of sweep gas NO concentration [**1**]. Even yet higher sweep gas NO concentrations have been tested. In work conducted by Sly et al 1996 [**8**], adult pigs undergoing CBP were supported on a membrane oxygenator infused with a 500ppm NO/N_2 sweep gas at 1 L/min. Platelet adherence and aggregation decreased compared to their controls ($p<0.05$), and no difference in flow, mean arterial pressure, and hematocrit was observed between control and NO groups. These conclusions held when sweep gas NO concentration was increased to1000 ppm. Methemoglobin however, doubled from 4% when sweep gas NO concentration was increased to 1000ppm [**7, 8**]. From these studies, it seems that the bases for selecting a sweep gas NO concentration solely relied on previous blood coagulation outcomes without regard for what the NO flux would be on the surfaces of gas exchange membranes. In this work, NO flux rates on the Biolung and Terumo CapioxRX25 were investigated using 10 - 1000ppm NO/N_2 sweep gas NO concentrations. Flux rates at different concentrations are also predicted and compared to endothelial levels of NO flux.

6.3 Materials and Methods

6.3.1 In vitro Study

Circulation Setup: To determine NO flux rate across oxygenator fibers, water was circulated in a circuit, as NO sweep gas flowed countercurrently through the oxygenators as shown in Figure 6.1. The concentration of NO in the fluid was then measured at different time points. Specifically, 1000 cc of fluid was pumped (stockert multiflow roller pump) from the reservoir into the lungs (Biolung MC3, Ann Arbor, MI and Terumo Capiox R_X 25) and returned to the reservoir through a $0.5''$ Tygon tubing at 4 L min^{-1}. 10, 100 and 1000 ppm NO/N_2(Cyrogenic gases, Detroit MI) sweep gases were separately supplied at 8 L min^{-1} and monitored with an air flow meter while a TS410 transit-time tubing flow meter (Transonic systems Inc. Ithaca, NY) monitored fluid velocity. The concentration of NO in the bulk fluid was measured by drawing 3 mL fluid samples from the outlet conduit of the lungs through a stopcock at baseline (time zero), 3, 5, 10, 15, and 30 minutes for each sweep gas concentration. After each 30 minute run, the circuit was filled with fresh water for the next run.

Procedure for Measuring Nitric Oxide Concentration in Water:
The concentration of NO in the bulk fluid was measured by drawing 3 mL samples from the outlet conduit of the lungs through a stopcock prior to the initiation of sweep gas flow and at 3, 5, 10, 15, and 30 minutes after initiation of flow. After each 30-minute run, the circuit was filled with fresh water for the next run. Drawn samples were immediately (<10 sec) introduced into a pre-prepared sample cell of a Sievers nitric oxide analyzer 280 unit (GE analytical instruments, Boulder, CO) setup to measure the NO content. Prior to sample introduction the sample cell was purged with N2 to remove oxidative species from the cell. A 3-minute baseline recording of the dry cell was then done before drawn samples were injected. At this point, no nitrate

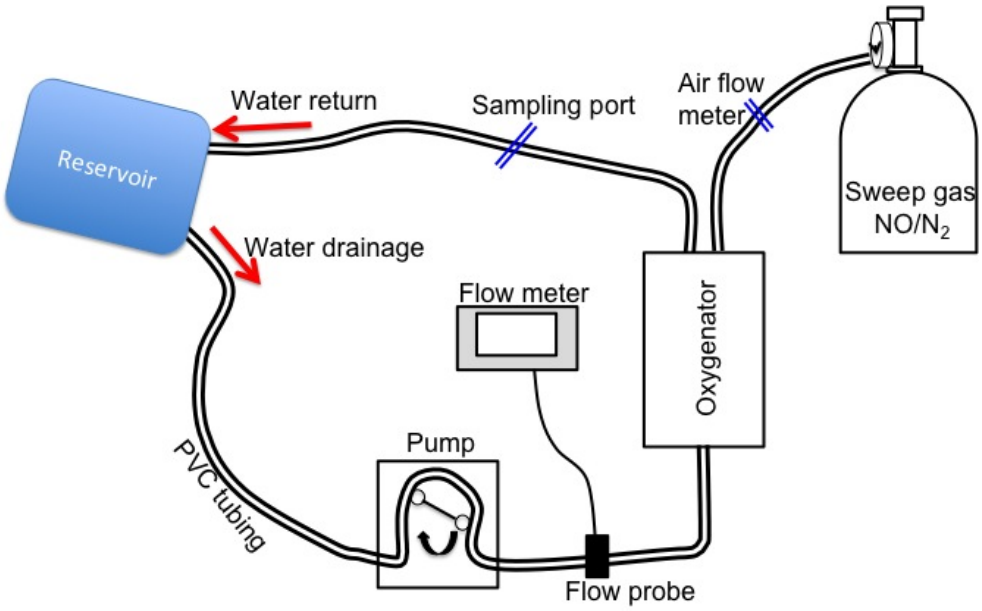

Figure 6.1: Nitric oxide in sweep gas circulation setup.

or nitrite reducing agents were added to the samples. Only NO dissolved in water during circulation was degassed out with N_2 into the Nitric Oxide Analyzer (NOA)s sample unit system for measurements. NO released from the samples was measured for at least 5 minutes after the measurement signal returned to baseline levels. N= 3 measurements were taken at each sampling time for each lung. A total of N=9 samples were analyzed at each sampling time.

Recovery of Scavenged Nitric Oxide:

A standard nitrite reduction protocol using a purge vessel (GE analytical instruments, Boulder, CO), acetic acid and potassium iodide (Sigma Aldrich, St Louis MO) was used to reduce any nitrites that were formed in the water during circulation. This procedure can be referred to in the Nitric Oxide Analyzer manual and it ensures that all NO scavenged into nitrites and nitrates by oxidative species was recovered. Nitrite is the predominant byproduct formed when nitrogen and oxidative species react in water so scavenged NO was recovered only from nitrites in this experiment. In short, three 50 μL aliquots of the degassed sample were injected in succession into the purge

vessel containing acetic acid and potassium iodide. The average of the areas under the NO release profile was then used to estimate total recovered NO.

Calculation of NO Concentration in Water:

In order to preserve convention, the units of concentration (parts per million/billion), as recorded by our NOA was converted to moles/L. The number of moles of NO, n(NO) (moles), per 3mL water samples, was the product of total NO content in the sample, NOtotal (ppb* sec), which was calculated as the area under the NO release curve, and NOA's sampling inlet system flow rate, Q (ml/sec), and mL-to-moles conversation factor for an ideal gas, C in equation (6.1e). This formulation was expressed as:

$$\mathrm{n(NO)} = \mathrm{NO}_{total} \times \mathrm{Q} \times \mathrm{C} \qquad \text{Nitric Oxide Concentration} \qquad (6.1a)$$

$$\mathrm{NO}_{total} = \mathrm{NO}_{time(t)} - \mathrm{NO}_{baseline} \qquad \text{Net Nitric Oxide (ppb.sec)} \qquad (6.1b)$$

$$\mathrm{Q} = 3.33 \text{ ml/sec} \qquad \text{NOA's Flow Rate} \qquad (6.1c)$$

$$\mathrm{ppb} = (\text{ x } 10^{-9}) \qquad \text{NOA's sensitivity unit} \qquad (6.1d)$$

$$\mathrm{C} = 22400 \text{ mole/mL} \qquad \text{Ideal gas molecules per miliLiter} \qquad (6.1e)$$

The data generated from equation (6.1a) was then used to calculate the n(NO) per liter of water (NO concentration in mol/L). Equations (6.1b), (6.1c), and (6.1d) represent the total NO measured, the nitric oxide analyzer's gas inlet flow rate, and its sensitivity unit respectively.

NO Flux Across Gas-exchange Membranes:

NO flux, J_{NO} (mol $\mathrm{min}^{-1}\mathrm{cm}^{-2}$), across each oxygenator was calculated by dividing the product of its total gas-exchange fibers surface area, SA (cm^2), and duration of

sweep gas flow, t (mins), into the change in NO concentration, [NO], as expressed in equation (6.2a).

$$J_{NO} = \Delta[\mathrm{NO}]/(\Delta t \times SA) \tag{6.2a}$$

Estimating NO Flux at Time Zero:

Solubility of NO in water at STP is reported to be 1.94 x 10^{-3} mol L^{-1} atm^{-1} [9]. For our flow conditions and sweep gas blend, the theoretical solubility of NO in water should be lower, as the solubility of gases in solvents is directly proportional to the partial pressure of the gas interfacing with the solvent. In our setup, the partial pressure exerted by NO, p(NO) (atm), will be approximately proportional to its gas proportion in the sweep gas, NO/N_2 (ppm). Assuming the sweep gas exerts a total pressure of 1 atm, the solubility and maximum theoretical concentration of NO, [NO]max (mol L^{-1}), in water can be estimated using equations (6.3a) and (6.3b) respectively.

$$\mathrm{Solubility(NO)} = 1.94 \text{ x } 10^{-3} \text{ (mol L}^{-1} \text{ atm}^{-1}) \times \mathrm{NO/N_2} \tag{6.3a}$$

$$[\mathrm{NO}]\mathrm{max} = \mathrm{Solubility(NO)} \times \mathrm{p(NO)} \tag{6.3b}$$

$$\text{where } \mathrm{p(NO)} = \mathrm{NO/N_2} \times 1\mathrm{atm} \tag{6.3c}$$

First, the [NO]max was estimated using the theoretical solubility of NO in water. Second, the mass transfer coefficient, Kc, at each time point was calculated using equation (6).

$$\mathrm{Kc} = \mathrm{J}_{NO}/([\mathrm{NO}]_{max} - [\mathrm{NO}]_t) \tag{6.4a}$$

In brief, Kc was calculated by dividing the difference between the maximum theoretical NO concentration and measured NO concentration into the NO flux. Finally, NO flux at time zero for each lung type was estimated as the product of their average Kc and the maximum theoretical NO concentration for each sweep gas blend.

6.4 Results

6.4.1 NO Concentration in Fluid

Typical purged NO profile as measured by the NOA is shown in Figure 6.2. The levels of purged NO detected by chemiluminescence decreased over time as the dissolved NO in the test solution purged. In addition, scavenged NO was recovered from samples that were already purged. Specifically, three 50 μL aliquots of the purged sample were injected into the purge vessel and the areas under their peaks were then calculated and averaged to estimate the total residual NO.

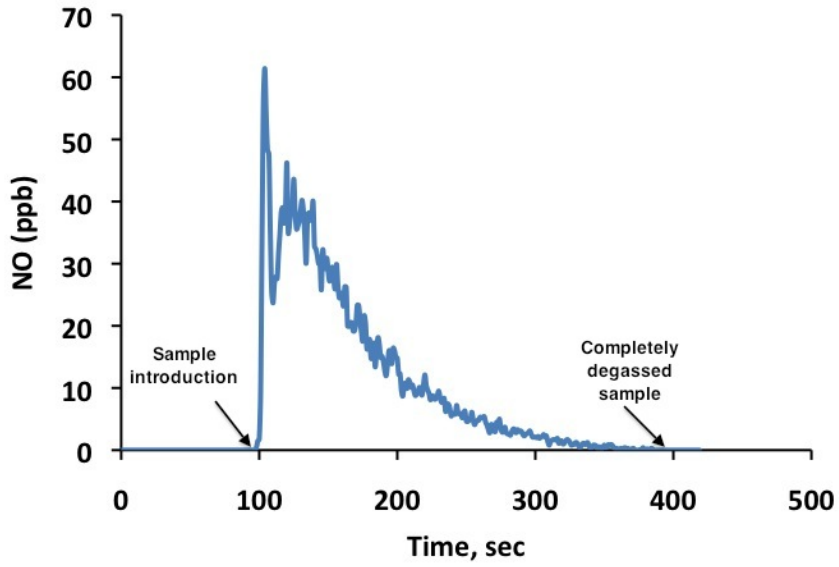

Figure 6.2: Representative nItric oxide release profile from degassed sample fluids.

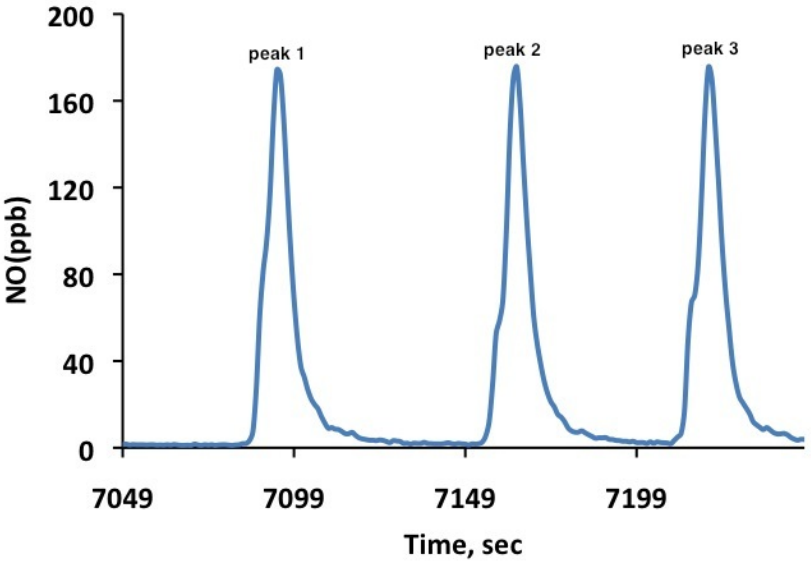

Figure 6.3: Representative nitric oxide release profile from reducing nitrites in degassed samples. Three 50 μL aliquotes(peak 1, peak 2 and peak 3) of the degassed sample were treated to reduce nitrites to nitric oxide gas which was then degassed from samples and measured with a nitric oxide analyzer. This NO release profile was from a sample perfused with 10 ppm NO/N_2 sweep gas for 30 minutes.

For each sweep gas blend, NO concentration in the circulating fluid was determined

using equation (6.1a). As shown in Figure 6.4, the NO concentration rapidly builds up in the fluid within 10 minutes and plateaus thereafter when the Biolung was used as the gas-exchanging device. For the 100ppm and 1000ppm NO/N_2 sweep gas blend, NO concentration (mol/L) dynamics was similar in both Biolung and Capoix devices. It increased from 1.5 x 10^{-7} at 1 minute to 2.8 x 10^{-7} at 30 minutes with the100ppm gas and from 9.16 x 10^{-7} to 1.80 x 10^{-6} with the 1000ppm gas. However in the 10ppm NO/N_2 blend, NO concentration was higher with the Capiox. With the capiox RX25, it increased from (3.87 x 10^{-7}) to (7.28 x 10^{-8}) and (1.4 x 10^{-8}) to (1.74 x 10^{-8}) with the Biolung.

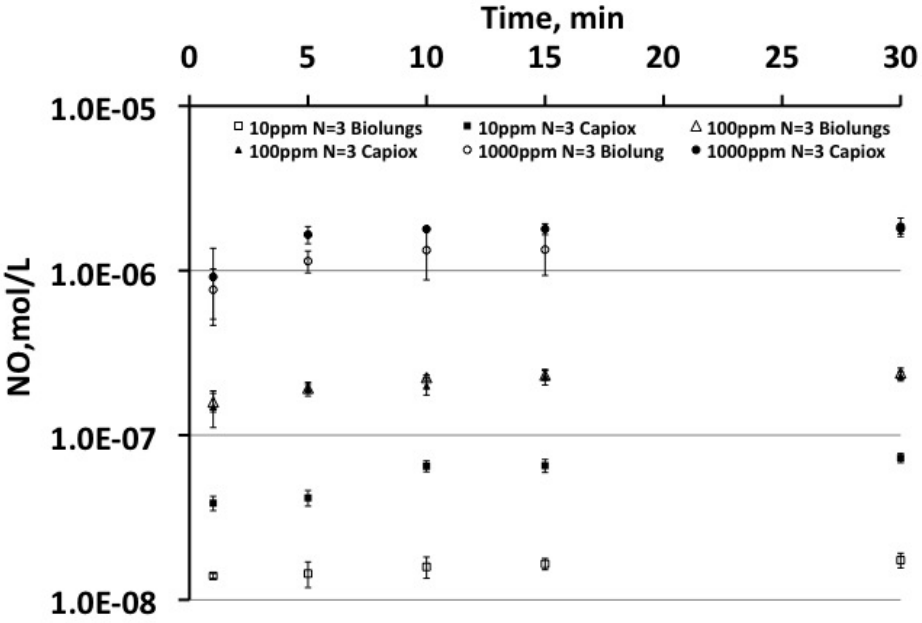

Figure 6.4: Nitric oxide gas dissolved in circulation water after diffusing through the gas exchange membranes of the Biolung and Capiox r_X25.

NO flux across each oxygenator was calculated by dividing the product of total surface area of its gas-exchanging fibers and duration of sweep gas flow by the change in NO concentration. As expected NO flux into the fluid was higher soon after flow began Figure 6.5, as NO concentration in the fluid at this point was low. For each

lung and sweep gas blend tested, flux gradually decreased as the NO concentration increased in the circulating fluid.

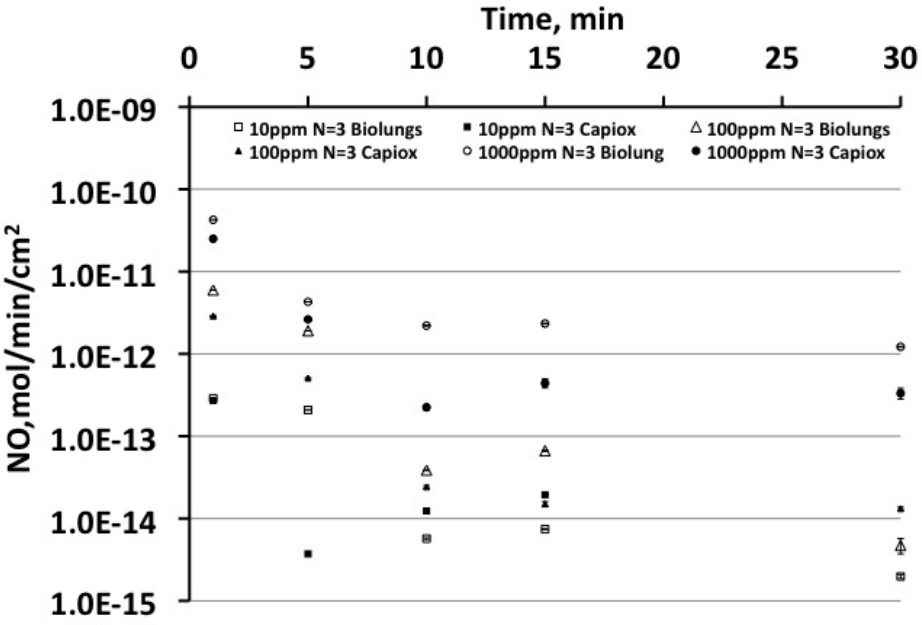

Figure 6.5: NO flux across membranes of the Biolung and Capiox RX25 using 10, 100, and 1000ppm NO/N_2 sweep gases.

6.4.2 Estimating NO Flux from the Biolung and Capiox RX25 fibers at Time Zero

Solubility of NO in water at standard temperature and pressure Standard Temperature and Pressure (STP) is reported to be 1.94 x 10^{-3} mol L^{-1} atm^{-1} [9]. For our flow conditions and sweep gas blend, the theoretical solubility of NO in the fluid should be lower, as NO gas exerts a partial pressure proportional to its percentage in the sweep gas. Table 6.1 shows the Solubilities of NO in different NO/N_2 concentrations and their corresponding maximum NO concentrations in fluid.

Theoretical solubilities of our various sweep gas blends, the NO concentration in the fluid, and the mass transfer coefficient of the gas exchange fibers of each lung were used to estimate the NO flux across the fibers at time zero. Time-zero NO flux

Table 6.1: Solubilities of NO in different NO/N_2 concentrations and their corresponding maximum NO concentrations in fluid

Sweep gas blend (NO/N_2, ppm)	**Solubility** (mol L^{-1} atm^{-1})	**Theoretical [NO]max** (mol/L-1)
10	1.94 x 10^{-8}	1.94 x 10^{-8}
100	1.94 x 10^{-7}	1.94 x 10^{-7}
250	4.85 x 10^{-7}	4.85 x 10^{-7}
1000	1.94 x 10^{-6}	1.94 x 10^{-6}
2000	3.88 x 10^{-6}	3.88 x 10^{-6}
2500	4.85 x 10^{-6}	4.85 x 10^{-6}
5000	9.70 x 10^{-6}	9.70 x 10^{-6}

is interpreted as flux just after sweep gas flow started.

The mass transfer coefficient at each time point in Figure 6.6 was calculated by dividing the difference between theoretical NO concentration and measured NO concentration by the calculated NO flux at that time point. The mass transfer coefficient of each oxygenator was then estimated by curve-fitting the dominating values (first ten minutes) of the mass transfer coefficient data for all sweep gas blends. See Figures 6.7 and 6.8. The estimated mass transfer coefficient at time zero for the Biolung and Capiox RX25 oxygenators were 0.05 cm/min and 0.025 cm/min respectively.

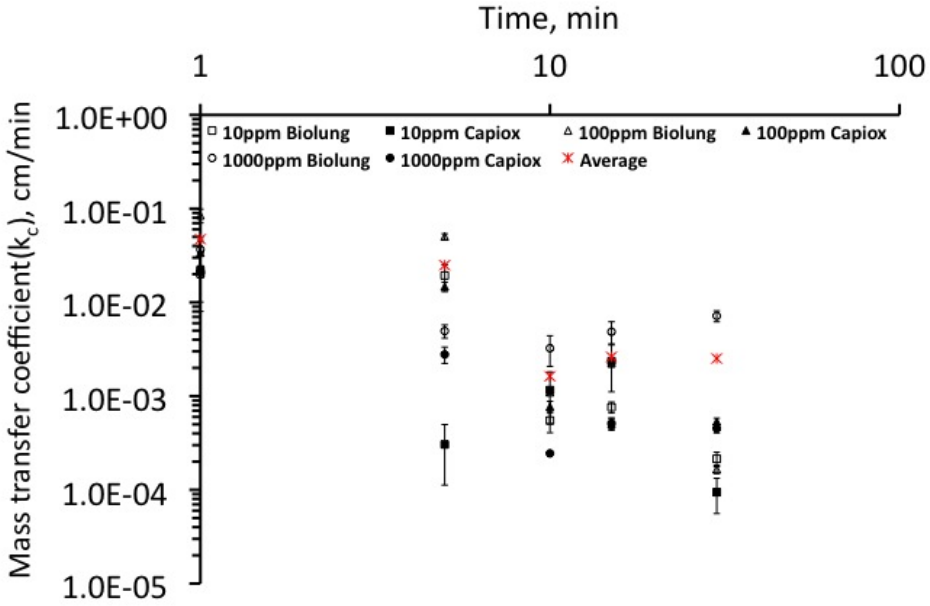

Figure 6.6: Evolution of the mass transfer coefficient, (k_c), of the Biolung and Capiox RX25 oxygenators at 10, 100, and 1000ppm NO/N_2 sweep gases.

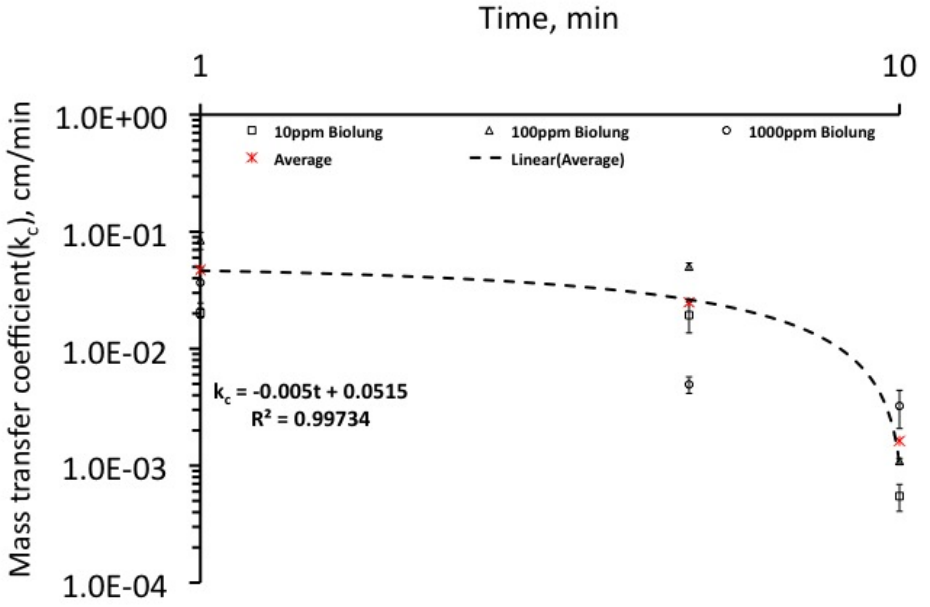

Figure 6.7: Time-zero estimation of the NO flux of the Biolung oxygenators N=4

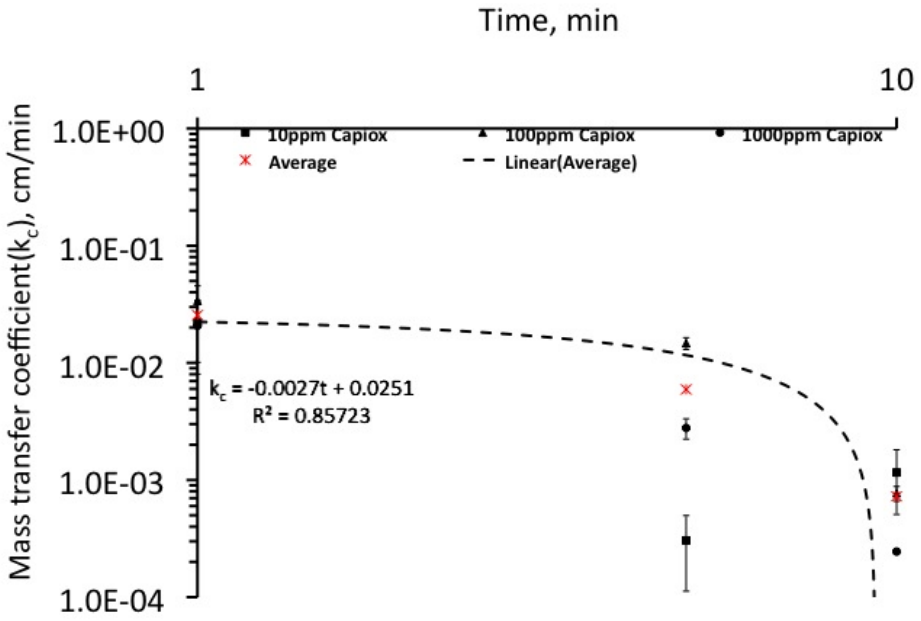

Figure 6.8: Time-zero estimation of the NO flux of the Capiox RX25 oxygenators N=4

NO flux at time zero for each lung was then calculated by multiplying the estimated mass transfer coefficient of the lung by the theoretical maximum NO concentration for each sweep gas blend. The predicted NO flux at time zero for various gas blends (tested and untested) per lung is shown in Table 6.2.

Table 6.2: Predicted peak flux of NO from fibers of primed Biolung and Capiox RX25 oxygenators in 1 L circulation setup

NO/N_2 sweep gas Concentration, (ppm)	**Predicted flux at time 0**, ($\times 10^{-10}$ mol/min/cm^2)	
	Biolung	**Terumo RX25**
10	0.009 ± 0.0002	0.005 ± 0.0001
100	0.097 ± 0.002	0.05 ± 0.001
1000	0.485±0.009	0.24±0.001
2000	0.970±0.02	0.48±0.001
5000	4.85±0.1	2.43±0.007

6.5 Discussion

NO fluxes generated from the tested range of NO sweep gas blends are able to effect small anticoagulatory benefits, as reported in [**11**] and also shown in this work. Although these flux levels offer some benefit, they are insufficient to significantly limit platelet deposition on biomaterials. Higher NO concentration is needed for platelet inhibition. However, high NO levels produce MetHb at levels incompatible with life. In the setting of our study, NO is fighting both the effects of protein deposition and of thrombin on blood coagulation. Our hypothesis is that if the biomaterial's surface is functionalized so that it inhibits protein or platelet deposition, low levels of NO may prove more effective at inhibiting blood activation. At such low levels, the problem with mHb buildup could also be avoided. Future studies should focus on passivating surfaces to platelet deposition such that lower NO flux rates may be sufficient to inhibit platelet activation.

The solubility of NO in water at standard temperature and pressure has been

extensively studied and, perhaps, the most comprehensive report [**10**] on this subject reported it to be 1.94 x 10^{-3} mol L^{-1} atm^{-1}. This value was used to calculate the NO solubility levels at partial pressure per each sweep gas blend (See Table 6.1). These theoretical solubility levels should dictate the maximum NO concentration levels in the circulating fluid per sweep gas blend. To check for this, the maximum NO concentrations calculated from theroretical NO solubility values were compared to maximum experimental NO concentration levels. For the 1000ppm NO sweep gas blend, the ratio of maximum experimental NO concentration for both Biolung and Capiox RX25 (1.80 x 10^{-6} mol L^{-1}) to the maximum theoretical NO concentration, 1.94 x10^{-6} mol L^{-1}, was 0.92. With the 100ppm sweep gas, this was ratio was 1.23 for both lungs. At the lowest end of NO sweep gas concentration tested (10ppm), this ratio was different for each lung type. We calculated 3.75 for the Capiox RX25 and 0.89 for the Biolung. The ratio was exceptionally higher for the Capiox lung with the 10ppm NO/N_2 sweep gas probably because the fluid used was below room temperature and thus increased the solubility of the NO. However, these ratios are generation close to 1, indicating agreement of our in vitro work with existing literature.

Based on our in vitro studies, we are able to provide a different interpretation of some of the NO sweep gas results reported in literature. Although different oxygenators were used in works cited, most of them had surface areas (1.3 -1.9 m^2) comparable to that of the Biolung (1.7 m^2) and Capiox RX25's (2.5 m^2). Therefore, the flux levels per NO sweep gas blend used in other studies should follow our predicted time-zero NO flux values. Another similarity that can be drawn between our oxygenators and those used in literature is their gas-exchange material. The gas exchange material of the Capiox RX25 is polypropylene and polymethyl pentene for the Biolung. Those in literature comprise of but not limited to polypropylene and polymethyl pentene. These similarities in material and surface area of the oxygenators perhaps can allow for the use of our time-zero NO flux values to justify why inhibition of platelet activa-

tion was insignificant in studies where 40ppm [**5**], 100ppm [**6**], and 500/1000ppm [**8**] was used. Their NO flux levels were too low to significantly inhibit platelet activation.

6.6 Reference

1. Konishi R, Shimizu R, Firestone L, Walters FR, Wagner WR, Federspiel WJ, Konishi H, and Hattler BG., Nitric oxide prevents human platelet adhesion to fiber membranes in whole blood. ASAIO.,1996 42(5): p.850-53

2. Mellgren K, Friberg LG, Mellgren G, Hedner T, Wennmalm A, and Wadenvik H., Nitric oxide in the oxygenator sweep gas reduces platelet activation during experimental perfusion. The Annals of Thoracic Surgery., 1996 61(4): p. 1194-8

3. Keh D, Gerlach M, Kurer I et al. Nitric oxide diffusion across membrane lungs protects platelets during simulated extracorporeal circulation. European Journal of Clinical Investigation 1999; 29: 344350

4. Mellgren K, Mellgren G, Lundin S, Wennmalm A, and Wadenvik H., Effect of Nitric Oxide Gas on Platelets During Open Heart Operations. Ann Thorac Surg., 1998 65: p.1335 41

5. Tevaearai HT, Mueller XM, Tepic S, Cotting J, Boone Y, P.M. Montavon PM, and Von Segesser LK., Nitric Oxide Added to the Sweep Gas Infusion Reduces Local Clotting Formation in Adult Blood Oxygenators. ASAIO., 2000 46: p. 719-22

6. Lowson SM, Hassan HM, and Rich GF., The Effect of Nitric Oxide on Platelets When Delivered to the Cardiopulmonary Bypass Circuit. Anesth Analg., 1999 89: p. 1360 5

7. Sly MK, Prager MD, Eberhart RC, Jessen ME, and Kulkarni PV., Inhibition of Surface-Induced Platelet Activation by Nitric Oxide. ASAIO journal 1995 41: p. 394-98

8. Sly MK, Prager MD, Li J, Harris FB, Shastri P, Bhujle R, Chao R, Kulkarni PV, Constantinescu A, Jessen ME, and Eberhart RC. Platelet and Neutrophil Distributions in Pump Oxygenator Circuits: Influence of Nitric Oxide Gas Infusion. ASAIO journal 1996 42: p. 494-99

9. Thakur, M.L., et al., Indium-111-labeled human platelets: improved method, efficacy, and evaluation. J Nucl Med, 1981. 22(4): p. 381-5

10. Zacharia IG and Deen WM., Diffusivity and solubility of nitric oxide in water and saline. Ann Biomed Eng. 2005 33(2): p.214-22

11. Amoako KA and Cook KE., Developing copper-doped nitric oxide-generating silicone for reduced platelet activation in artificial lungs. Journal of Biomaterials Research Part B: Applied Biomaterials (under review)

CHAPTER VII

CONTRIBUTIONS, LIMITATIONS AND FUTURE WORKS, AND CONCLUSION

7.1 Contributions

The presented study has many contributions to the knowledge base on the synthesis, fabrication, characterization, and non-thrombogenic evaluation of nitric oxide releasing and generating surfaces. In summary:

Synthesis and characterization of nitric oxide-generating silicone for use as a blood-contacting biomaterial:

1. To the best of the author's knowledge, the characterization of Cu-mediated NO generation from S-nitrosothiols on silicone polymer is the most advanced and complete characterization, which considers polymer surface microstructure, effect of wt% Cu on surface expression of Cu and NO flux and gives an insight into blood coagulation on Cu-mediated NO-generation silicone.

2. Micro and nano Cu particles coalesce to form dendritic structures inside the polymer membrane and on the surface of the polymer. The expression of the dendrites on the surface is necessary for NO generation from S-nitrosothiols especially in hydrophobic polymers.

3. NO flux bears linear relationships with wt% Cu range tested and clotting time of whole blood.

4. This study provides many interesting conclusions regarding NO generation through Cu-mediated S-nitrosothiol decomposition: At 10 wt%, the clotting time is 4.24 times greater than with pure silicone, additional Cu will have diminishing returns, as the surface concentration of copper does not increase markedly with increasing wt% in this range.

Nitric oxide-generating silicone application to hollow fiber oxygenator technology: development and biocompatibility evaluation:

1. To the best of the author's knowledge, the developed Cu-mediated NO-generating hollow silicone fiber oxygenator is the first and most complete study regarding the application of NO-generation coating to a clinical device and its non-thrombogenic evaluation.

2. Many interesting findings important for assessing the applicability of this novel approach to clinical oxygenators is made. They include, surface morphology of the silicone hollow fiber, NO flux levels from fibers, flow pattern of NO-generating oxygenator, non-thrombogenic evaluation by device resistance, flows, platelet consumption and fibrinogen consumption.

3. This work also provides important information on Cu leaching into plasma and thus an assessment of the toxic effects of leached Cu levels.

Non-thrombogenic characterization of extruded nitric oxide-releasing silicone catheters:

1. To the best of the author's knowledge, silicone catheters extruded with chemical species that allow post-extrusion NO charging to create a nitric oxide-releasing

($\geq$ 2 x 10^{-10} mol $min^{-1}cm^{-2}$) catheters is the first and foremost of its kind. This study fully describes the effect of catheter structure, wall chemistry, and post NO-charging storage condition on NO release levels and duration of silicone catheters. Their non-thrombogenicity evaluation and outcomes are also presented.

2. The extrusion-over-mandrel process is, for the first time, applied to the fabrication of nitric oxide releasing catheters. The process is adequate for the manufacturing of 12 gauge OD catheters implantable in the right and left internal jugular veins of adult rabbits for non-thrombogenicity evaluation.

3. In the synthesis and fabrication process used, it was found that the NO releasing catheter produced endothelial NO flux levels, the flux level is a function of DACA-6 content and is affected by anionic agents and catheter storage conditions.

4. The level of NO flux released by the catheters is adequate for significant reduction of catheter occlusion in a 4h non-thrombogenicity testing.

Nitric oxide in sweep gas for local clot inhibition in oxygenators:

1. To the best of the author's knowledge, nitric oxide in sweep gas for the reduction of blood coagulation in oxygenators has been studied for over 15 years. However, characterization of the gas's flux level in oxygenators has never been studied hence making it impossible to settle on what sweep gas NO concentration can produce endothelial NO flux level or flux levels effective for significantly reducing blood coagulation in oxygenators without systemic anticoagulation.

2. An experimental procedure for quantifying NO flux at the surface of gas exchange fibers of commercial oxygenators for different sweep gas NO concentrations is described.

3. NO flux levels in the Biolung and Capiox RX25 oxygenators using 10, 100 and 1000 ppm sweep gas NO concentrations is presented. It is found that between a 1000 and 2000 ppm sweep gas NO concentrations will produce endothelial levels of NO flux on those oxygenators. This implies that previous studies examining NO in sweep gas were largely underpowered in terms of sweep gas NO concentration used.

7.2 Limitations and Future Works

This study, however, bears some limitations due to differences in simulated *in vivo* environment and the actual *in vivo* milieu. Those limitations, along with related suggestions for each study, can be largely summarized as follows:

1. In the nitric oxide sweep gas work water, instead of blood, was used for studying NO flux on the gas exchange membranes of oxygenators as no reliable technique currently exists for measuring dissolved NO in blood. Blood has far more NO scavenging species that may increase the transfer of NO across gas exchange membranes and thus, perhaps, a lesser sweep gas NO concentration may produce endothelial NO flux levels with blood flow. In clinical practice oxygen is bled into oxygenators to oxygenate flowing blood. When NO is also swept into the artificial lung, it can be oxidized into nitrite by oxygen. Hence the NO concentration inhibiting platelet activation at the polymer/blood interface may be different from that provided by the NO sweep gas.

2. The NO release duration and *in vivo* non-thrombogenicity of the nitric oxide-releasing catheters were studied and evaluated for 24h and 4h respectively. Clinical need requires these catheters to remain patent for weeks to months, and therefore a longer-term study is required. The duration of NO release should be studied in order to extend their patency up to 30 d and beyond. To get there,

different NO immobilizing compounds and anionic sites must be investigated.

3. The NO-generating silicone for blood-contacting coating study showed many positive results. However, the study is limited by the short periods of blood biomaterial contact and the relatively static setting. The effectiveness of the Cu/Si PMC on coagulation for periods of hours to days under appropriate blood flows must be studied. Cu leaching from the surface of the coating into the bulk fluid was not addressed. These concerns are however addressed in the NO-generating membrane lung study.

7.3 Conclusion

The research conducted herein investigated the use of nitric oxide as a means of inhibiting clot formation at the surfaces of blood-contacting artificial materials. Different surfaces were functionalized with NO production using three methods that involved chemical and physical modifications of materials. The chemical methods included: (1) NO generation at the surface of artificial materials via the decomposition of NO donors using Cu catalysts and (2) NO release from surfaces after incorporation of NO donors inside their bulk. And by the physical method, artificial materials were functionalized to produce NO after flowing NO gas over their surfaces.

For long-term use of artificial lungs, both physical and chemical means of NO functionalization may help inhibit clot formation. The catalytic means of NO production from using Cu catalysts and NO donors allows for continuous NO generation as long as the physical interaction between the catalyst and the NO donor remains unhindered. The ability of this method to generate NO continuously makes it a good candidate for applications requiring blood-contacting devices to remain functional for months. The hollow thin-walled gas exchange fibers of artificial lungs is a good fit for this method of NO production. It interfaces with blood only at their outer surface so NO donors infused into flowing blood can drive a continuous generation of NO from these fibers. NO supplementation into sweep gas may prove even more efficient for long-term use of artificial lungs. It does not involve modification of materials using complex and expensive chemical formulations, and the gas is also commercially available at several concentrations. All of these methods, however do have one potential underlining drawback of the formation of metHemoglobin when they lead to high NO flux production. In addition, the use of Cu as a catalyst for NO generation can lead to Cu toxicity. NO generation from this method may also decrease due to protein adsorption and Cu leaching from fibers.

In short-term (up to 4h) respiratory support by ECMO, AVCO2R, and CPB, their

artificial lungs' gas exchange fibers and extracorporeal circulatory surfaces could be modified to incorporate NO releasing materials for a controlled release. It should be noted that NO flux from such thin walls (up to 50 μm) may be limited to near low-end endothelial NO flux levels. During hemodialysis, dialysis membranes filter blood anywhere up to 4 h at a time, and therefore NO releasing coatings on their membranes is a more practical approach for controlling clot formation.

Catheters, on the other hand, interact with blood both on their lumen and on their outer surfaces. NO production is thus required on both sides of their walls although more so on their outer surfaces where blood continuously flows. The incorporation of NO releasing materials in their walls for controlled release from both surfaces appear to be a more efficient method for functionalizing catheters.

Ultimately, the selection of a surface functionalization with NO method for a device will depend on the intended duration of use, how the device works, and the structure and size of the blood-contacting surface. Long term use of blood-contacting devices require methods able to sustain long term NO production, gas exchange devices is a natural fit for NO supplementation, and small diameter pediatric catheters is a good fit for NO release material incorporation.